SDHD-related Head and Neck Paragangliomas

& their natural course

Berdine Louise Heesterman

ISBN: 978-94-6361-131-2

The publication of this thesis was financially supported by:
IG&H

SDHD-related Head and Neck Paragangliomas

& their natural course

Proefschrift

ter verkrijging van
de graad van Doctor aan de Universiteit Leiden,
op gezag van Rector Magnificus prof.mr.C.J.J.M. Stolker
volgens besluit van het college voor promoties
te verdedigen op donderdag 13 september 2018
klokke 16.15 uur

door
Berdine Louise Heesterman
Geboren te Baarn
in 1990

Promotor:	Prof. dr. P.P.G. van Benthem
Copromotores:	Dr. J.C. Jansen Dr. B.M.Verbist
Leden promotiecommissie:	Prof. dr. ir. J.H.M. Frijns Prof. dr. B. Kremer (Maastricht UMC+) Prof. dr. B.F.A.M. van der Laan (UMCG) Dr. F.J. Hes Dr. E.P.M. van der Kleij-Corssmit

Contents

"Incipiens necdum a me perfecta hiftoria eft; ramorum magnorum ex Ganglio hoc longiffimo Intercortalis ortorum, qui retro Carotides euntes, ad ipfum Internae ab Externa fecedentis angulum Ganglion minitum effeciunt, cujus ramuli quantum video, in tunicis hujus arteriae definunt."

H.W.L. Taube, 1743

1

Introduction

Paragangliomas

Paragangliomas (PGL) are rare neuroendocrine tumors associated with the autonomic nervous system. They may occur from the skull base to the pelvic floor and can be segregated into sympathetic and parasympathetic paragangliomas. The former, arise in close proximity to the paravertebral sympathetic trunk and from the adrenal medulla (pheochromocytoma). Parasympathetic paragangliomas are primarily located in the head and neck region and therefore commonly referred to as head and neck paragangliomas (HNPGL).

History

The history of head and neck paragangliomas begins with the discovery of the "Ganglion minitum", by Taube in 1743. A few years later, Carl Samuel Andersch published a detailed description of what he named the "gangliolum intercaroticum", in his work *Tractatio anatomico-physiologica de nervis corporis humani*. Although Andersch accurately described branches of the glossopharyngeal nerve to enter the gangliolum intercaroticum, its function remained unknown until the 1920s. Fernando De Castro was the first to postulate the sensory function of the small structure located at the bifurcation of the carotid artery, today known as the carotid body. It was however Corneille J.F. Heymans, who demonstrated that the carotid body could detect arterial hypoxia, hypercapnia and acidosis with subsequent reflexiogenic hyperventilation and increased blood pressure, for which he was awarded the Nobel Prize in Physiology or Medicine in 1938 [1–5].

The first histological examination of the carotid body was performed by Luschka in 1862 [6]. However, the presence of both type I (Chief) an type II (Sustentacular) cells, in the pathognomonic "Zellballen" configuration, was not discovered until the 1950s [7, 8]. Approximately two decades later, the neural crest origin of type I and II cells was identified by le Douarin [9].

The first reports on carotid body tumors, date back to 1891 [10–12]. Publications describing paragangliomas arising at other locations in the head and neck region, followed during the first half of the 20th century [13–15]. Although, familial occurrence of head and neck paragangliomas was first recognized during the same time period, several

decades past before the genetic basis for hereditary head and neck paragangliomas was discovered (table 1.0.1) [16–19].

Carotid & cardioaortic bodies

The carotid and cardioaortic bodies are sensitive to changes in arterial pO_2 and to lesser extent to changes in pCO_2 and pH. Oxygen deprivation causes neurotransmitter release, the subsequent action potential is transmitted to the cardiorespiratory centers in the medulla oblongata via afferent fibers of the glossopharyngeal (carotid body) and vagus nerve (cardioaortic body). In addition, prolonged oxygen deprivation results in upregulation of hypoxia-inducible factors with subsequent erythropoiesis and angiogenesis [8, 31, 32].

Hereditary paragangliomas

In the early 1990s, a gene locus associated with hereditary head and neck paragangliomas (PGL1) was mapped to chromosome 11q22.3-q23.1 [18]. Considering the similarities between hypoxia induced carotid body hyperplasia/anaplasia and PGL1-related paragangliomas, Baysal et al. postulated PGL1 to be involved in oxygen sensing and signaling. This astute proposition, resulted in the discovery of mutations in the gene encoding subunit-D of succinate dehydrogenase (SDH), the only mitochondrial protein that functions in both the aerobic electron transport chain and the tricarboxylic acid (TCA) cycle. SDH consists of 4 subunits (SDHA-SDHD) and is dependent on 2 assembly factors (SDHAF1 & SDHAF2). SDHAF2 promotes the covalent incorporation of flavin adenine dinucleotide (FAD, a redox cofactor) in SDHA (flavoprotein-subunit), the subunit that stabilizes succinate. SDHB (iron-sulfur subunit) contains the 2Fe-2S, 4Fe-4S and 3Fe-4S clusters. The catalytic core is anchored to the inner mitochondrial membrane by the hydrophobic subunits SDHC and SDHD (heme-protein cytochrome b). As FAD is reduced to $FADH_2$, succinate is oxidized into fumurate (TCA cycle). Subsequently, the 2 electrons are transferred from $FADH_2$ to the iron-sulfur clusters. Thereafter ubiquinone is reduced to ubiquinol (electron transport chain). Although the function of Heme is not proven, it probably prevents the production of reactive oxygen species (ROS) (figure 1.0.1) [19, 33–37].

Table 1.0.1: History

1563	First description of adrenal glands (Eustachius[20])
1743	Discovery of the carotid body (Taube[1])
1857	Color reaction of adrenal medulla after chromium staining (Werner[21])
1862	First histological description of carotid body (Luschka[6])
1878	Discovery of tympanic ganglion at the promontory (Krause[22])
1891	First comprehensive descriptions of carotid body tumors & first successful surgery (Marchand & Paultauf[10,11])
1903	Extensive description of abdominal sympathetic paraganglia tissue (Kohn[23])
1909	Discovery of paraganglion at the nodose ganglion of the vagus nerve (Aschoff[24])
1912	Adrenal medulla tumors first named pheochromocytoma (Pick[25])
1930	Discovery of cardioaortic bodies (Penitschka[26])
1932	Chemoreceptor function of carotid body established (De Castro & Heymans[2,4])
1933	Familial occurrence of carotid body paragangliomas recognized (Chase[16])
1935	First description of vagal body tumor (Stout[13])
1941	Discovery of jugular paraganglion, located at the adventitia of the jugular bulb (Guild[14])
1945	First successful surgery for temporal bone paraganglioma (Rosenwasser[15])
1958	Recognition of type I and II cells in typical "Zellballen" pattern, usually preserved in paraganglioma tissue (i.a., Garner[7])
1972	Neural crest origin of type I and II cells identified (Le Douarin[9])
1973	Association between chronic hypoxia (medical conditions, high altitude dwellers) and carotid body hyperplasia/anaplasia (Arias-Stella[27])
1980	Introduction of WHO classification into pheochromocytomas, extra-adrenal sympathetic paragangliomas and parasympathetic paragangliomas[28]
1982	Co-occurence of head and neck paragangliomas and pheochromocytomas (Pritchett[29])
1989	Parent-of-origin-dependent inheritance established in Dutch families (van der Mey[17])
1992	Genetic linkage (PGL1) to chromosome 11q22-23 in large Dutch family with hereditary paragangliomas (Heutink[18])
1998	Founder effect at PGL1 locus in the Netherlands (van Schothorst[30])
2000	Discovery of germline mutations in SDHD gene (Baysal[19])

Following the discovery of germline mutations in SDHD, mutations in SDHC, SDHB, SDHAF2 and SDHA were found in families with hereditary paragangliomas [34, 38–40]. All result in function loss of succinate dehydrogenase, with subsequent accumulation of succinate and increased production of ROS [41]. Not only mutations in SDHx are involved in the pathogenesis of paragangliomas. Germline (table 1.0.2 and 1.0.3)and/or somatic mutations have been identified in over 15 PGL susceptibility genes, and more will likely be discovered in the near future [33, 42].

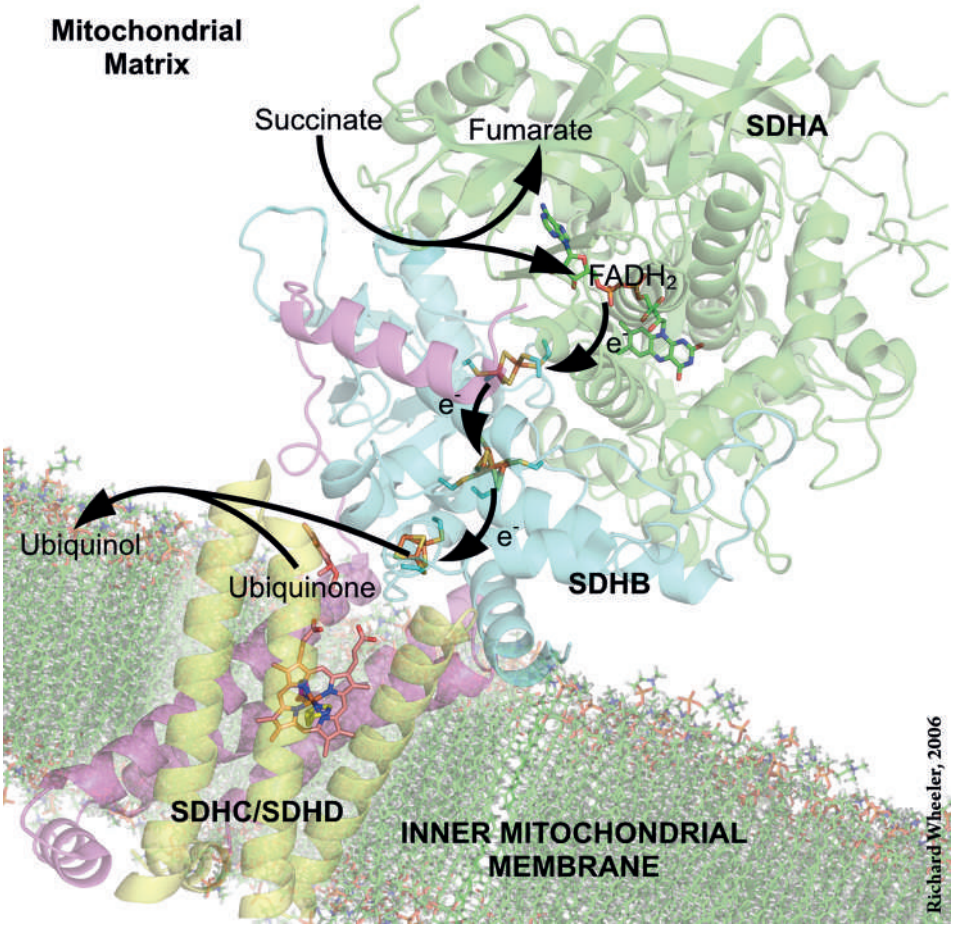

Figure 1.0.1: Function of succinate dehydrogenase in the tricarboxylic acid cycle and aerobic electron transport chain.

Although the exact molecular mechanisms resulting in tumor formation are still unknown, hereditary paragangliomas can be divided into 2 main clusters, based on their gene expression profile. Hypoxia-inducible factors (HIFs) are the main regulators of tumorigenesis in cluster 1 related paragangliomas (table1.0.2). HIFs can be subdivided into oxygen sensitive α-subunits and constitutively expressed β-subunits. Under normoxic conditions, HIF-1α and HIF-2α are hydroxylated by prolyl hydroxylase domain proteins (PHDs), enabling degradation via the von Hippel-Lindau (VHL) protein mediated ubiquitin proteasome pathway. Succinate, fumurate, and ROS inhibit PHD enzyme activity with subsequent stabilization of HIF-α. Stabilization of HIF-α also occurs in the absence of functional VHL, impaired PHD function and mutations in endothelial PAS domain protein 1 (EPAS1). HIF-α binds to HIF-β and translocates to the cell nucleus, with subsequent activation of HIF-responsive elements (HRE). As a result, transcription of pathways associated with cell proliferation, survival, and migration as well as angiogenesis and haematopoiesis occur [33, 43].

Succinate and fumurate do not only inhibit prolyl hydroxylase, but multiple α-ketoglutarate (α-KG)-dependent dioxygenases, including 5-methylcytosine (5mC) hydroxylases and histone demethylases, resulting in aberrant histone and DNA hypermethylation. A hypermethylator phenotype has been identified in SDHx, fumurate hydratase (FH) and, malate dehydrogenase 2 (MDH2) related paragangliomas [44–46]. Likewise, the pathogenic effect of ROS are not limited to inhibition of PHDs, but also cause direct mitochondrial DNA damage and activation of other pro-oncogenic pathways [41, 47]. Furthermore, upregulation of the G-protein-coupled receptor (GPR91), involved in numerous physio-pathological functions, might be involved in tumorigenesis of SDHx, VHL and EPAS1 related tumorigenesis (figure 1.0.2) [48].

Tumorigenesis in cluster 2 related paragangliomas is characterized by aberrant activation of kinase signaling pathways, promoting angiogenesis, cell proliferation, and survival (table 1.0.3) [33]. Finally, genes from both cluster 1 and cluster 2 are involved in c-jun dependent apoptosis of neuronal precursor cells. It is currently unknown if this pathway is involved in SDHx-related tumorigenesis [41].

Table 1.0.2: Cluster 1 (pseudohypoxia pathway) PGL susceptibility genes

Gene	Pathogenesis	Features
Von Hippel-Lindau (VHL, 1993)[49]	Absence of functional VHL protein	i.a., CNS and retinal hemangioblastomas, RCC, Visceral cysts, PCC, sPGL, and occasional HNPGL
Succinate dehydrogenase	Accumulation of succinate & increased ROS production	
SDHD (2000)[19]		Multiple HNPGL, sPGL, PCC, RCC, GIST, and PA
SDHC (2000)[38]		HNPGL, sPGL, PCC, RCC, and GIST
SDHB (2001)[39]		sPGL, PCC, HNPGL, GIST, PTC, NB, and RCC
SDHAF2 (2009)[34]		HNPGL
SDHA (2010)[40]		HNPGL, PCC, sPGL, GIST, and PA
Endothelial PAS domain protein 1/hypoxia-inducible factor 2α (EPAS1/HIF2α, 2013)[50]	Stabilization of HIF-2α	Polycythemia, PCC, sPGL, and somatostatinoma
Fumurate hydratase (FH, 2013)[44]	Accumulation of fumurate (TCA cycle)	Leiomyomatosis, RCC, PCC, sPGL, and HNPGL
Malate dehydrogenase 2 (MDH2, 2015)[46]	Accumulation of fumurate (TCA cycle)	Multiple malignant PGL

Abbreviations: central nervous system (CNS), renal cell carcinoma (RCC), pheochromocytoma (PCC), extra-adrenal sympathetic paraganglioma (sPGL), head and neck paraganglioma (HNPGL), gatrointestinal stromal tumor (GIST), pituitary adenoma (PA) and papillary thyroid carcinoma (PTC), neuroblastoma (NB)

Table 1.0.3: Cluster 2 (kinase signaling pathways) PGL susceptibility genes

Gene	Pathogenesis	Features
Neurofibromatosis type 1 (NF1, 1990)[51,52]	Failed RAS-GTPase activation (Ras-Raf-MEK-ERK pathway)	i.a., cafe-au-lait spots, neurofibromas, PCC, seldomly sPGLs and HNPGLs
Rearranged during transfection proto-oncogene (RET, 1993)[53]	Activation tyrosine kinase receptor (Ras-Raf-MEK-ERK & PI3K-AKT-mTOR pathway)	Multiple endocrine neoplasia type 2: i.a., MTC, primary hyperparathyroidism, PCC, seldomly sPGLs and HNPGLs
Kinesin family member1Bβ (KIF1Bβ, 2008)[54]	Involved in Ras-Raf-MEK-ERK pathway & perhaps prevention of apoptosis	NB, GN, LC, and PCC
Transmembrane protein 127 (TMEM127, 2010)[55]	Impaired negative regulation of mTOR signaling	PCC, rarely RCC
Myc associated factor X (MAX, 2013)	Association between Myc signaling and Ras-Raf-MEK-ERK & PI3K-AKT-mTOR pathways	sPGL, PCC
MET kinase receptor (MET, 2016)[56]	MET is associated with multiple pathways (i.a., PI3K/AKT)	PCC, RCC
C-MER proto-oncogene tyrosine kinase (MERTK, 2016)[56]	MERTK is associated with multiple pathways (i.a., MAPK-ERK)	PCC

Abbreviations: Ras-Raf-MEK-extracellular signal-regulated kinases (ERK) pathway, PI3 kinase (PI3 K) - AKT- mammalian target of rapamycin (mTOR) pathway, pheochromocytoma (PCC), extra-adrenal sympathetic paraganglioma (sPGL), head and neck paraganglioma (HNPGL), medullary thyroid carcinoma (MTC), neuroblastoma (NB), ganglioneuroma (GN), lung carcinoma (LC), renal cell carcinoma (RCC)

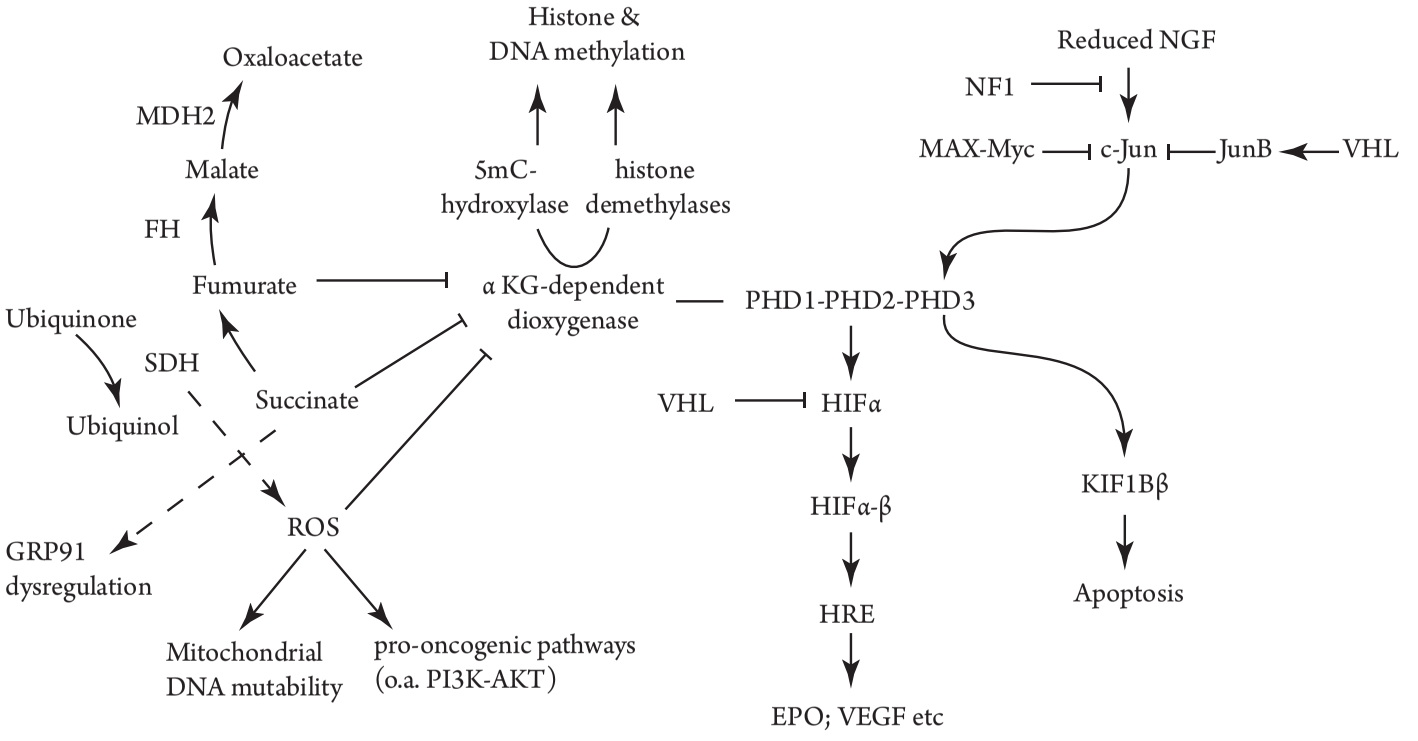

Figure 1.0.2: Mechanisms that are (possibly) involved in tumorigenesis of cluster 1 related paragangliomas. Primarily the pathways that might explain tumor development in SDHx-related cases are depicted.

Abbreviations: malate dehydrogenase 2 (MDH2), fumurate hydratase (FH), succinate dehydrogenase (SDH), G-protein-coupled receptor (GPR91), reactive oxygen species (ROS), PI3 kinase (PI3 K),5-methlycytosine (5mC) hydroxylases, α-ketoglutarate (α-KG)-dependent dioxygenases, prolyl hydroxylase domain proteins (PHDs), Von Hippel-Lindau (VHL), Hypoxia-inducible factor (HIF), HIF-responsive elements (HRE), erytropoetin (EPO), vascular endothelial growth factor (VEGF), nerve growth factor (NGF), Myc associated factor X (MAX), Kinesin family member1Bβ (KIF1Bβ)

Genetic testing

Approximately 35% - 40% of paragangliomas are hereditary [42, 57]. Germline mutations are detected in 92-99%, if multiple paragangliomas are present or in case of a positive familiy history [58]. However, due to low penetrance (e.g., SDHA, B & C) and paternal imprinting (SDHD & SDHAF2), a clear family history is not always present and genetic testing is therefore recommended for all paraganglioma patients [59, 60]. Genetic testing traditionally included polymerase chain reaction based amplication followed by Sanger sequencing and multiplex ligation-dependent probe amplification (MLPA) to detect larger defects. Targeted sequential algorithms, based on characteristics such as syndromic features, secretory phenotype (adrenergic, noradrenergic, or dopaminergic), malignancy, tumor location(s), and immunohistochemical analysis, were introduced to improve cost-effectiveness. Next generation sequencing (NGS), provides the opportunity to simultaneously test multiple susceptibility genes, while costs are reduced. In addition, if a mutation is not detected among the hitherto identified susceptibility genes, whole exome and genome sequencing is possible. A drawback of NGS is the increased detection of variants of unknown significance. Other limitations include the decreased sensitivity/accuracy in A/T or G/C rich ($\geq$65%) regions and in regions with homopolymer repeats [57, 61].

Founder effect

Mutations in the SDHD gene are the most common cause of hereditary paragangliomas in the Netherlands [42, 57, 62, 63]. The Dutch population is furthermore characterized by a high prevalence of founder mutations [62, 63]. A founder effect at the PGL1 locus was first recognized by van Schothorst et al., who demonstrated that paraganglioma patients from 11 families originating from the same geographical area, shared an approximately 6 centrimorgans (cM) haplotype [30]. Connections between the families were not detected by genealogical surveys going back as early as 1770 -1830. However, the authors argue that it would be extremely unlikely that the haplotype would be linked by chance, particularly because it was not shared by 41 unrelated subjects from the same area, in the vicinity of Leiden.

In 2000, Baysal et al. discovered 5 different germline mutations in SDHD in 8 families,

including the Dutch founder mutation: a missense mutation that changes Asp^{92} into Tyr^{92}. The SDHD gene consists of 8978 base pairs (bp) and 4 exons of 52, 117, 145 and 163 bp. Presently over 100 germline mutations have been identified, including missense, frameshift and nonsense changes (www.lovd.nl/sdhd) [64]. A second founder mutation in SDHD, that changes Leu^{139} into Pro^{139} was identified by Taschner et al.in 2001 [62]. The c.274G>T, p.Asp92Tyr and c.416T>C, p.Leu139Pro variants are present in approximately 80% and 11% of Dutch SDHD germline mutation carriers [65, 66].

Parent-of-origin-dependent inheritance

SDHD germline mutations are inherited in an autosomal dominant fashion. However, a phenotype develops almost exclusively upon paternal transmission [67]. This parent-of-origin-dependent tumorigenesis was initially attributed to epigenetic modification of the maternally derived allele [17]. Deficiency of SDH-activity, as is to be expected if the wild-type SDHD allele is imprinted, is however associated with severe developmental defects. In addition, biallelic expression of the SDHD gene has been observed in kidney, brain and lymphoid tissue. Selective imprinting in paraganglia cells is improbable, as loss of the maternal SDHD allele is observed in tumor tissue [19, 62, 67, 68]. Several models, that attempt to explain this remarkable parent-of-origin effect, have been proposed of which the Hensen model is the most plausible [68, 69].

Hensen et al. observed that not only the maternal SDHD allele, but the entire maternal chromosome 11 is lost in tumor tissue and proposed that, one ore more paternally imprinted genes, residing on the 11p15 region (the only known region on chromosome 11 that contains imprinted genes) are involved in tumorigenesis. Loss of the maternal chromosome 11 would than result in loss of the wild-type SDHD allele and the nonimprinted tumor modifier allele(s) on the 11p15 region. The authors furthermore hypothesized that mitotic recombination, succeeded by loss of the maternal 11q and paternal 11p region would be required for tumorigenesis if the SDHD mutation is transmitted via the maternal line. Somatic recombination has since been observed in one of the very few patients with maternally transmitted disease [67].

The absence of tumor development in heterozygous SDHD knockout mice, supports the proposition that additional genetic changes are required [70, 71]. Considering tissue spe-

cific homozygous knockdown resulted in early death, Hoekstra et al. argue that loss of the nonimprinted modifier allele(s) increases apoptosis resistance. They considered several paternally imprinted genes located at 11p15, including cyclin-dependent kinase inhibitor 1c (CDKN1C) and polyspecific organic cation transporter (SLC22A18). CDKN1c prevents cell cycle progression and SLC22A18 has a proapoptotic function. Expression of both genes was reduced in tumor, compared to normal tissue. In addition, increased cell proliferation and reduced apoptosis were observed in combined SDHD/CDKN1C and SDHD/SLC22A18 in vitro knockdown models compared to SDHD knockdown alone. Occasionally, heterogeneity of chromosome 11 is preserved. However, reduced expression of CDKN1C and SLC22A18 was also observed in these cases. The authors thus concluded that it is probable that, CDKN1C and/or SLC22A18 are involved in tumorigenesis of SDHD-related paragangliomas [71, 72].

Clinical manifestations

Mutations in SDHD are predominantly associated with head and neck paragangliomas. The life time penetrance is high, with estimates at age 70 ranging from approximately 85 - 100% [73–75]. Most SDHD germline mutation carriers will even develop multiple head and neck paragangliomas ($\approx$ 60 - 70%), pheochromocytomas and extra-adrenal sympathetic paragangliomas are observed less frequently. Renal cell carcinomas, gastrointestinal stromal tumors and pituitary adenomas have also been associated with germline mutations in SDHD in rare cases [74, 76, 77]. The prevalence of malignant paragangliomas is approximately 3% [78].

Carotid body tumors are the most common manifestation, followed by vagal body and jugulotympanic tumors. Head and neck paragangliomas at other locations, including the thyroid gland, sympathetic chain, and larynx are extremely rare [65, 79]. Signs and symptoms vary with tumor size and location, although HNPGL may also remain asymptomatic throughout life, and only detected as incidental finding or following screening by genetic testing and imaging in context of hereditary disease.

Carotid body tumors typically present as a slowly expanding, painless mass, lateral to the hyoid bone. In advanced disease, symptoms resulting from compression or invasion of the lower cranial nerves, primarily the vagus nerve, may be present. Due to attach-

ment to the carotid arteries, carotid body tumors are more mobile in horizontal rather than vertical direction (Fontaine's sign). A painless lateral neck mass is also the most common symptom of vagal body paragangliomas. As they are located more medially, they may remain undetected for longer periods of time. Medial bulging of the lateral pharyngeal wall with displacement of the tonsil, soft palate and uvula is often observed. Vagal body tumors more frequently present with hoarseness due to involvement of the vagus nerve. The other lower cranial nerves are affected less often. Although, vagal body paragangliomas most commonly arise at the nodose ganglion, they may also occur at the jugular ganglion and mimic symptoms of jugular paragangliomas. Jugulotympanic tumors usually present with pulsatile tinnitus and hearing loss. Nonetheless, due to their anatomic location these tumors more often cause dysfunction of the glossopharyngeal, vagus, and accessory nerve (jugular foramen syndrome), compared to carotid and vagal body paragangliomas. In addition, the 7th, 8th and 12th cranial nerves may be affected. Characteristic findings are a red mass behind the eardrum and positive Brown's pulsation sign. If the tumor is touching the tympanic membrane, pulsation may also be observed without applying positive pressure [75, 80–82].

Most patients with pheochromocytomas and extra-adrenal sympathetic paragangliomas present with paroxysmal or sustained hypertension. Other common symptoms/signs of catecholamine excess include the classical triad of paroxysmal headache, palpitations and diaphoresis, anxiety, weakness, flushing and nausea. Seldomly, patients present with a catecholaminergic crisis [83, 84].

Symptoms indicative for renal cell carcinoma are flank pain and heamaturia. Common symptoms of gastrointestinal stromal tumors include abdominal pain, nausea and gastrointestinal bleeding. Pituitary adenomas may present with symptoms of increased cranial pressure, bitemporal hemianopsia or other visual field defects and hyperpituitarism [76, 84].

Diagnosis

Biochemical screening

Catecholamines (epinephrine, norepinephrine, and dopamine) are primarily synthesized, stored, and secreted by chromaffin (or chief) cells. Although catecholamine re-

lease fluctuates, there is continuous leakage of catecholamines from chromaffin granules into the cell cytoplasm. Due to subsequent metabolism, there is a relatively constant release of metanephrines (metanephrine, normetanephrine, and 3-methoxytyramine; further metabolized into homovanillic acid and vanillylmandelic acid). If a biochemical active paraganglioma is present, metanephrines are thus consistently elevated, whereas catecholamine levels may be normal at the time of measurement. Therefore biochemical screening should not only include measurement of plasma or urine catecholamines, but also measurement of metanephrines (figure 1.0.7) [83, 85].

SDHD-related pheochromocytomas and extra-adrenal sympathetic paragangliomas are generally characterized by a noradrenergic or dopaminergic phenotype. Which is readily explained by hypermethylation of the phenylethanolamine N-methyltransferase (PNMT) promotor due to succinate accumulation. PNMT converts norepinephrine into epinephrine, downregulation of PNMT thus results in reduced or absent levels of epinephrine. Although biochemically silent PCCs and sPGLs are rare, increased secretion of catecholamines and/or their metabolites is only detected in $\approx$ 30% of head and neck paragangliomas (mainly 3-methoxytyramine) [57, 83, 86].

Imaging

Magnetic resonance imaging (MRI) is generally used for the detection and follow-up of head and neck paragangliomas, as it displays more soft tissue contrasts compared to computed tomography (CT). However, high resolution CT is the modality of choice to appraise temporal bone involvement. Paragangliomas typically exhibit low signal intensity on T1 and proton density weighted images and appear hyperintense on T2 weighted images. Small lesions generally show intense homogeneous enhancement after gadolinium injection. However, as lesions become larger, heterogeneous enhancement may be observed, corresponding with areas of necrosis. The "salt and pepper" appearance on spin-echo sequences, used to describe areas of signal flow foids, interspersed with areas of low flow and hemorrhagic foci, is characteristic for paragangliomas. The contrast enhanced 3D Time of Flight MR Angiography sequence (3D TOF MRA), has proven to be more sensitive ($\approx$ 90%) for the detection of hereditary paragangliomas compared to T1 and T2 (fat suppressed) weighted images. In addition, 3DTOF MRA is better

suited for showing the hypervascularity of paragangliomas than conventional spin-echo sequences [81, 82, 87].

Carotid body tumors cause splaying of the carotid bifurcation with anterio-lateral/anterio-medial displacement of the external carotid artery (ECA) and posterio-lateral displacement of the internal carotid artery (ICA). Carotid body tumors are commonly categorized according to the Shamblin classification (table 1.0.4 and figure 1.0.3). Vagal body tumors can be distinguished from carotid body tumors, as they do not cause splaying of the carotid bifurcation. Furthermore, both the ICA and ECA are displaced anterio-medially. Vagal body tumors may be classified according their extension and skull base involvement (figure 1.0.4). Due to the proximity of the jugular bulb and cochlear promontory, distinction between jugular and tympanic paragangliomas is no longer attainable if tumors become larger. Therefore, these tumors are often referred to as jugulotympanic tumors (table 1.0.4 and figure 1.0.5) [87–90].

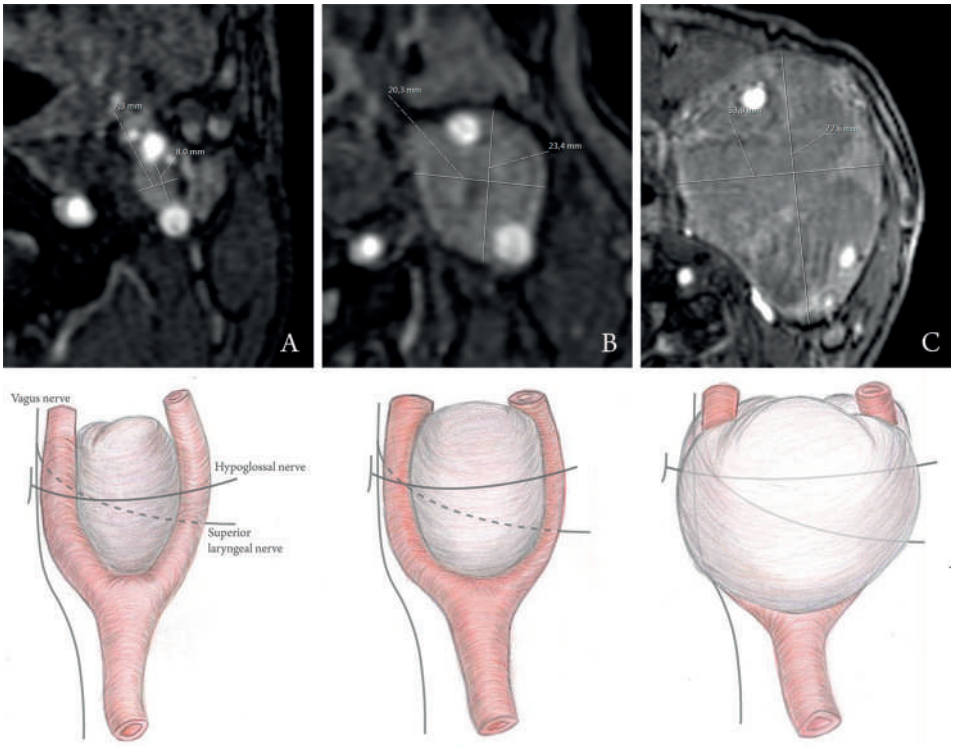

Figure 1.0.3: Shamblin type I (A), type II (B), and type III (C) carotid body paragangliomas.[88]

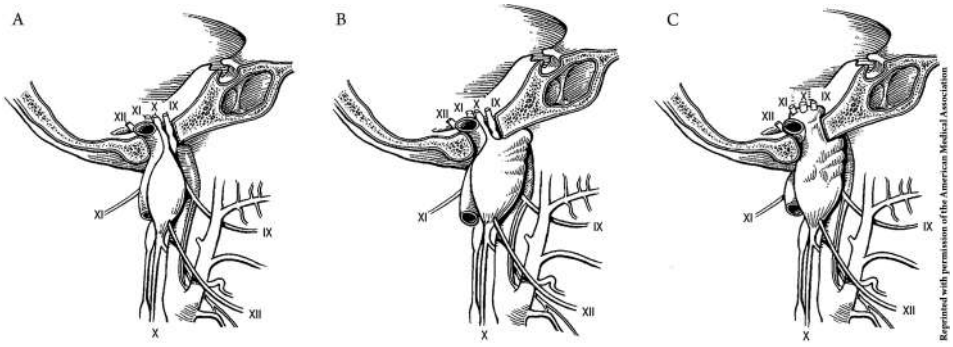

Figure 1.0.4: Netterville classification for vagal body paragangliomas.[89]

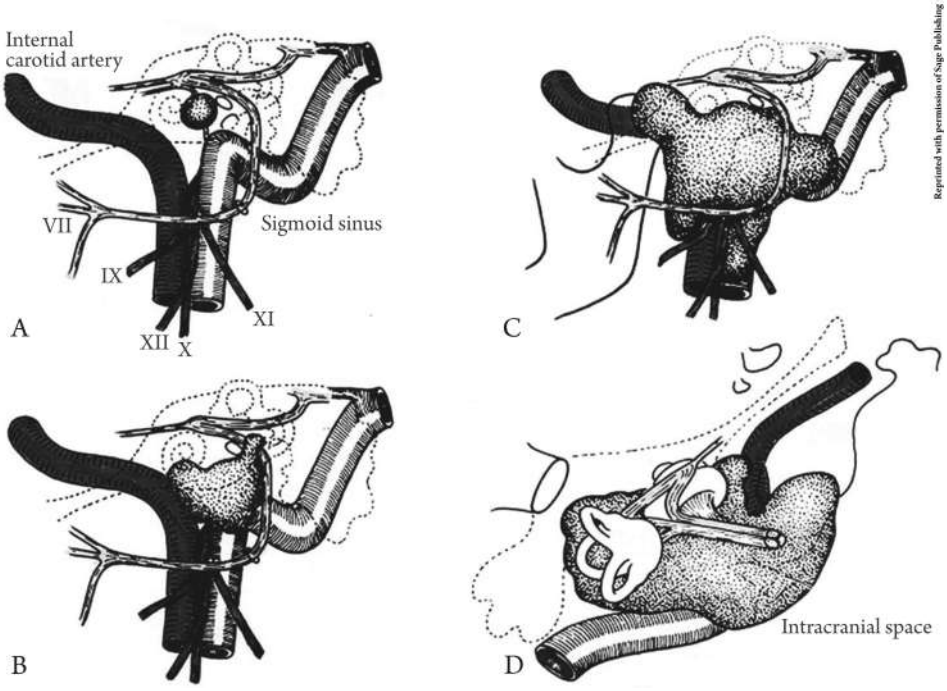

Figure 1.0.5: Fisch type A, B (Tympanic) C, and D (Jugular/Jugulotympanic) paragangliomas.[90]

Table 1.0.4: Classifications commonly used for head and neck paragangliomas.

Carotid body tumors: Shamblin[88]
Type I: Splaying of the carotid bifurcation with no or little involvement of the carotid arteries
Type II: Partial involvement of the carotid arteries
Type III: Complete encasement of the carotid arteries (A/B: absence/presence of contact with the skull base)

Vagal body tumors: Netterville[89]
A: Confined to the cervical region
B: Contact with the jugular foramen and encasement of ICA
C: Extending through the jugular foramen, often with cranial extension

Tympanic paragangliomas: Fisch[90]
A: Limited to mesotympanum
B: Limited to the tympanomastoid compartment without erosion of the jugular bulb

Jugular/Jugulotympanic paragangliomas: Fisch[90]
C: Erosion of the jugular foramen and:
C1: Erosion of carotid foramen
C2: Involvement of vertical segment of the carotid canal
C3: Involvement of horizontal segment of the carotid canal
C4: Involvement of foramen lacerum and cavernous sinus
D: Intracranial extension
De_1: Extradural extension, displacement of dura $<$ 2 cm
De_2: Extradural extension, displacement of dura $>$ 2 cm
Di_1: Intradural extension, invasion into posterior fossa $<$ 2cm
Di_2: Intradural extension, invasion into posterior fossa 2 - 4 cm
Di_3: Intradural extension, invasion into posterior fossa $>$ 4 cm

With the increasing availability of radiopharmaceuticals that detect metabolic changes specific to paragangliomas, functional imaging techniques have become more widely applied. ^{123}I-metaiodobenzylguanidine (MIBG) scintigraphy is often used for the detection of paragangliomas, and is available in most centers. However, functional imaging techniques with higher sensitivity and specificity have been introduced. Until recently ^{18}F-fluordopa (^{18}F-FDOPA) PET/CT was the preferred metabolic imaging method, but the necessity of a cyclotron to produce ^{18}F-FDOPA, precludes routine application. In

addition, ^{68}Gallium-DOTATATE PET/CT has proven to be superior in the detection of HNPGL compared to ^{18}F-FDOPA PET/CT. Although this might be reversed in cases of PCC, a cyclotron is not required to synthesize ^{68}Ga-DOTATATE. Therefore it will likely become the functional imaging technique of choice. It has been demonstrated that both ^{18}F-FDOPA and ^{68}Ga-DOTATATE PET/CT provide superior sensitivity and specificity compared to anatomical imaging. Nonetheless, MRI/MRA and/or high resolution CT needs to be added for locoregional staging [42, 83, 91].

Digital substraction angiography (DSA), historically used for the detection of paragangliomas, enables identification of dominant feeding and collateral vessel. However, following the introduction of MR angiography, DSA should only be performed if embolization is necessary[81, 92].

Histopathology

Clinical and radiologic findings are generally very characteristic and the added value of fine needle aspiration and incisional biopsy are limited. Moreover, due to the highly vascular nature of paragangliomas, these procedures are not without risks. Therefore, the diagnosis is only confirmed by histopathology following surgical resection [93, 94]. The typical pattern of chief (type I) cell nests, separated from the surrounding stroma by sustentacular (type II) cells is usually preserved in paraganglioma tissue (figure 1.0.6). Loss of heterogeneity is demonstrated in chief cells while retention of both SDHD alleles is observed in sustentacular cells. Therefore chief cells are considered the neoplastic component of paragangliomas, whereas proliferation of sustentacular cells is induced by the former [95, 96]. Chief cells stain positive for chromogranin as well as other neuroendocrine markers (synaptophysin, neuron-specific enolase, neural cell adhesion molecule), whereas S-100 protein is a marker for sustentacular cells. In addition, negative SDHB immunostaining of chief cells, but not of sustentacular cells is typical for SDHx-related paragangliomas [42, 79, 97].

Although correlations between several tumor markers, including ki-67 index, multiple mitotic figures, absent S-100 staining, and high HIF-1α expression, and metastatic disease have been found, reliable criteria for malignancy are lacking. Therefore, metastatic disease is defined as the presence of metastases, i.e., tumor cells at locations were paraganglia tissue is usually not present. Most often it concerns regional lymph nodes [42, 98–100].

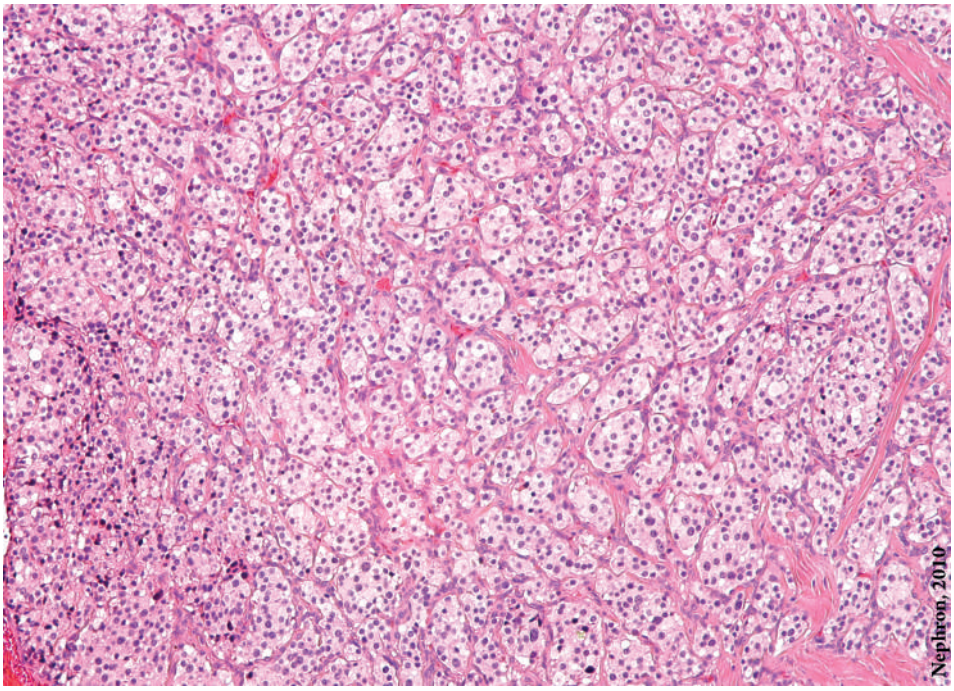

Figure 1.0.6: Micrograph of a carotid body tumor (hematoxylin & eosin stain), with characteristic "Zellballen" pattern

Treatment

Head and neck paragangliomas, particularly SDHD-linked cases, are generally benign tumors. The main goal of treatment should thus be achievement of tumor control and preservation of cranial nerve function rather than complete removal.

Surgery

Prior to surgery, urinary/plasma catecholamine levels should be evaluated. If elevated, sufficient α- and potentially β-adrenergic blockage is required to prevent a hypertensive crisis.

Since the first successful resection of a carotid body tumor in 1891, the risk at perioperative complications including stroke and even death have been reduced considerably [10, 81, 101]. Mainly due to advances in vascular reconstructive techniques, the use of intraluminal vascular shunts, and ligation of arterial supply (primarily branches of

the ascending pharyngeal artery). Nonetheless, intraoperative manipulation may still result in detachment of plaques in the common and internal carotid artery with subsequent cerebrovascular ischemia. Currently, the incidence of permanent stroke following surgery for carotid body tumors is approximately 3%. Although, only one patient (2.4 %) suffered from a minor stroke, with no evidence of permanent damage, in our own recent series [102]. In addition, there is a considerable risk at iatrogenic damage to the lower cranial nerves, primarily the vagus and hypoglossal nerve. The reported incidence varies from roughly 0 - 75% and is particularly high for Shamblin type III tumors. Other complications include hemorrhage and aspiration pneumonia. Total resection is achieved in nearly 97% and the risk at tumor recurrence is low ($\approx$ 3%). Total removal of shamblin type III tumors is most challenging [101, 103].

Surgery for vagal body tumors almost invariably results in vagus nerve dysfunction. In addition, iatrogenic damage of the glossopharyngeal and hypoglossal nerve have been reported in approximately 30%. Other serious, and relatively common, complications include aspiration/pneumonia ($\approx$ 10%), cerebrospinal fluid leakage ($\approx$ 3%) and stroke ($\approx$ 2%). Thus, surgery for vagal tumor paragangliomas is only advisable if tumor progression already caused lower cranial nerve dysfunction, and in case of malignant disease (or symptomatic catecholamine excess).

Tympanic tumors can usually be removed via a transmeatal (Fisch type A) or combined postauricular/endaural (Fisch type B) approach. Pulsatile tinnitus generally resolves and hearing loss often improves, whether or not ossicular chain reconstruction is necessary. The risk of serious complications is low and surgery is recommended in most cases [42, 104, 105]. In contrast, surgery for jugulotympanic paragangliomas is very challenging. Postoperative cranial nerve dysfunction is common, Suarez et al. reported 965 new cranial nerve deficits following surgery for 1084 jugulotympanic tumors. Functional hearing is seldomly preserved and the risk at other serious complications is considerable. Complete removal is achieved in approximately 85%, and the recurrence rate is nearly 7% [42, 106, 107].

The risk of debilitating bilateral cranial nerve dysfunction due to multifocal head and neck paragangliomas, further complicates the management of SDHD-linked cases. Primarily bilateral carotid body tumors are common. Some authors recommend to surgically remove the largest tumor first, while others argue that is is best to primarily

resect the smallest tumor and thereby increase the chance that at least unilateral neurovascular function is preserved [81, 101]. One should furthermore consider the risk of acute baroreflex failure syndrome due to bilateral denervation of the carotid sinus. Acute baroreflex failure is characterised by severe, volatile hypertension accompanied with dizziness or lightheadedness, palpitations, diaphoresis, headache, and emotional lability. Signs and symptoms may gradually resolve over the course of months. However, symptoms may also persist for years. Even in patients, that never experienced symptoms of baroreflex failure following bilateral carotid body resection, chronically decreased baroreflex sensitivity with increased blood pressure volatility have been observed. Bilateral carotid body resection furthermore causes dysfunction of the ventilatory response to hypoxia and apneic spells may occur [31, 32, 108].

Pheochromocytomas and extra-adrenal sympathetic paragangliomas are generally treated surgically, by choice via an endoscopic approach. Although, this is often feasible for small pheochromocytomas and abdominal extra-adrenal paragangliomas, an open procedure may be required for larger tumors. Cortex-sparing surgery is preferred to adrenalectomy, particularly in hereditary cases with high risk of bilateral disease, as it reduces the necessity for life long steroid substitution therapy. Fluid replacement and administration of vasopressors are required to counterbalance postoperative hypotension resulting from an abrupt decrease in plasma catecholamines [83, 109, 110].

Preoperative embolization

The advantages of preoperative embolization are reduced intraoperative blood loss and tumor shrinkage. However, embolization is not without risks. Migration of the embolic agent may result in stroke, mucosal, tong, or, skin necrosis, as well as ocular damage. Other complications include lower cranial nerve palsies and arterial dissection [42, 80, 111]. Surgery should be performed after 24-48 hours, in order that maximum thrombosis has occurred, but before the formation of collateral blood supply. To reduce the inflammatory response, that may hamper surgical resection, steroids should be administered. Most authors agree that there is no added value of embolization prior to surgery of Fisch type A and B paragangliomas. In contrast, preoperative embolization is generally recommended for Fisch type C and D tumors. However, the necessity of preoperative embolization of cervical paragangliomas remains controversial. Van der Bogt et al. argued

that the risks outweigh the benefits, mainly because a craniocaudal approach to carotid body tumors, facilitates early ligation of feeding vessels with statistically significant reduced blood loss [42, 81, 101, 104].

External beam radiotherapy

Historically, radiotherapy was used adjuvant to surgery, or if surgical removal was unattainable. However, radiotherapy is increasingly offered as primary treatment. Conventional fractionated radiotherapy is effective as it causes DNA damage with subsequent postmitotic cell death. The biological effective dose, depends on the total dose, dose per fraction and the radiosensitivity of irradiated cells. Unfortunately, the radioresistance of chief cells is high, and the close proximity of important neurovascular structures limits the possibility to increase the total radiation dose. Nevertheless, fibrosis around chief cell nests is observed in irradiated tumor specimens, 6 months after treatment. A total dose of approximately 45Gy in 25 daily fraction is currently recommended. Radiosurgery, causes direct cell death by using a highly focused, single ablative dose ($\approx$ 15Gy). Aside from the clear advantage that radiosurgery requires only one radiation session, treatment efficacy is less influenced by radioresistance. However, as radiosurgery is dependent on a steep dose gradient, the application of radiosurgery is limited in large tumors [42, 104, 112].

Local control, defined as the absence of tumor progression following radiotherapy, is achieved in $\approx$ 80 -100%. Approximately 25% of patients, irradiated for jugulotympanic tumors, have reported improvement of symptoms including, pulsatile tinnitus, headache, dizziness, and symptoms associated with cranial nerve impairment. However, new cranial nerve deficits may develop as well ($\approx$7%). It should furthermore be noted that supposed improvement of vagus nerve function is not always objectified and may also be attributed to compensation of the controlateral vocal cord. Although hearing may improve, permanent hearing loss following radiation therapy for jugulotympanic tumors is observed more often. Serious complications, such as osteonecrosis, brain necrosis, acute radiation syndrome, and radiation induced secondary malignancies are rare but should be considered. Common side affects include mucositis, nausea, dermatitis, chronic otitis, and fatigue [42, 81, 103, 106, 113].

Wait & Scan

A "wait and scan" strategy was first introduced in the early 90s by van der Mey et al. who argued that treatment did not necessarily improve the natural course of head and neck paragangliomas [114]. Growth of head and neck paragangliomas have since been addressed in several case series. All confirmed the generally indolent growth pattern of these tumors [115–118]. A "wait and scan" strategy entails, periodic imaging of the head and neck region. Active treatment is considered if rapid tumor growth or progression of symptoms is observed. Other reasons to change to active treatment are symptomatic catecholamine excess and malignant disease. This conservative approach is usually adopted in the Leiden University Medical Center (figure 1.0.7), and will have a central role throughout this thesis.

Objective

The main objective of this thesis is to gain more insight in the natural course of SDHD-related head and neck paragangliomas and ultimately improve surveillance and treatment strategies, as well as counseling of both patients and their family members.

Outline of this thesis

Chapter 2: Genetic testing has been offered to asymptomatic relatives of SDHD germline mutation carriers from 2002 onward. With the aim to estimate the prevalence of occult paragangliomas in asymptomatic SDHD germline mutation carriers, the results of genetic testing and surveillance are evaluated.

Chapter 3: We cannot say anything about tumor growth, without knowledge of the measurement method used. In this chapter, three measurement techniques are compared, with respect to reproducibility and practicability.

Chapter 4: Focuses on growth of carotid and vagal body paragangliomas. Possible predictors for tumor growth are evaluated and a prediction model is created.

Chapter 5: The insights gained in *chapter 4* are further explored, and mathematical models are fitted to growth data.

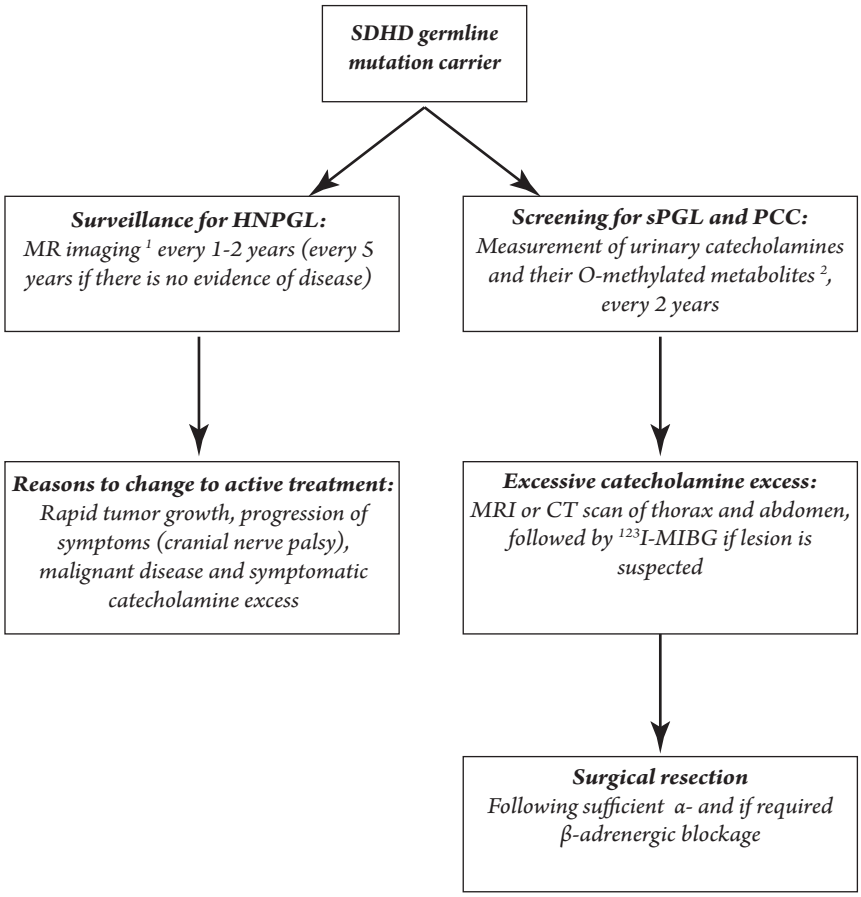

Figure 1.0.7: Current screening & surveillance strategy for head and neck paragangliomas (HNPGL), pheochromocytomas (PCC) and sympathetic extra-adrenal paragangliomas (sPGL) in SDHD germline mutation carriers.
Note 1: Computed tomography (CT) is used if there are contraindications for MR imaging.
Note 2: Measurement of (nor)epinephrine, dopamine, (nor)metanephrine, 3-methoxytyramine, and vanillylmandelic acid in two 24-hour urinary collections. Dietary restrictions during and two days prior to urinary collection are required and medication that may interfere with measurements are discontinued if possible.

Chapter 6: Multiple head and paragangliomas are typically observed in SDHD germline mutation carriers. However, the risk at metachronous lesions is presently unknown. In addition, sizable studies reporting the evolution of symptoms and cranial nerve dysfunction in patients managed with primary observation are lacking. Both the risk of metachronous lesions and clinical progression are addressed.

Chapter 7: Mortality rates and survival of SDHD germline mutation carriers are compared with those in the general population.

Chapter 8: In this final chapter, the acquired insights (*chapter 2 - 7*) and future research perspectives are discussed.

References

1. H. Taube. *De vera riervi intercostalis origine. Gottingae, A. Vandenhoeck.* 1743.
2. C. Heymans, J. Bouckaert, U. S. Von Euler, and L. Dautrebande. "Sinus carotidiens et reflexes vasomoteurs". In: *Arch. Int. Pharmacodyn* 43 (1932), pp. 86–110.
3. J. Pick. "The discovery of the carotid body". In: *J. Hist. Med. Allied Sci.* 14.1 (1959), pp. 61–73.
4. F. de Castro. "Sur la structure et l'innervation du sinus carotidien de l'homme et des mammifères. Nouveaux faits sur l'innervation et la fonction du glomus caroticum". In: *Trav. Lab. Rech. Biol.* 25 (1928), pp. 331–380.
5. F. de Castro. "Towards the sensory nature of the carotid body: hering, de castro and heymansdagger." In: *Front. Neuroanat.* 3.December (2009), p. 23.
6. H. Luschka. "Ueber die drusenartige Natur des sogenannten Ganglion intercaroticum". In: *Arch Anat Physiol Lpz* (1862), pp. 405–414.
7. C. M. Garner and D. Duncan. "Observations on the fine structure of the carotid body." In: *Anat. Rec.* 130.4 (1958), pp. 691–709.
8. P. Kumar and N. R. Prabhakar. "Peripheral chemoreceptors: function and plasticity of the carotid body." In: *Compr. Physiol.* 2.1 (2012), pp. 141–219.
9. N. Le Douarin, C. Le Lièvre, and J. Fontaine. "Experimental research on the embryologic origin of the carotid body in birds". In: *C. R. Acad. Sci. Hebd. Seances Acad. Sci. D.* 275.4 (1972), pp. 583–6.
10. R. Paltauf. "Ueber Geschwuelste der Glandula carotica". In: *Beitrage zur Pathol. Anat. und Allg. Pathol.* 11 (1891), pp. 260–301.
11. F. Marchand. "Beitraege zur Kenntnis der normalen und pathologischen Anatomie der Glandula carotica und der Nebennieren." In: *Int. Beiträge zur wissenschaftlichen Medizin. Festschrift für Rudolf Virchow* 1.1047-1050 (1891).
12. T. Else. "Pheochromocytoma, paraganglioma and genetic syndromes: A historical perspective". In: *Endocr. Relat. Cancer* 22.4 (2015), T147–T159.
13. A. Stout. "Malignant tumors of peripheral nerves". In: *Am. J. Cancer* 25 (1935), pp. 1–35.
14. S. Guild. "A hitherto Unrecognized Structure, the Glomus Jugularis, in man". In: *Am. Assoc. Anat.* 57 (1941), p. 28.
15. H. Rosenwasser. "Carotid body like tumor involving the middle ear and mastoid bone". In: *Arch. Otolaryngol.* 41 (1945), pp. 64–67.
16. H. Chase. "Familial and bilateral tumours of the carotid body". In: *J. Pathol. Bacteriol.* 36 (1933), pp. 1–12.
17. A. G. van der Mey, P. D. Maaswinkel-Mooy, C. J. Cornelisse, P. H. Schmidt, and J. J. van de Kamp. "Genomic imprinting in hereditary glomus tumours: evidence for new genetic theory." In: *Lancet* 2.8675 (1989), pp. 1291–1294.
18. P. Heutink, A. G. van der Mey, L. A. Sandkuijl, et al. "A gene subject to genomic imprinting and responsible for hereditary paragangliomas maps to chromosome 11q23-qter." In: *Hum. Mol. Genet.* 1.1 (1992), pp. 7–10.

19. B. E. Baysal, R. E. Ferrell, J. E. Willett-Brozick, et al. "Mutations in SDHD, a mitochondrial complex II gene, in hereditary paraganglioma." In: *Science* 287.5454 (2000), pp. 848–851.
20. B. Eustachi. "Tabulae Anatomicae Clarissimi Viri Bartholomaei Eustachii." In: *Rome, Italy Fr. Gonzagae.* (1714).
21. B. Werner. "De Capsulis Suprarenalibus." In: *Dorpat, Est. J. C. Schuemann, C. Mattiesen* (1857).
22. W. Krause. "Die Glandula tympanica des Menschen." In: *Zentralbl Med Wiss* 16 (1878), pp. 737–739.
23. A. Kohn. "Kohn A 1903 Die Paraganglien. A 62 263–367." In: *Arch. für mikroskopische Anat.* 62 (), pp. 263–637.
24. L. Arschoff and G. Goodhart. "Vorkommen von Paraganglien im periferschen Stamm des N. Vagus". In: *Dtsch Med Wochenschr* 35 (1909), p. 1461.
25. L. Pick. "Das Ganglioma embryonale sympathicum (sympathoma embryonbosartige gesale), eine typische chwuestform des sym- pathischen nervensystems". In: *Berliner Klin.* 49 (1912), pp. 67–69.
26. W. Penitschka. "Paraganglion aorticum". In: *Med. Klin* 26 (1930), pp. 1312–1313.
27. J. Arias-Stella and J. Valcarcel. "The human carotid body at high altitudes." In: *Pathol. Microbiol. (Basel).* 39.3 (1973), pp. 292–7.
28. E. Williams, L. Sobin, and R. E. Siebenmann. *Histological typing of endocrine tumours*. Geneva: World Health Organization, 1980.
29. J. W. Pritchett. "Familial concurrence of carotid body tumor and pheochromocytoma." In: *Cancer* 49.12 (1982), pp. 2578–9.
30. E. M. van Schothorst, J. C. Jansen, E. Grooters, et al. "Founder effect at PGL1 in hereditary head and neck paraganglioma families from the Netherlands." In: *Am. J. Hum. Genet.* 63.2 (1998), pp. 468–73.
31. H. J. L. M. Timmers, J. M. Karemaker, W. Wieling, H. A. M. Marres, H. T. M. Folgering, and J. W. M. Lenders. "Baroreflex and chemoreflex function after bilateral carotid body tumor resection." In: *J. Hypertens.* 21.June 2001 (2003), pp. 591–599.
32. T. Ketch, I. Biaggioni, R. Robertson, and D. Robertson. "Four faces of baroreflex failure: Hypertensive crisis, volatile hypertension, orthostatic tachycardia, and malignant vagotonia". In: *Circulation* 105.21 (2002), pp. 2518–2523.
33. S. Pillai, V. Gopalan, R. A. Smith, and A. K.-Y. Lam. "Updates on the genetics and the clinical impacts on phaeochromocytoma and paraganglioma in the new era." In: *Crit. Rev. Oncol. Hematol.* 100 (2016), pp. 190–208.
34. H.-X. Hao, O. Khalimonchuk, M. Schraders, et al. "SDH5, a gene required for flavination of succinate dehydrogenase, is mutated in paraganglioma." In: *Science* 325.5944 (2009), pp. 1139–42.
35. D. Ghezzi, P. Goffrini, G. Uziel, et al. "SDHAF1, encoding a LYR complex-II specific assembly factor, is mutated in SDH-defective infantile leukoencephalopathy." In: *Nat. Genet.* 41.6 (2009), pp. 654–656.
36. J. Rutter, D. R. Winge, and J. D. Schiffman. "Succinate Dehydrogenase-Assembly, Regulation and Role in Human Disease". In: *Mitochondrion* 10.4 (2010), pp. 393–401.

37. V. Yankovskaya, R. Horsefield, S. Tornroth, et al. "Architecture of succinate dehydrogenase and reactive oxygen species generation". In: 299.5607 (2003), pp. 700–704.
38. S. Niemann and U. Müller. "Mutations in SDHC cause autosomal dominant paraganglioma, type 3." In: *Nat. Genet.* 26.3 (2000), pp. 268–270.
39. D. Astuti, F. Latif, A. Dallol, et al. "Gene mutations in the succinate dehydrogenase subunit SDHB cause susceptibility to familial pheochromocytoma and to familial paraganglioma." In: *Am. J. Hum. Genet.* 69.1 (2001), pp. 49–54.
40. N. Burnichon, J. J. Briere, R. Libe, et al. "SDHA is a tumor suppressor gene causing paraganglioma". In: *Hum Mol Genet* 19.15 (2010), pp. 3011–3020.
41. C. Bardella, P. J. Pollard, and I. Tomlinson. "SDH mutations in cancer". In: *Biochim. Biophys. Acta - Bioenerg.* 1807.11 (2011), pp. 1432–1443.
42. D. Taïeb, A. Kaliski, C. C. Boedeker, et al. "Current approaches and recent developments in the management of head and neck paragangliomas." In: *Endocr. Rev.* 35.5 (2014), pp. 795–819.
43. I. Hussain, Q. Husain, S. Baredes, J. A. Eloy, R. W. Jyung, and J. K. Liu. "Molecular genetics of paragangliomas of the skull base and head and neck region: implications for medical and surgical management." In: *J. Neurosurg.* 120.2 (2014), pp. 321–30.
44. E. Letouzé, C. Martinelli, C. Loriot, et al. "SDH Mutations Establish a Hypermethylator Phenotype in Paraganglioma". In: *Cancer Cell* 23.6 (2013), pp. 739–752.
45. M. Xiao, H. Yang, W. Xu, et al. "Inhibition of *α*-KG-dependent histone and DNA demethylases by fumarate and succinate that are accumulated in mutations of FH and SDH tumor suppressors". In: *Genes Dev.* 26.12 (2012), pp. 1326–1338.
46. A. Cascón, I. Comino-Méndez, M. Currás-Freixes, et al. "Whole-exome sequencing identifies MDH2 as a new familial paraganglioma gene". In: *J. Natl. Cancer Inst.* 107.5 (2015), pp. 1–5.
47. S. S. Sabharwal and P. T. Schumacker. "Mitochondrial ROS in cancer: initiators, amplifiers or an Achilles' heel?" In: *Nat. Rev. Cancer* 14.11 (2014), pp. 709–21.
48. M. D. C. Fonseca, C. J. Aguiar, J. Antônio, and R. N. Gingold. "GPR91 : expanding the frontiers of Krebs cycle intermediates". In: *Cell Commun. Signal.* (2016), pp. 1–9.
49. F. Latif, K. Tory, J. Gnarra, et al. "Identification of the von Hippel-Lindau Disease Tumor Suppressor Gene". In: *Source Sci. New Ser.* 260.5112 (1993), pp. 1317–1320.
50. F. R. Lorenzo, C. Yang, M. Ng Tang Fui, et al. "A novel EPAS1/HIF2A germline mutation in a congenital polycythemia with paraganglioma". In: *J. Mol. Med.* 91.4 (2013), pp. 507–512.
51. M. R. Wallace, D. A. Marchuk, L. B. Andersen, et al. "Type 1 neurofibromatosis gene: identification of a large transcript disrupted in three NF1 patients." In: *Science* 249.4965 (1990), pp. 181–6.
52. R. M. Cawthon, R. Weiss, G. F. Xu, et al. "A major segment of the neurofibromatosis type 1 gene: cDNA sequence, genomic structure, and point mutations." In: *Cell* 62.1 (1990), pp. 193–201.
53. L. M. Mulligan, J. B. Kwok, C. S. Healey, et al. "Germ-line mutations of the RET proto-oncogene in multiple endocrine neoplasia type 2A." In: *Nature* 363.6428 (1993), pp. 458–60.
54. I. T. Yeh, R. E. Lenci, Y. Qin, et al. "A germline mutation of the KIF1B?? gene on 1p36 in a family with neural and nonneural tumors". In: *Hum. Genet.* 124.3 (2008), pp. 279–285.

55. Y. Qin, L. Yao, E. E. King, et al. "Germline mutations in TMEM127 confer susceptibility to pheochromocytoma." In: *Nat. Genet.* 42.3 (2010), pp. 229–33.
56. R. A. Toledo, Y. Qin, Z. M. Cheng, et al. "Recurrent Mutations of Chromatin-Remodeling Genes and Kinase Receptors in Pheochromocytomas and Paragangliomas". In: *Clin. Cancer Res.* 22.9 (2016), pp. 2301–2310.
57. J. Favier, L. Amar, and A.-P. Gimenez-Roqueplo. "Paraganglioma and phaeochromocytoma: from genetics to personalized medicine." In: *Nat. Rev. Endocrinol.* 11.2 (2015), pp. 101–11.
58. N. Burnichon, V. Rohmer, L. Amar, et al. "The succinate dehydrogenase genetic testing in a large prospective series of patients with paragangliomas." In: *J. Clin. Endocrinol. Metab.* 94.8 (2009), pp. 2817–2827.
59. M. Iacobone, F. Schiavi, M. Bottussi, et al. "Is genetic screening indicated in apparently sporadic pheochromocytomas and paragangliomas?" In: *Surgery* 150.6 (2011), pp. 1194–1201.
60. J. A. Rijken, N. D. Niemeijer, E. P. M. Corssmit, et al. "Low penetrance of paraganglioma and pheochromocytoma in an extended kindred with a germline SDHB exon 3 deletion." In: *Clin. Genet.* 89.1 (2016), pp. 128–32.
61. NGS in PPGL (NGSnPPGL) Study Group, R. A. Toledo, N. Burnichon, et al. "Consensus Statement on next-generation-sequencing-based diagnostic testing of hereditary phaeochromocytomas and paragangliomas." In: *Nat. Rev. Endocrinol.* (2016).
62. P. E. M. Taschner, J. C. Jansen, B. E. Baysal, et al. "Nearly all hereditary paragangliomas in the Netherlands are caused by two founder mutations in the SDHD gene". In: *Genes Chromosom. Cancer* 31.3 (2001), pp. 274–281.
63. E. F. Hensen, N. van Duinen, J. C. Jansen, et al. "High prevalence of founder mutations of the succinate dehydrogenase genes in the Netherlands". In: *Clin. Genet.* 81.3 (2012), pp. 284–288.
64. J.-P. Bayley, P. Devilee, and P. E. M. Taschner. "The SDH mutation database: an online resource for succinate dehydrogenase sequence variants involved in pheochromocytoma, paraganglioma and mitochondrial complex II deficiency." In: *BMC Med. Genet.* 6 (2005), p. 39.
65. L. T. van Hulsteijn, A. C. den Dulk, F. J. Hes, J. P. Bayley, J. C. Jansen, and E. P. M. Corssmit. "No difference in phenotype of the main Dutch SDHD founder mutations". In: *Clin. Endocrinol. (Oxf).* 79.6 (2013), pp. 824–831.
66. L. T. van Hulsteijn, B. Heesterman, J. C. Jansen, et al. "No evidence for increased mortality in SDHD variant carriers compared with the general population." In: *Eur. J. Hum. Genet.* 23.12 (2015), pp. 1713–6.
67. J.-P. Bayley, R. a. Oldenburg, J. Nuk, et al. "Paraganglioma and pheochromocytoma upon maternal transmission of SDHD mutations." In: *BMC Med. Genet.* 15.1 (2014), p. 111.
68. E. F. Hensen, E. S. Jordanova, I. J. H. M. van Minderhout, et al. "Somatic loss of maternal chromosome 11 causes parent-of-origin-dependent inheritance in SDHD-linked paraganglioma and phaeochromocytoma families." In: *Oncogene* 23.23 (2004), pp. 4076–4083.
69. A. S. Hoekstra, P. Devilee, and J.-P. Bayley. "Models of parent-of-origin tumorigenesis in hereditary paraganglioma". In: *Semin. Cell Dev. Biol.* (2015), pp. 1–8.

70. J. P. Bayley, I. van Minderhout, P. C. W. Hogendoorn, et al. "Sdhd and Sdhd/H19 knockout mice do not develop paraganglioma or pheochromocytoma". In: *PLoS One* 4.11 (2009), pp. 1–7.
71. A. S. Hoekstra, R. D. Addie, C. Ras, et al. "Parent-of-origin tumorigenesis is mediated by an essential imprinted modifier in SDHD -linked paragangliomas: SLC22A18 and CDKN1C are candidate tumor modifiers". In: *Hum. Mol. Genet.* 25.17 (2016), ddw218.
72. A. S. Hoekstra, E. F. Hensen, E. S. Jordanova, and E. Korpershoek. "Loss of maternal chromosome 11 is a signature event in SDHAF2 , SDHD , and VHL -related paragangliomas , but less significant in SDHB -related paragangliomas". In: (2017).
73. D. E. Benn, A. P. Gimenez-Roqueplo, J. R. Reilly, et al. "Clinical presentation and penetrance of pheochromocytoma/paraganglioma syndromes". In: *J. Clin. Endocrinol. Metab.* 91.3 (2006), pp. 827–836.
74. C. J. Ricketts, J. R. Forman, E. Rattenberry, et al. "Tumor risks and genotype-phenotype-proteotype analysis in 358 patients with germline mutations in SDHB and SDHD". In: *Hum. Mutat.* 31.1 (2010), pp. 41–51.
75. E. F. Hensen, J. C. Jansen, M. D. Siemers, et al. "The Dutch founder mutation SDHD.D92Y shows a reduced penetrance for the development of paragangliomas in a large multigenerational family." In: *Eur. J. Hum. Genet.* 18.1 (2010), pp. 62–66.
76. P. Xekouki, K. Pacak, M. Almeida, et al. "Succinate dehydrogenase (SDH) D subunit (SDHD) inactivation in a growth-hormone-producing pituitary tumor: A new association for SDH?" In: *J. Clin. Endocrinol. Metab.* 97.3 (2012), pp. 357–366.
77. J. A. Carney and C. A. Stratakis. "Familial paraganglioma and gastric stromal sarcoma: A new syndrome distinct from the Carney triad". In: *Am. J. Med. Genet.* 108.2 (2002), pp. 132–139.
78. L. T. van Hulsteijn, O. M. Dekkers, F. J. Hes, J. W. A. Smit, and E. P. M. Corssmit. "Risk of malignant paraganglioma in SDHB-mutation and SDHD-mutation carriers: a systematic review and meta-analysis". In: *J. Med. Genet.* (2012), pp. 768–776.
79. C. C. Boedeker, E. F. Hensen, H. P. H. Neumann, et al. "Genetics of hereditary head and neck paragangliomas." In: *Head Neck* 36.6 (2014), pp. 907–16.
80. S. Woolen and J. J. Gemmete. "Paragangliomas of the Head and Neck." In: *Neuroimaging Clin. N. Am.* 26.2 (2016), pp. 259–78.
81. C. C. Boedeker. "Paragangliomas and paraganglioma syndromes." In: *GMS Curr. Top. Otorhinolaryngol. Head Neck Surg.* 10 (2011), Doc03.
82. R. van den Berg. "Imaging and management of head and neck paragangliomas". In: *Eur. Radiol.* 15.7 (2005), pp. 1310–1318.
83. V. L. Martucci and K. Pacak. "Pheochromocytoma and paraganglioma: Diagnosis, genetics, management, and treatment". In: *Curr. Probl. Cancer* 38.1 (2014).
84. D. E. Benn, B. G. Robinson, and R. J. Clifton-Bligh. "15 Years of paraganglioma: Clinical manifestations of paraganglioma syndromes types 1-5." In: *Endocr. Relat. Cancer* 22.4 (2015), T91–103.
85. J. Barron. "Phaeochromocytoma: diagnostic challenges for biochemical screening and diagnosis." In: *J. Clin. Pathol.* 63.8 (2010), pp. 669–74.

86. N. van Duinen, D. Steenvoorden, I. P. Kema, et al. "Increased urinary excretion of 3-methoxytyramine in patients with head and neck paragangliomas". In: *J. Clin. Endocrinol. Metab.* 95.1 (2010), pp. 209–214.
87. R. Van Den Berg, A. Schepers, F. T. De Bruïne, et al. "The value of MR angiography techniques in the detection of head and neck paragangliomas". In: *Eur. J. Radiol.* 52.3 (2004), pp. 240–245.
88. W. R. Shamblin, W. H. ReMine, S. G. Sheps, and E. G. Harrison. "Carotid body tumor (chemodectoma). Clinicopathologic analysis of ninety cases." In: *Am. J. Surg.* 122.6 (1971), pp. 732–9.
89. J. L. Netterville, C. G. Jackson, F. R. Miller, J. R. Wanamaker, and M. E. Glasscock. "Vagal paraganglioma: a review of 46 patients treated during a 20-year period." In: *Arch. Otolaryngol. Head. Neck Surg.* 124.10 (1998), pp. 1133–40.
90. U. Fisch. "Infratemporal fossa approach for glomus tumors of the temporal bone." In: *Ann. Otol. Rhinol. Laryngol.* 91.5 Pt 1 (1982), pp. 474–9.
91. A. Archier, A. Varoquaux, P. Garrigue, et al. "Prospective comparison of 68Ga-DOTATATE and 18F-FDOPA PET/CT in patients with various pheochromocytomas and paragangliomas with emphasis on sporadic cases". In: *Eur. J. Nucl. Med. Mol. Imaging* 43.7 (2016), pp. 1248–1257.
92. J.-P. Guichard, N. Fakhry, J. Franc, P. Herman, C.-A. Righini, and D. Taieb. "Morphological and functional imaging of neck paragangliomas". In: *Eur. Ann. Otorhinolaryngol. Head Neck Dis.* (2016).
93. T. Anttila, V. Häyry, T. Nicoli, et al. "A two-decade experience of head and neck paragangliomas in a whole population-based single centre cohort." In: *Eur. Arch. Otorhinolaryngol.* 272.8 (2015), pp. 2045–53.
94. A. G. van der Mey, J. C. Jansen, and J. M. van Baalen. "Management of carotid body tumors." In: *Otolaryngol. Clin. North Am.* 34.5 (2001), pp. 907–24, vi.
95. E. M. Van Schothorst, M. Beekman, P. Torremans, et al. "Paragangliomas of the head and neck region show complete loss of heterozygosity at 11q22-q23 in chief cells and the flow-sorted DNA aneuploid fraction". In: *Hum. Pathol.* 29.10 (1998), pp. 1045–1049.
96. P. B. Douwes Dekker, W. E. Corver, P. C. W. Hogendoom, A. G. L. van der Mey, and C. J. Cornelisse. "Multiparameter DNA flow-sorting demonstrates diploidy and SDHD wild-type gene retention in the sustentacular cell compartment of head and neck paragangliomas: Chief cells are the only neoplastic component". In: *J. Pathol.* 202.4 (2004), pp. 456–462.
97. F. H. van Nederveen, J. Gaal, J. Favier, et al. "An immunohistochemical procedure to detect patients with paraganglioma and phaeochromocytoma with germline SDHB, SDHC, or SDHD gene mutations: a retrospective and prospective analysis." In: *Lancet. Oncol.* 10.8 (2009), pp. 764–71.
98. J. H. Lee, F. Barich, L. H. Karnell, et al. "National cancer data base report on malignant paragangliomas of the head and neck". In: *Cancer* 94.3 (2002), pp. 730–737.
99. P. De Wailly, L. Oragano, F. Radé, et al. "Malignant pheochromocytoma: New malignancy criteria". In: *Langenbeck's Arch. Surg.* 397.2 (2012), pp. 239–246.

100. D. J. Pinato, R. Ramachandran, S. T. K. Toussi, et al. "Immunohistochemical markers of the hypoxic response can identify malignancy in phaeochromocytomas and paragangliomas and optimize the detection of tumours with VHL germline mutations." In: *Br. J. Cancer* 108.2 (2013), pp. 429–37.

101. K. E. van der Bogt, M.-P. F. M. Vrancken Peeters, J. M. van Baalen, and J. F. Hamming. "Resection of carotid body tumors: results of an evolving surgical technique." In: *Ann. Surg.* 247.5 (2008), pp. 877–884.

102. M. P. M. Paridaans, K. E. A. Van Der Bogt, J. C. Jansen, et al. "Results from craniocaudal carotid body tumor resection: Should it be the standard surgical approach?" In: *Eur. J. Vasc. Endovasc. Surg.* 46.6 (2013), pp. 624–629.

103. C. Suárez, J. P. Rodrigo, W. M. Mendenhall, et al. "Carotid body paragangliomas: a systematic study on management with surgery and radiotherapy." In: *Eur. Arch. Otorhinolaryngol.* 271.1 (2014), pp. 23–34.

104. K. Hu and M. S. Persky. "Treatment of Head and Neck Paragangliomas." In: *Cancer Control* 23.3 (2016), pp. 228–41.

105. M. L. Carlson, A. D. Sweeney, S. Pelosi, G. B. Wanna, M. E. Glasscock, and D. S. Haynes. "Glomus Tympanicum: A Review of 115 Cases over 4 Decades." In: *Otolaryngol. Head. Neck Surg.* 152.1 (2015), pp. 136–42.

106. C. Suárez, J. P. Rodrigo, C. C. Bödeker, et al. "Jugular and vagal paragangliomas: Systematic study of management with surgery and radiotherapy." In: *Head Neck* 35.8 (2013), pp. 1195–204.

107. D. S. Hoyne, S. E. Mowry, and M. R. Hansen. "Canal wall reconstruction and conductive hearing preservation for temporal bone paraganglioma." In: *Laryngoscope* 126.4 (2016), pp. 988–91.

108. G. De Toma, V. Nicolanti, M. Plocco, et al. "Baroreflex failure syndrome after bilateral excision of carotid body tumors: an underestimated problem." In: *J. Vasc. Surg.* 31.4 (2000), pp. 806–810.

109. Z. Erlic and H. P. H. Neumann. "Familial pheochromocytoma". In: *Hormones* 8.1 (2009), pp. 29–38.

110. R. Ramachandran and V. Rewari. "Current perioperative management of pheochromocytomas." In: *Indian J. Urol.* 33.1 (2017), pp. 19–25.

111. R. S. Jackson, J. a. Myhill, T. a. Padhya, J. C. McCaffrey, T. V. McCaffrey, and R. S. Mhaskar. "The Effects of Preoperative Embolization on Carotid Body Paraganglioma Surgery: A Systematic Review and Meta-analysis." In: *Otolaryngol. Head. Neck Surg.* 153.6 (2015), pp. 943–50.

112. G. J. Spector, J. Compagno, C. A. Perez, R. H. Maisel, and J. H. Ogura. "Glomus jugulare tumors: effects of radiotherapy." In: *Cancer* 35.5 (1975), pp. 1316–21.

113. L. T. Van Hulsteijn, E. P. M. Corssmit, I. E. M. Coremans, J. W. A. Smit, J. C. Jansen, and O. M. Dekkers. "Regression and local control rates after radiotherapy for jugulotympanic paragangliomas: Systematic review and meta-analysis". In: *Radiother. Oncol.* 106.2 (2013), pp. 161–168.

114. A. G. van der Mey, J. H. Frijns, C. J. Cornelisse, et al. "Does intervention improve the natural course of glomus tumors? A series of 108 patients seen in a 32-year period." In: *Ann. Otol. Rhinol. Laryngol.* 101.8 (1992), pp. 635–42.

115. J. C. Jansen, R. van den Berg, A. Kuiper, A. G. van der Mey, A. H. Zwinderman, and C. J. Cornelisse. "Estimation of growth rate in patients with head and neck paragangliomas influences the treatment proposal." In: *Cancer* 88.12 (2000), pp. 2811–2816.

116. A. Langerman, S. M. Athavale, S. V. Rangarajan, R. J. Sinard, and J. L. Netterville. "Natural History of Cervical Paragangliomas: Outcomes of Observation of 43 Patients". In: *Arch. Otolaryngol. - Head Neck Surg.* 138.4 (2012), pp. 341–345.

117. S. C. Prasad, H. A. Mimoune, F. D'Orazio, et al. "The role of wait-and-scan and the efficacy of radiotherapy in the treatment of temporal bone paragangliomas." In: *Otol. Neurotol.* 35.5 (2014), pp. 922–31.

118. M. L. Carlson, A. D. Sweeney, G. B. Wanna, J. L. Netterville, and D. S. Haynes. "Natural History of Glomus Jugulare: A Review of 16 Tumors Managed with Primary Observation". In: *Otolaryngol. – Head Neck Surg.* 152.1 (2014), pp. 98–105.

Berdine L Heesterman, Jean-Pierre Bayley, Carli M Tops , Frederik J Hes, Bernadette T J van Brussel, Eleonora P M Corssmit, Jaap F Hamming, Andel G L van der Mey and Jeroen C Jansen

European Journal of Human Genetics, 2013

2

High prevalence of occult paragangliomas in asymptomatic carriers of SDHD and SDHB gene mutations

Abstract

Background: Hereditary paraganglioma is a benign tumor syndrome with an age-dependent penetrance. Carriers of germline mutations in the SDHB or SDHD genes may develop parasympathetic paragangliomas in the head and neck region or sympathetic catecholamine-secreting abdominal and thoracic paragangliomas (pheochromocytomas). In this study, we aimed to establish paraganglioma risk in 101 asymptomatic germline mutation carriers and evaluate the results of our surveillance regimen.

Methods: Asymptomatic carriers of an SDHD or SDHB mutation were included once disease status was established by MRI diagnosis.

Results: Clinical surveillance revealed a head and neck paraganglioma in 28 of the 47 (59.6%) asymptomatic SDHD mutation carriers. Risk of tumor development was significantly lower in SDHB mutation carriers: 2/17 (11.8%, p= 0.001). Sympathetic paragangliomas were encountered in two SDHD mutation carriers and in one SDHB mutation carrier.

Conclusions: Asymptomatic carriers of an SDHD mutation are at a high risk for occult parasympathetic paraganglioma. SDHB carrier risk is considerably lower, consistent with lower penetrance of SDHB mutations. For both syndromes, the risk of symptomless sympathetic paragangliomas is small.

Introduction

Hereditary paraganglioma syndrome is caused by mutations in genes encoding subunits or cofactors of mitochondrial succinate dehydrogenase (SDH): SDHA, SDHB, SDHC, SDHD or SDHAF2 [1–4]. Mutations of RET, NF1 and VHL have also been noted in rare cases of head and neck paragangliomas [5]. The penetrance of SDHD-related paragangliomas is modulated by genomic imprinting, resulting in an almost complete absence of disease following maternal transmission. Paternal transmission is associated with incomplete penetrance (43–100%) [6]. Head and neck paragangliomas and multiple concurrent paragangliomas are most frequently observed in SDHD-linked cases, whereas extra-adrenal abdominal and thoracic (sympathetic) paragangliomas are most frequently found in SDHB-linked cases. In addition, mutations in SDHB, SDHC and SDHD, but not in SDHAF2, are associated with the development of adrenal pheochromocytomas. Malignancy, defined as metastatic paraganglioma, can occur in SDHD-linked patients but is most common in SDHB mutation carriers [7, 8]. We have offered genetic testing to asymptomatic relatives of patients with SDHD mutations at Leiden University Medical Center (LUMC) since 2002, and more recently, for SDHB, SDHC or SDHAF2 mutations. We have now evaluated the outcome of SDHD/SDHB testing and surveillance, with the aim of establishing the prevalence of paragangliomas in asymptomatic carriers.

Methods

The database of the Laboratory for Diagnostic Genome Analysis (LDGA) of the Leiden University Medical Center (LUMC) was used to identify asymptomatic carriers of a known mutation in SDHD or SDHB. Subsequently, relevant clinical parameters were derived from the records of the Departments of ENT and Endocrinology (LUMC).

An MRI scan (3D/TOF with gadolinium) was considered the gold standard for diagnosis of head and neck paragangliomas. For the diagnosis of sympathetic paragangliomas, catecholamines and their *O*-methylated metabolites were measured as described by Havekes et al. and, if elevated, were followed by MRI or CT scans of the thorax and abdomen and, when positive for a suspected sympathetic paraganglioma, by MIBG-scintigraphy [9].

A χ^2-test was used to analyze the association between mutation type and the number of parasympathetic paragangliomas. A two-sided Fisher's exact test and a Mantel-Haenszel test were used to compare SDHD and SDHB carriers.

Results

From 2002 to 2011, 294 asymptomatic relatives underwent genetic testing, and 101 were found to carry an SDHD or SDHB mutation. An additional history taken during the first visit to the ENT clinic revealed that four subjects had existing symptoms before genetic testing and were thus excluded. Another 16 persons inherited an SDHD mutation via the maternal line and were therefore not considered to be at risk for paragangliomas. In addition, disease status could not be established in 17 cases due to a lack of MRI screening, including seven SDHB mutation carriers who declined further examination following genetic counseling. Disease status was established in the remaining 64 asymptomatic cases, including 47 SDHD carriers and 17 SDHB carriers.

SDHD mutation carriers

Following physical examination, six of the 47 SDHD mutation carriers were suspect for head and neck paraganglioma, and the diagnosis was confirmed by MRI. An additional 22 patients carrying a total of 57 tumors (38 carotid body, 17 vagal body and 2 jugulotympanic tumors) were identified by MRI. Thus, a head and neck paraganglioma was found in 59.6% of asymptomatic SDHD carriers and multiple tumors were seen in 34%. A sympathetic paraganglioma was diagnosed in two patients (4.3%). Although the sample size was too small to show significance, individuals with c.416T>C, p.Leu139Pro mutation were affected more often, and with multiple tumors (p = 0.07), compared with those with most common mutation (c.274G>T, p.Asp92Tyr) (table 2.0.1).

Table 2.0.1: Mutation type SDHD

Mutation	No tumor	1 tumor	Multiple tumors	Total
c.274G>T, p.Asp92Tyr	17	11	9	37
c.416T>C, p.Leu139Pro	1	0	5	6
c.284T>C, p.Leu95Pro	1	1	2	4
Total	19	12	16	47

A carotid body tumor was resected in three patients, two of whom showed postoperative hypoglossal nerve paresis that improved with time. In one case the superior laryngeal nerve was sacrificed and the other showed accidental accessory nerve paresis. Both patients with a sympathetic paraganglioma were treated surgically without complications.

A "wait and scan" policy was adopted in the other cases, which gave the opportunity to follow the natural course of 28 tumors radiologically. Growth was observed in five tumors (17.9%) during a mean follow-up time of 3.2 ($\pm$ 2.5) years. None of these patients developed symptoms during follow-up.

SDHB mutation carriers

Seventeen asymptomatic SDHB mutation carriers were investigated and MRI identified a vagal body tumor in two carriers (11.8%), significantly less than in SDHD mutation carriers (odds ratio 11.1; 2.3–54.0 95% confidence interval, p = 0.001). These patients and 13 others carried the c.423 + 1G>A splice mutation, while the remaining two had a large deletion affecting exon 3. No association was found between the mutation and type tumor (p = 0.58). An additional sympathetic paraganglioma was found in one patient and was surgically removed without complications.

Discussion

Clinical surveillance of asymptomatic SDHD mutation carriers reveals a high prevalence of occult head and neck paragangliomas, and even multiple tumors may go undetected. No sizable jugulotympanic tumors were found, probably because these tumors give rise to symptoms at an early stage. The relatively large number of affected individuals carrying the c.416T>C, p.Leu139Pro mutation suggests that this mutation may be more penetrant, but larger sample sizes will be necessary to confirm this suspicion.

In contrast to SDHD, SDHB mutations were responsible for asymptomatic head and neck tumors in only 12% of the tested cases, consistent with the low penetrance previously reported [10].

The results presented here support the use of genetic testing and clinical surveillance in families with paraganglioma, not only for the exclusion of disease in genuinely healthy subjects, but also because screening allows the detection and treatment of early-stage

paragangliomas. This may be particularly valid for adrenal and extra-adrenal secreting pheochromocytomas, for which surgery is recommended even in the absence of clinical signs [11]. The uneventful resection of the sympathetic paragangliomas in this study underlines the fact that this is a safe procedure. In contrast, surgery of parasympathetic paragangliomas of the head and neck is associated with cranial nerve injury. These risks must be weighed against the frequently indolent natural course of the disease and a "wait and scan" policy should be considered.

In conclusion, genetic testing facilitates the detection of head and neck paragangliomas in a high proportion of asymptomatic carriers and provides the opportunity to treat patients at an early stage of the disease.

References

1. D. Astuti, F. Latif, A. Dallol, et al. "Gene mutations in the succinate dehydrogenase subunit SDHB cause susceptibility to familial pheochromocytoma and to familial paraganglioma." In: *Am. J. Hum. Genet.* 69.1 (2001), pp. 49–54.
2. B. E. Baysal, R. E. Ferrell, J. E. Willett-Brozick, et al. "Mutations in SDHD, a mitochondrial complex II gene, in hereditary paraganglioma." In: *Science* 287.5454 (2000), pp. 848–851.
3. H.-X. Hao, O. Khalimonchuk, M. Schraders, et al. "SDH5, a gene required for flavination of succinate dehydrogenase, is mutated in paraganglioma." In: *Science* 325.5944 (2009), pp. 1139–42.
4. S. Niemann and U. Müller. "Mutations in SDHC cause autosomal dominant paraganglioma, type 3." In: *Nat. Genet.* 26.3 (2000), pp. 268–270.
5. G. Opocher and F. Schiavi. "Genetics of pheochromocytomas and paragangliomas". In: *Best Pract. Res. Clin. Endocrinol. Metab.* 24.6 (2010), pp. 943–956.
6. E. F. Hensen, J. C. Jansen, M. D. Siemers, et al. "The Dutch founder mutation SDHD.D92Y shows a reduced penetrance for the development of paragangliomas in a large multigenerational family." In: *Eur. J. Hum. Genet.* 18.1 (2010), pp. 62–66.
7. H. P. M. Kunst, M. H. Rutten, J. P. De Mönnink, et al. "SDHAF2 (PGL2-SDH5) and hereditary head and neck paraganglioma". In: *Clin. Cancer Res.* 17.2 (2011), pp. 247–254.
8. H. P. H. Neumann, C. Pawlu, M. Peczkowska, et al. "Distinct clinical features of paraganglioma syndromes associated with SDHB and SDHD gene mutations." In: *JAMA* 292.8 (2004), pp. 943–51.
9. B. Havekes, A. A. van Der Klaauw, M. M. Weiss, et al. "Pheochromocytomas and extra-adrenal paragangliomas detected by screening in patients with SDHD-associated head-and-neck paragangliomas". In: *Endocr. Relat. Cancer* 16.2 (2009), pp. 527–536.
10. F. J. Hes, M. M. Weiss, S. A. Woortman, et al. "Low penetrance of a SDHB mutation in a large Dutch paraganglioma family". In: *BMC Med. Genet.* 11.1 (2010), p. 92.
11. "NIH state-of-the-science statement on management of the clinically inapparent adrenal mass ("incidentaloma")." In: *NIH Consens. State. Sci. Statements* 19.2 (2002), pp. 1–25.

Berdine L Heesterman, Berit M Verbist, Andel G L van der Mey, Jean-Pierre Bayley, Eleonora P M Corssmit, Frederik J Hes and Jeroen C Jansen

Clinical Otolaryngology, 2016

3

Measurement of head and neck paragangliomas: is volumetric analysis worth the effort? A method comparison study

Abstract

Background: The aim of this study was to assess the reproducibility of different measurement methods and define the most workable technique for measuring head and neck paragangliomas, to determine the best method for evaluating tumour growth. The evaluation of tumour growth is vital for a "wait and scan" policy, a management strategy that became increasingly important.

Study design: Method comparison study.

Setting and participants: Thirty tumours, including carotid body, vagal body, jugulotympanic tumours and conglomerates of multiple tumours, were measured in duplicate, using linear dimensions, manual area tracing and an automated segmentation method.

Main outcome measures: Reproducibility was assessed using the Bland-Altman method.

Results: The smallest detectable difference using the linear dimension method was 11% for carotid body and 27% for vagal body tumours, compared with 17% and 20% for the manual area tracing method. Due to the irregular shape of paragangliomas in the temporal bone and conglomerates, the manual area tracing method showed better results in these tumours (26% and 8% versus 54% and 47%). The linear dimension method was significantly faster (median 4.27 versus 18.46 minutes, $p < 0.001$). The automatic segmentation method yielded smallest detectable differences between 39% and 75%, and although fast (2.19 ± 1.49 minutes), it failed technically.

Conclusions: Due to a relatively good reproducibility, fast and easy application, we found the linear dimension method to be the most pragmatic approach for evaluation of growth of carotid and vagal body paragangliomas. For jugulotympanic tumours, the preferred method is manual area tracing. However, volumetric changes of these tumours may be of less clinical importance than changes in relation to surrounding anatomical structures.

Introduction

Head and neck paragangliomas are neuroendocrine tumours related to the parasympathetic nervous system. Approximately 35% of head and neck paragangliomas are associated with hereditary syndromes. Mutations in subunit-D of the succinate dehydrogenase gene (SDHD) are the most common [1]. Inheritance of paragangliomas in SDHD-linked families is characterised by parent-of-origin-related tumorigenesis. Development of paragagangliomas after maternal transmission is extremely rare [2].

Surgery is the only definitive treatment for head and neck paragangliomas; however, due to location close to large vessels and lower cranial nerves, resection is challenging. This is especially true for jugular and vagal body paragangliomas; in the latter case, sacrificing the vagus nerve is almost inevitable [3]. Treatment of patients with hereditary syndromes, particularly SDHD-linked cases, is further complicated as these patients often develop multiple head and neck paragangliomas that may grow together and form a conglomerate. In addition, they are at risk for debilitating bilateral lower cranial nerve impairment. With the evolvement of radiotherapy and stereotactic radiosurgery, local control rates vary from 76% to 100% while the complication rate is significantly lower compared to surgery. Although risk of radiation induced malignancy is low, it should be considered, especially in younger patients [3–5].

Surgery and radiotherapy thus carry disadvantages and head and neck paragangliomas generally show a very favourable natural course. This has led our institution, among others, to advocate an initial policy of "watchful waiting". Only tumours that cause complaints, (impending) cranial nerve impairment or exhibit progressive growth are treated. A "wait and scan" strategy is not the first choice in hormonally active and malignant paragangliomas or in case of skull base lesions with significant intracranial extension [1, 3, 4, 6–9].

A "wait and scan" treatment strategy has become increasingly important as pre-symptomatic testing for causative gene defects in family members of paraganglioma patients has increased the detection of very small and predominantly asymptomatic paragangliomas [10].

For the surveillance of these tumours, it is essential to determine whether presumed growth is true tumour progression or could still be explained by measurement variation alone (i.e., reproducibility). Several measurement methods are available for the assessment of tumour volume, these include linear dimension methods, manual area tracing and automated segmentation techniques.

Three previous studies that addressed growth of paragangliomas used linear dimensions [6–8]. However several studies comparing linear dimension methods with volumetric analysis in the assessment of growth of other tumours, for example schwannomas and meningiomas, concluded that volumetric analysis is more accurate [11–14]. Although head and neck paragangliomas are usually well defined, they are not always homogeneously enhancing and due to their hypervascularity often difficult to delineate from carotid arteries and the jugular vein. These features hamper the use of automated techniques and make manual area tracing more laborious.

To the best of our knowledge, no study has yet compared linear dimension measurements and volumetric analysis in head and neck paragangliomas. The aim of this study was to assess the reproducibility of these methods and define the most workable technique for measuring head and neck paragangliomas, taking also practicability into account.

Methods

Ethical considerations

This method comparison study was approved by the review board of the department of Radiology, of the Leiden University Medical Center.

Patients

A database detailing all SDHD mutation carriers tested in the Leiden University Medical Center before 1, July 2012 and their affected family members (obligate SDHD mutation carriers) was ranked by follow-up time. The 10 carotid body paragangliomas, 10 vagal body paragangliomas and 10 jugulotympanic paragangliomas with the longest follow-up were selected. Furthermore, nine conglomerates, consisting of a total of 20 paragangliomas (five conglomerates of carotid and vagal body tumours, two vagal and

jugulotympanic conglomerates and two conglomerates consisting of carotid body, vagal body, and jugulotympanic tumours) were included. The 50 paragangliomas included in this study were from 26 patients, and the most recent MRI scan of the head and neck region was retrospectively analysed.

MRI technique

We used 3D Time of Flight MR angiography with gadolinium, as this method was previously indicated the modality of choice for detection of head and neck paragangliomas [15]. Examinations completed between June 2006 and December 2012 were performed on a 1.5T (Philips Medical Systems, Best, the Netherlands) using a head and neck coil (repetition time/echo time, 21/7 ms; flip angle, 20; slice thickness, 0.75 mm; field of view, 210 mm; matrix, 256 x 256; reconstructed voxel size, 0.82/0.82/0.75 mm) or on a 3T (Philips Medical Systems) using a neurovascular coil (repetition time/echo time, 20/3.5 ms; flip angle, 15; slice thickness, 0.75 mm; field of view, 200 mm; matrix, 384 x 384; reconstructed voxel size, 0.39/0.39/0.75 mm).

Measurements

All measurements were taken twice by a trained first observer (BLH), with an interval of at least 4 days, and subsequently verified and, if necessary, corrected by an experienced head and neck radiologist (BMV, 12.5 years of experience). The time required to take measurements was also recorded, by observer 1 during the second session of measurements.

Tumour volume (cm^3) was calculated using linear dimensions, computer-assisted manual area tracing method and automatic segmentation tool. A Vitrea workstation version 6.0.1540.7188 (Vital images, Minnetonka, Minnesota, USA) was used for all measurements. For the linear dimension method, the largest diameter in the axial plane (A) was measured using a linear digital caliper tool, followed by the diameter perpendicular to A in the same plane (B). Finally, the largest craniocaudal diameter (C) was measured in the sagittal plane (figure 3.0.1 a & b). Tumours were assumed to be ellipsoid and volume was therefore estimated using the equation:

$$Volume(V) = \frac{4}{3}\pi(\frac{1}{2}A * \frac{1}{2}B * \frac{1}{2}C) \tag{3.1}$$

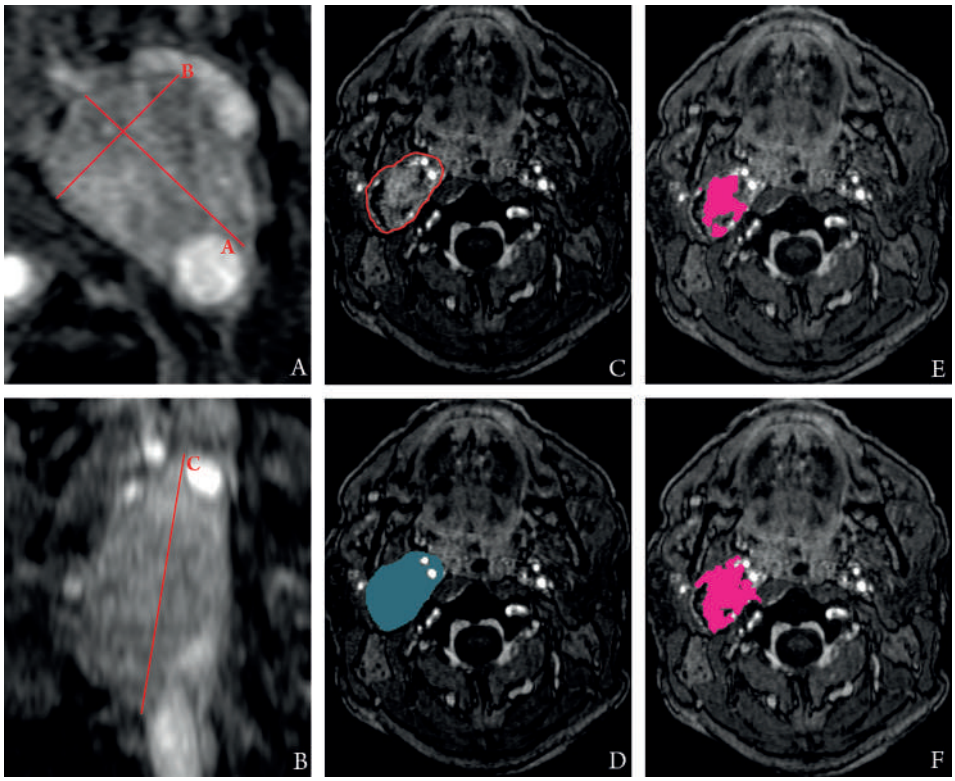

Figure 3.0.1:
Linear dimension measurements (a & b). To estimate volume based on linear dimensions, paragangliomas were considered to have an ellipsoid shape, and consequently, volume was calculated using equation 3.1. *A* is the largest diameter in the axial plane (a), *B* is the diameter perpendicular to *A*, and *C* is the largest craniocaudal diameter measured in the sagittal plane (b).
Manual area tracing method (c & d). As shown, the tumour was manually delineated in the axial plane excluding the main vessels.
Automatic segmentations technique (e & f). These are images of the same tumour as shown in c & d, it clearly illustrates the measurement error associated with the automatic segmentation technique.

Segmentation of the tumour was performed using two methods. Manual segmentation was performed using the computer-assisted free-sculpting tool (Vitrea, Vital Images, Minnetonka, Minnesota, USA). The tumour was manually delineated excluding the main vessels in axial slices using the free-sculpting tool (figure 3.0.1 c & d). Automatic segmentation was performed using a tool provided by Vitrea (Vital Images, Minnetonka, Minnesota, USA). With this tool, the tumour was automatically segmented by selecting a region of interest inside the tumour. Subsequently, the volume of the tumour was calculated based on both segmentation methods.

Statistics

IBM SPSS Statistics version 20.0 (IBM Corp.: Armonk, NY, USA) was used for statistical analysis. The Bland and Altman method was used to assess intra-observer agreement [16]. Relative differences (% differences) rather than absolute differences between two measurements were used, as a small absolute difference may still represent a large percentage of tumour volume in small paragangliomas. Relative differences were calculated as follows:

$$\frac{(measurement1 - measurement2)}{0.5 * (measurement1 + measurement2)} * 100 \tag{3.2}$$

The 95% limits of agreement: mean $\pm$ 1.96 $*$ SD of differences and the smallest detectable difference (SDD): 1.96 $*$ SD of differences were calculated [12, 16–18]. The linear dimension method was compared with the manual area tracing method using a linear mixed model and Wilcoxon signed-rank test. An independent t-test was used to compare the mean time necessary to take measurements. As sample sizes were small, a Shapiro-Wilk test was used to assess normality. A test statistic of $\leq$ 0.9 was considered to be the cut-off value. Finally, equality of variances was assessed by Levene's test of equality ($p < 0.05$). Continuous data are represented as mean $\pm$ SD, unless stated otherwise.

Results

Reproducibility

Intra-observer agreement was objectified for all measurement methods separately. The mean difference between consecutive measurements and the calculated limits of agree-

ment are displayed for carotid body, vagal body, jugulotympanic paragangliomas and conglomerates individually (figure 3.0.2). The Shapiro-Wilk test was used to assess normality of the relative differences of all measurement methods for all tumour categories individually. The test statistic was (approximately) 0.9 in all cases, indicating a normal distribution. The mean and SD of the relative differences were also approximately constant throughout the range of measurements (data not shown); therefore, the limits of agreement were considered to be constant. As shown by similar limits of agreement, the reproducibility of the linear dimension and manual area tracing method were comparable for vagal body and carotid body tumours, whereas the limits of agreement of the automatic segmentation method were wider, indicating an inferior reproducibility. This was also apparent from the calculated smallest detectable differences (SDD), which ranged from 8% to 75% depending on tumour location and measurement method (table 3.0.1). In addition, median tumour volumes of paragangliomas at different locations were estimated using each method; the results are displayed in table 3.0.1.

Technical notes

When calculating tumour volumes based on linear dimensions, paragangliomas were assumed to have an ellipsoid shape. Although this is broadly true for most carotid body tumours and many vagal body tumours, jugulotympanic tumours often do not have a clear geometrical shape. Consequently, conglomerates involving jugulotympanic tumours are often non-ellipsoid. Conglomerates of a carotid and vagal body paraganglioma are more likely to be ellipsoid or double ellipsoid in shape. In the latter case, the volume of both tumours can be measured separately. The linear dimension method was performed with a mean time of 4.27 ± 1.36 min.

The manual area tracing method involves separate review of each image in which the paraganglioma appears; therefore, any judgment errors only affect calculations for that particular image. In addition, this technique allows the inclusion or exclusion of each voxel and therefore provides an opportunity to exclude vessels even when they are surrounded by tumour tissue. However, with a mean time of 18.46 ± 10.67 min, the technique was the most time-consuming.

With a mean time of 2.19 ± 1.49 min, the automatic segmentation technique was the fastest measurement technique. However, as paragangliomas may contain necrotic por-

tions, the technique was (even after selecting several voxels inside the tumour with a different grey scale) frequently unable to select the entire paraganglioma. Furthermore, the provided tool often selected structures outside the tumour, leading to a calculated volume that did not correspond to the actual tumour size (figure 3.0.1 e & f). Because reproducibility was also poor, the technique was not further assessed.

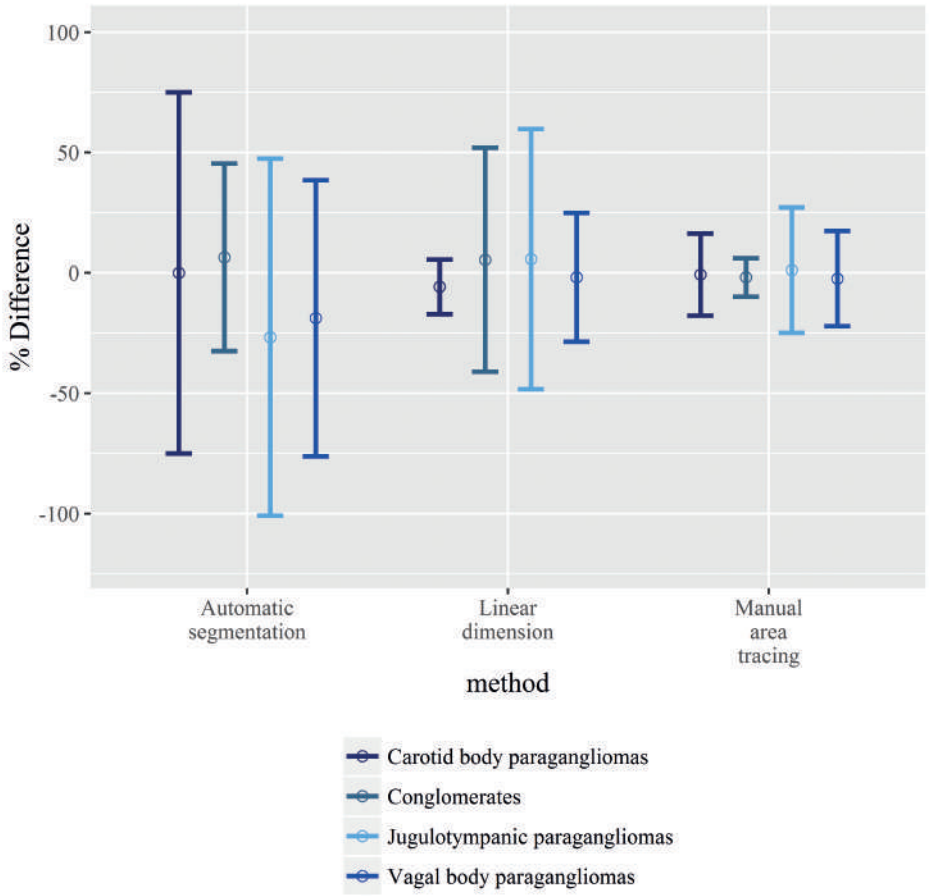

Figure 3.0.2: Reproducibility. Intra-observer agreement assessed by the Bland and Altman method: the mean difference and the 95% limits of agreement (mean $\pm$ 1.96 $*$ SD) are shown for each method. On the x-axis, the different measurement techniques are shown. The y-axis represents the % difference (equation 3.2).

Table 3.0.1: Median estimated volume (cm^3) and smallest detectable difference (SDD, 1.96 * SD of differences).

	Carotid body paragangliomas	Vagal body paragangliomas	Jugulotympanic paragangliomas	Conglomerates
Linear dimension method				
Median volume (cm^3), (range)	5.31 (1.28-27.86)	5.19 (1.88-34.34)	3.08 (0.70- 15.14)	33.97 (21.35-77.03)
Smallest detectable differences (%)	11.4	26.8	54.1	46.5
Manual area tracing method				
Median volume (cm^3), (range)	6.11 (0.81-25.49)	5.65 (2.29-31.96)	2.95 (0.64-13.16)	27.15 (18.37-83.20)
Smallest detectable differences (%)	17.0	19.8	26.0	8.0
Automatic segmentation method				
Median volume (cm^3), (range)	4.31 (0.74-20.85)	5.00 (1.28-23.10)	3.10 (1.22-10.18)	24.43 (15.53-68.72)
Smallest detectable differences (%)	75.0	57.3	74.2	39.0

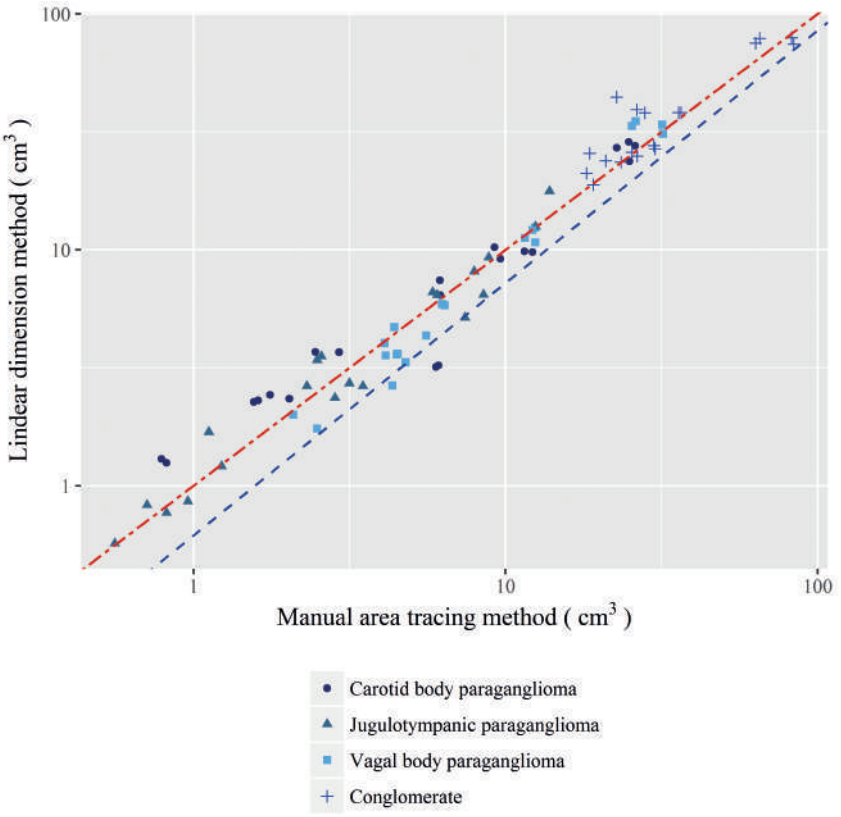

Figure 3.0.3: Linear dimension versus manual area tracing method. The values on the y-axis represent the measurements obtained by the linear dimension method, and the values on the x-axis represent the measurements obtained by the manual area tracing method. With the fitted regression line (blue line; $y = 1.07x - 0.21$) and the line of equality (red line; $y = x + 0$)

Linear dimension versus manual area tracing method

The linear dimension method was compared with the manual area tracing method using a linear mixed model, resulting in a fitted regression line with the following equation: $y = 1.07x - 0.21$. As the 95% confidence interval (CI) of the slope was -1.6-1.1 and the 95% CI of the intercept was 1.0-1.1, the fitted regression line resembled the line of equality ($y = x + 0$) (figure 3.0.3). Furthermore, there was no significant difference between the median volume estimated by the manual area tracing and linear dimension method, 7.68 (0.64-83.20) cm^3 and 6.93 (0.70-77.03) cm^3 (p = 0.332), respectively. A

significant difference was found in the variance of measurements ($p = 0.013$). However, if only carotid and vagal body tumours were analysed, the variance of measurement did not differ significantly ($p = 0.57$). With a mean time of 4.27 ± 1.36 min, the linear dimension method was significantly faster ($p < 0.001$).

Discussion

Since a "wait and scan" policy was first introduced in the early nineties as alternative management strategy for head and neck paragangliomas, it became more important with the increasing detection of very small paragangliomas following pre-symptomatic screening. Although tumour progression is not the only reason to treat these tumours, the decision to resort to surgery or radiotherapy of head and neck paragangliomas is often determined by tumour growth [10, 19, 20].

Understanding the practicability and reproducibility of measurement methods that estimate tumour volume is of great importance to evaluate growth. Although hardware and scanning techniques (e.g., slice thickness) can influence measurements, this influence is trivial compared to the impact of measurement methods and observer interpretation [21, 22]. In general, the more accurate the method used, the more time-consuming it is. For this study, we compared three methods with differing complexity: estimation of the volume using linear dimensions, manual area tracing and an automated segmentation technique.

Synopsis of key findings and comparison with other studies

The poor reproducibility of the automatic segmentation technique was a particularly disappointing finding. This poor performance was primarily attributable to inhomogeneous enhancement of tumours and to the close proximity of similarly enhancing large vessels. While new techniques and algorithms may be developed to improve (semi) automated methods, in the current setting, they are not (yet) useful in the evaluation of volume and growth of head and neck paragangliomas [23].

The manual area tracing method was the most robust of the three methods investigated, but was also the most time-consuming. For vagal body and carotid body tumours, volume estimates based on the linear dimensions of the tumour and the assumption that these

tumours have an ovoid shape produced intra-observer variability and tumour volumes comparable to manual area tracing but could be performed four times faster. These findings are in line with studies that measured glioblastomas and gliomas [24, 25].

Irregularly shaped tumours are difficult to consistently measure with any method. In the case of jugular paragangliomas, defining the tumour is further hampered by the intimate relationship of the tumour with the jugular bulb, and to a lesser extent, the internal carotid artery; including the jugular bulb in the measurement of tumour volume may reduce the variability but will overestimate tumour volume. For follow-up, this strategy is only useful when the vessel is already encompassed at the time of first imaging. When vessels are initially distinguishable but become gradually involved (as is often the case in head and neck paragangliomas), the inclusion of these vessels in subsequent measurements of tumour volume will result in an exaggerated growth rate. Studies comparing volumetric analysis and linear dimension methods for the measurement of irregularly shaped tumours such as vestibular schwannoma also concluded that volumetric analysis is the most accurate method to evaluate tumour growth [12–14]. These results are in line with our findings; jugular paragangliomas are most reliably measured using the manual area tracing method.

The tumour conglomerates included in this study consisted of vagal body tumours with jugular components. Linear dimension analysis was not suited to these generally dumbbell-shaped conglomerates, but circumferential tracing yielded good results. Linear dimension analysis was more suitable for conglomerates consisting of a carotid body and vagal body paraganglioma as these conglomerates are more likely to be ellipsoid or double ellipsoid in shape. In the latter case, it is often possible to separate the two tumour locations in a slightly arbitrary manner and then apply the linear dimension method.

Our experience is that growth of benign tumours of the head and neck, such as schwannomas, meningiomas and paragangliomas, is often measured in the axial plane only. This can provide a false sense of reassurance, especially as paragangliomas tend to expand in a craniocaudal direction. While the alternative approach of using volumetric measurement is often regarded as being excessively time-consuming, we have shown that measuring in three dimensions in paragangliomas in the neck is fast, reproducible and yields volume estimates similar to manual area tracing methods.

Clinical applicability

The smallest detectable differences of 11.4% for carotid body tumours and 26.8% for vagal body tumours can be used in practice to define the cut-off points to differentiate growth from measurement errors volume increases of 10% and 25%, respectively. Jugular paragangliomas are best measured using manual area tracing, which also shows a 25% error. It is important to realise that MRI images carry a substantial measurement error; therefore, the use of tumour growth as the sole indicator for surgery means that a longer observation period will be needed to confirm tumour progression. Consequently, growth can easily be overlooked if comparison is only made between subsequent MRI scans; therefore, the most recent image should also be compared with the first (digitally) available scan.

References

1. D. Taïeb, A. Kaliski, C. C. Boedeker, et al. "Current approaches and recent developments in the management of head and neck paragangliomas." In: *Endocr. Rev.* 35.5 (2014), pp. 795–819.
2. J.-P. Bayley, R. a. Oldenburg, J. Nuk, et al. "Paraganglioma and pheochromocytoma upon maternal transmission of SDHD mutations." In: *BMC Med. Genet.* 15.1 (2014), p. 111.
3. C. Suárez, J. P. Rodrigo, C. C. Bödeker, et al. "Jugular and vagal paragangliomas: Systematic study of management with surgery and radiotherapy." In: *Head Neck* 35.8 (2013), pp. 1195–204.
4. R. E. Lieberson, J. R. Adler, S. G. Soltys, C. Choi, I. C. Gibbs, and S. D. Chang. "Stereotactic radiosurgery as the primary treatment for new and recurrent paragangliomas: Is open surgical resection still the treatment of choice?" In: *World Neurosurg.* 77.5-6 (2012), pp. 745–761.
5. C. Suárez, J. P. Rodrigo, W. M. Mendenhall, et al. "Carotid body paragangliomas: a systematic study on management with surgery and radiotherapy." In: *Eur. Arch. Otorhinolaryngol.* 271.1 (2014), pp. 23–34.
6. J. C. Jansen, R. van den Berg, A. Kuiper, A. G. van der Mey, A. H. Zwinderman, and C. J. Cornelisse. "Estimation of growth rate in patients with head and neck paragangliomas influences the treatment proposal." In: *Cancer* 88.12 (2000), pp. 2811–2816.
7. A. Langerman, S. M. Athavale, S. V. Rangarajan, R. J. Sinard, and J. L. Netterville. "Natural History of Cervical Paragangliomas: Outcomes of Observation of 43 Patients". In: *Arch. Otolaryngol. - Head Neck Surg.* 138.4 (2012), pp. 341–345.
8. M. L. Carlson, A. D. Sweeney, G. B. Wanna, J. L. Netterville, and D. S. Haynes. "Natural History of Glomus Jugulare: A Review of 16 Tumors Managed with Primary Observation". In: *Otolaryngol. – Head Neck Surg.* 152.1 (2014), pp. 98–105.
9. S. Manolidis, J. A. Shohet, C. G. Jackson, and M. E. Glasscock. "Malignant glomus tumors." In: *Laryngoscope* 109.1 (1999), pp. 30–34.
10. B. L. Heesterman, J. P. Bayley, C. M. Tops, et al. "High prevalence of occult paragangliomas in asymptomatic carriers of SDHD and SDHB gene mutations." In: *Eur. J. Hum. Genet.* 21.4 (2013), pp. 469–70.
11. S. Oya, S.-H. Kim, B. Sade, and J. H. Lee. "The natural history of intracranial meningiomas." In: *J. Neurosurg.* 114.5 (2011), pp. 1250–1256.
12. R. Van De Langenberg, B. J. De Bondt, P. J. Nelemans, B. G. Baumert, and R. J. Stokroos. "Follow-up assessment of vestibular schwannomas: Volume quantification versus two-dimensional measurements". In: *Neuroradiology* 51.8 (2009), pp. 517–524.
13. P. C. Walz, M. L. Bush, Z. Robinett, C. F. E. Kirsch, and D. B. Welling. "Three-Dimensional Segmented Volumetric Analysis of Sporadic Vestibular Schwannomas: Comparison of Segmented and Linear Measurements". In: *Otolaryngol. – Head Neck Surg.* 147.4 (2012), pp. 737–743.
14. G. J. Harris, S. R. Plotkin, M. MacCollin, et al. "Three-dimensional volumetrics for tracking vestibular schwannoma growth in neurofibromatosis type II". In: *Neurosurgery* 62.6 (2008), pp. 1314–1319.

15. R. van den Berg. "Imaging and management of head and neck paragangliomas". In: *Eur. Radiol.* 15.7 (2005), pp. 1310–1318.
16. J. M. Bland and D. G. Altman. *Statistical methods for assessing agreement between two methods of clinical measurement.* Tech. rep. 8476. 1986, pp. 307–310.
17. H. C. W. de Vet, C. B. Terwee, D. L. Knol, and L. M. Bouter. "When to use agreement versus reliability measures". In: *J. Clin. Epidemiol.* 59.10 (2006), pp. 1033–1039.
18. K. Dewitte, C. Fierens, D. Stöckl, and L. M. Thienpont. "Application of the Bland-Altman plot for interpretation of method-comparison studies: A critical investigation of its practice". In: *Clin. Chem.* 48.5 (2002), pp. 799–801.
19. J. B. Farrior. "Infratemporal approach to skull base for glomus tumors: anatomic considerations." In: *Ann. Otol. Rhinol. Laryngol.* 93.6 Pt 1 (1984), pp. 616–22.
20. A. G. van der Mey, J. H. Frijns, C. J. Cornelisse, et al. "Does intervention improve the natural course of glomus tumors? A series of 108 patients seen in a 32-year period." In: *Ann. Otol. Rhinol. Laryngol.* 101.8 (1992), pp. 635–42.
21. F. S. Luppino, E. Grooters, F. T. de Bruïne, A. H. Zwinderman, and A. G. L. van der Mey. "Volumetrical measurements in vestibular schwannoma, the influence of slice thickness and patient's repositioning." In: *Otol. Neurotol.* 27.7 (2006), pp. 962–968.
22. J. W. Snell, J. Sheehan, M. Stroila, and L. Steiner. "Assessment of imaging studies used with radiosurgery: a volumetric algorithm and an estimation of its error. Technical note." In: *J. Neurosurg.* 104.1 (2006), pp. 157–162.
23. M. Dang, J. Modi, M. Roberts, C. Chan, and J. R. Mitchell. "Validation study of a fast, accurate, and precise brain tumor volume measurement". In: *Comput. Methods Programs Biomed.* 111.2 (2013), pp. 480–487.
24. G. D. Shah, S. Kesari, R. Xu, et al. "Comparison of linear and volumetric criteria in assessing tumor response in adult high-grade gliomas." In: *Neuro. Oncol.* 8.1 (2006), pp. 38–46.
25. M. Y. Wang, J. L. Cheng, Y. H. Han, Y. L. Li, J. P. Dai, and D. P. Shi. "Measurement of tumor size in adult glioblastoma: Classical cross-sectional criteria on 2D MRI or volumetric criteria on high resolution 3D MRI?" In: *Eur. J. Radiol.* 81.9 (2012), pp. 2370–2374.

Berdine L Heesterman, Lisa M H de Pont, Berit M Verbist, Andel G L van der Mey, Eleonora P M Corssmit, Frederik J Hes, Peter Paul G van Benthem and Jeroen C Jansen

Journal of Neurological Surgery Part B: Skull Base, 2017

4

Age and tumor volume predict growth of carotid and vagal body paragangliomas

Abstract

Background: Treatment for head and neck paragangliomas (HNGPL) can be more harmful than the disease. After diagnosis, an initial period of surveillance is often indicated, and surgery or radiotherapy is reserved for progressive disease. With the aim to optimize this "wait and scan" strategy, we studied growth and possible predictors.

Design: A retrospective cohort study was conducted.

Setting: This study was conducted at a tertiary referral center for patients with HNPGL.

Methods: Tumor volume was estimated for 184 SDHD-related carotid and vagal body paragangliomas using sequential MR imaging. Cox regression was used to study predictors of tumor growth.

Results: The estimated fraction of growing tumors ranged from 0.42 after 1 year of follow-up to 0.85 after 11 years. A median growth rate of 10.4 and 12.0 %/year was observed for carotid and vagal body tumors, respectively. Tumor location, initial volume, and age ($p < 0.05$) were included in our prediction model. The probability of growth decreased with increasing age and volume, indicating a decelerating growth pattern.

Conclusions: We created a prediction model (available online), enabling a more individualized "wait and scan" strategy. The favorable natural course of carotid and vagal body paragangliomas was confirmed; although with long follow-up growth will be observed in most cases.

Introduction

Head and neck paragangliomas (HNPGL) are neuroendocrine tumors that arise from paraganglionic tissue associated with the parasympathetic nervous system. The most common location is the carotid body, other locations include the vagal, jugular, tympanic, and aortic bodies. Paragangliomas are often hereditary, in the Netherlands mutations in subunit-D of the succinate dehydrogenase (SDH) gene are the most common [1–3]. Mutations in this gene are associated with the occurrence of multiple head and neck paragangliomas, occasional pheochromocytomas, and a very low frequency of malignant transformation [4, 5]. Surgical resection is the primary treatment of head and neck paragangliomas, but radiotherapy may also be used to gain local control of the disease. However, head and neck paragangliomas generally show a very favorable natural course, and surgery carries a high risk of cranial nerve impairment due to their location near neurovascular structures. Therefore, a "wait and scan" policy is often adopted [6–12]. With the introduction of presymptomatic testing for causative genes, an increasing number of small paragangliomas is detected. For these asymptomatic tumors with no recorded growth, observation may be the best management initially [13]. Surgical or radiation therapy must be considered if evident growth occurs or if the tumor causes debilitating symptoms. To optimize this treatment strategy and further improve counseling of patients and their families, knowledge of the likelihood of (rapid) progression is essential. The natural course of head and neck paragangliomas was addressed in five case series [6–9]. All concluded that many paragangliomas (30 - 65%) remain stable and if progression is observed, growth is very slow [6–9]. However, predictors remain to be determined. Also, we recently defined new cut-off points for growth in carotid (10%) and vagal (25%) body tumors enabling more accurate estimation of tumor progression [14]. On a cohort of 184 SDHD-related head and neck paragangliomas, we studied growth rate and prognostic factors for growth.

Methods

Subjects

The database of the Laboratory for Diagnostic Genome Analysis (LDGA) of the Leiden University Medical Center (LUMC) was used to identify carriers of an SDHD germline

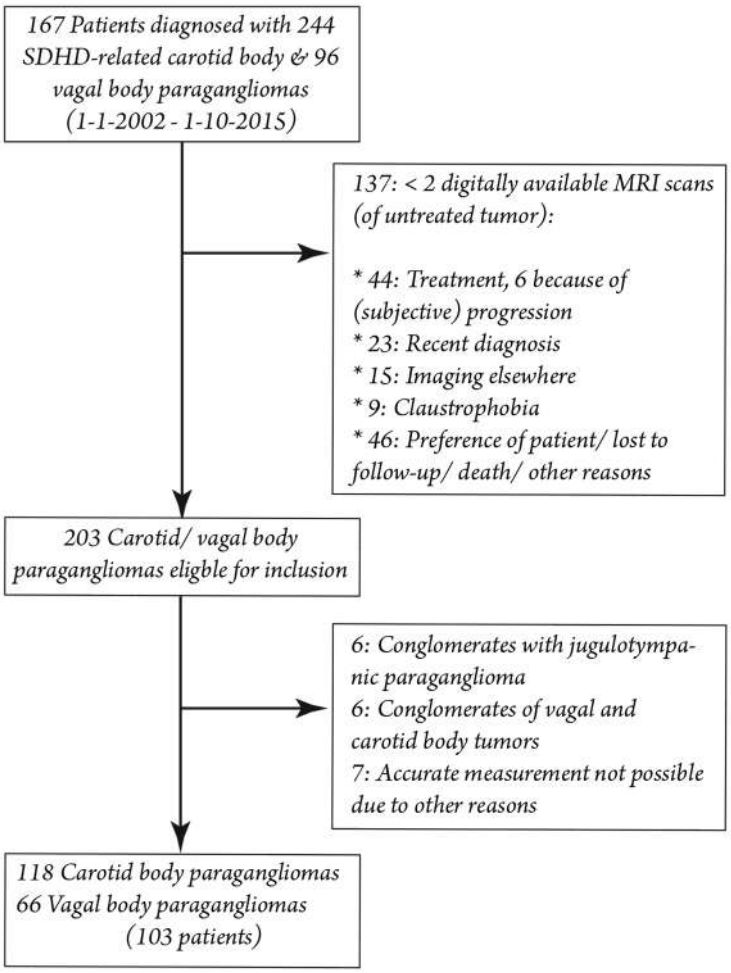

Figure 4.0.1: Carotid and vagal body paragangliomas included in this study

mutation. Subjects with a carrier status confirmed by molecular genetic testing as well as family members affected with paragangliomas (obligate carriers) were both eligible for inclusion if diagnosed with paragangliomas between January 2002 and October 2015. SDHD germline mutation carriers with the carotid body and/or vagal body paragangliomas managed with primary observation, and at least two digital available magnetic resonance imaging (MRI) scans of the head and neck region were selected. MRI scans are digitally available since 2002, to prevent selection bias, only subjects diagnosed since January 2002 were eligible for inclusion. Jugulotympanic tumors were not included as

we previously described that it was difficult to measure these tumors consistently [14]. Conglomerates of carotid and vagal body paragangliomas were measured as two separate tumors if possible, and otherwise excluded (figure 4.0.1). The date of the first digitally available MRI was considered the date of inclusion and time between the first and most recent digitally available MRI scan was considered the follow-up time. Relevant clinical parameters were retrieved from medical records.

According to the Dutch law, approval of the institutional ethics committee was not required, because all data used, were collected for routine patient care.

Volume estimation

At our institution, MRI is used as a diagnostic tool and for follow-up of patients with head and neck paragangliomas. Examinations were performed on 1.5T and 3T scans. Volume was estimated at the first ($T1$) and most recent ($T2$) digitally available MRI, on the contrast enhanced 3D Time of Flight (TOF) MR angiography sequence [14, 15]. Three perpendicular dimensions were used to calculate tumor volume, assuming an ellipsoid shape (figure 3.0.1 a & b).

$$Volume(V) = \frac{4}{3}\pi(\frac{1}{2}A * \frac{1}{2}B * \frac{1}{2}C) \tag{4.1}$$

All measurements were performed by two observers (BLH and LMHP). If measurements at the same time point differed more than the previously determined smallest detectable difference (10% for carotid body and 25% for vagal body parangliomas), consensus was reached [14]. Otherwise, the mean of both measurements was used for further calculations. Subsequently growth rate was calculated,

$$Growthrate(cm3/year) = \frac{V2 - V1}{T2 - T1} \tag{4.2}$$

$$Growthrate(\%/year) = \frac{1}{V1} * \frac{V2 - V1}{T2 - T1} \tag{4.3}$$

with $V1$ being the estimated volume at $T1$ and $V2$ the estimated volume at $T2$.

Statistics

The Statistical Package for Social Science (IBM SPSS Statistics, version 23.0, Armonk, New York, United States) and R version 3.2.5 were used for statistical analysis [16]. The Kaplan-Meier product limit estimator provided the estimated fraction of growing tumors and median time to growth. Cox proportional hazards regression with grouped jackknife variance estimator, to account for dependence amongst tumors from the same patient, was used to assess the relation between possible predictors and growth [17]. To differentiate growth from measurement error, growth was defined as a volume increase of at least 10% for carotid body and 25% for vagal body tumors [14]. If regression or progression less than the applicable cut-off value was observed, the censoring time was equal to follow-up time. If growth was observed, linear growth between $T1$ and $T2$ was assumed and time to growth (i.e., time to a volume increase of 10% or 25%) was calculated [18]. Age at inclusion, sex, mutation (p.Asp92Tyr versus other mutations in SDHD), initial volume ($V1$), tumor location (carotid versus vagal body paragangliomas) and whether a tumor was symptomatic or asymptomatic at its diagnosis, were considered possible predictors. Initial volume was positively skewed, and therefore $\log_2$ transformed, also natural cubic splines (df = 3) were used to relax the assumption of linearity. The proportional hazards assumption was checked, using scaled Schoenfeld residuals. To appraise the discriminative capability and predictive value, time-dependent receiver operating characteristic (ROC) curves (method: Nearest Neighbor Estimation, span 0.05) were produced and calibration plots (bootstrap cross-validated, with 100 cross-validation steps drawn with replacement, to prevent overfitting) were generated [19, 20]. To assess the relation between the development of new signs or symptoms and initial volume, volume increase and tumor location, a generalized estimation equation approach with robust estimator was used to account for within-patient correlation (exchangeable correlation matrix). Volume increase (cm^3) was positively skewed and for that reason categorized. Growth rate (%/year) of carotid and vagal body tumors, as well as, the initial volume of symptomatic and asymptomatic tumors were compared with a Mann-Whitney U Test. Statistical significance was considered for p-values <0.05. Continuous data are expressed as mean $\pm$ standard deviation if the data follows a normal distribution, if not, the median and interquartile range (IQR) are given unless stated otherwise.

Results

Subjects

A total of 184 paragangliomas, 118 carotid body and 66 vagal body tumors, diagnosed in 103 SDHD germline mutation carriers were included (figure 4.0.1). Overall, 64 (62%) subjects were males, and the median age at inclusion was 37 (range:13-62) years. The majority (80%) carried the c.274G>T, p.Asp92Tyr Dutch founder mutation, the remaining 21 subjects carried other previously described germline mutations in SDHD.

Growth characteristics

In a median follow-up time of 4.7 (IQR: 2.6-6.3) years, growth was observed in 75% of the carotid body (CBT) and 64% of vagal body paragangliomas (VBT). Regression was observed in 5%; the remaining tumors were stable. The median growth rate was 10.4 %/year for carotid body and 12.0%/year for vagal body tumors (p = 0.51). If only progressive tumors were considered, the median growth rate increased to 15.1% and 21.3% per year, for carotid and vagal body tumors, respectively, corresponding to a tumor doubling time of 5.9 and 4.7 years (table 4.0.1). The median time to growth was 1.4 (IQR: 0.5-5.1) years, and the estimated fraction of growing tumors was 0.42 (95% CI: 0.35-0.49) 1 year after inclusion and increased to 0.85 (95% CI: 0.70-0.92) after 11 years (figure 4.0.2).

Overall, 52 tumors were classified as clinically detected, with a lateral neck mass being the most reported symptom. Cranial nerve impairment attributable to tumor progression was observed in nine cases (4.9%), of which one developed during follow-up. The vagus nerve was affected most often. At the date of inclusion, 32% of the carotid body and 27% of vagal body tumors were symptomatic. The median volume of symptomatic tumors was substantially larger compared with asymptomatic tumors, 15.2 cm^3 (IQR: 6.4-24.3) versus 1.9 cm^3 (IQR: 0.7-4.9, p <0.001).

Clinical progression, defined as the progression of existing or development of new signs or symptoms, was reported in 66 cases (35.9%). In 45 cases new signs or symptoms were recorded, while in the remaining 21 cases it concerned progression of existing signs or symptoms. In most cases, it concerned the detection of a neck mass or progression of a

preexisting swelling. Other signs or symptoms, including medial bulging of the lateral pharynx wall, pain or discomfort, and dysphagia, were reported less often. There was a statistically significant relation between initial volume and the development of new signs or symptoms (odds ratio: 1.23, p = 0.04). With increasing volume expansion, new signs or symptoms were reported more often, although this relation was not statistically significant (odds ratio: 1.21 p = 0.07, appendix table 4.0.4). A total of 19 (10%) tumors (13 carotid and 6 vagal body tumors) were treated after *T2*. Conservative management was mainly (74%) discontinued because of evident progression. In the remaining cases, patients' preference was the most important reason for the switch to active treatment.

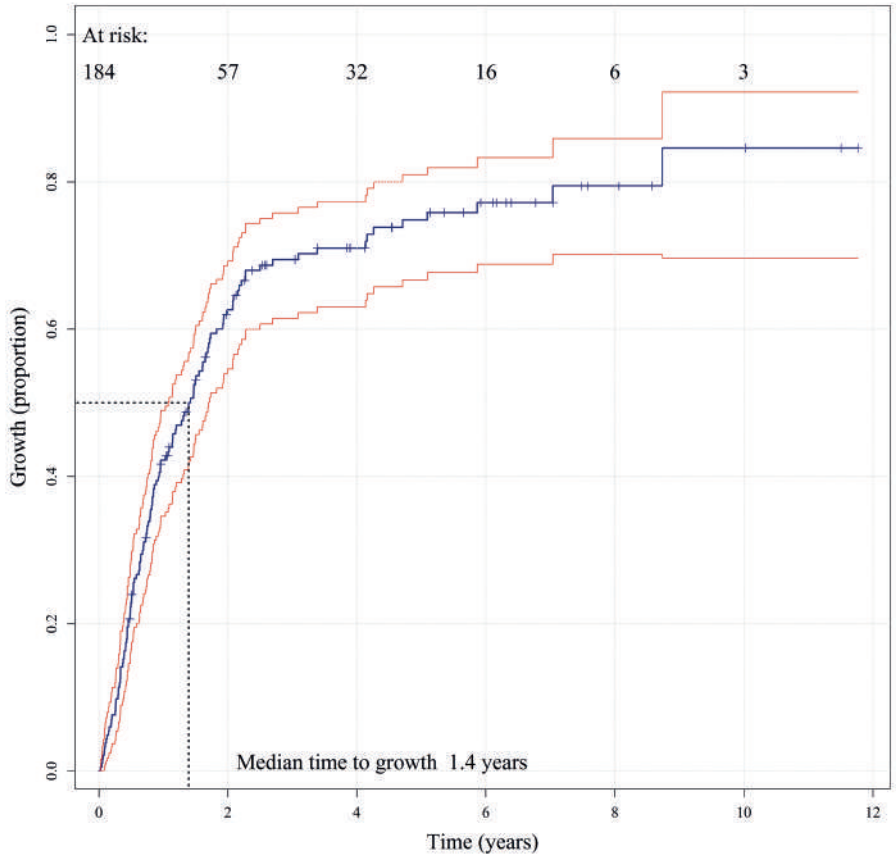

Figure 4.0.2: The cumulative proportion of growing tumors over time, with 95% confidence interval and numbers at risk.

Table 4.0.1: Growth characteristics and descriptives for carotid body tumors (CBT) and vagal body tumors (VBT)

	CBT		VBT	
	Median/N	IQR/%	Median/N	IQR/%
All	118		66	
Male	73	62 %	42	64 %
c.274G> T (p.Asp92Tyr)	89	75 %	52	79 %
Screening detected	82	69 %	50	76 %
Age (years)	37	30-50	40	30-51
Volume (cm^3)	3.0	0.9-9.3	3.8	1.2-16.8
Growth rate (cm^3/year)	0.26	0.05-0.76	0.41	0.08-1.46
Growth rate (%/year)	10.4	3.0-22.7	12.0	3.6-27.7
Growth	88	75 %	42	64 %
Male	55	62 %	27	64 %
c.274G> T (p.Asp92Tyr)	67	76 %	33	79 %
Screening detected	62	70 %	32	76 %
Age (years)	37	30-50	38	30-47
Volume (cm^3)	2.5	0.8-8.1	3.8	1.1-11.3
Growth rate (cm^3/year)	0.35	0.18-1.17	0.72	0.27-1.97
Growth rate (%/year)	15.1	6.8-30.0	21.3	12.3-35.3
T_d (years)	5.9	3.5-11.2	4.7	3.6-7.3
Stable	22	19 %	23	35 %
Regression	8	7 %	1	2 %

Predictors

At univariate and multivariate analysis tumor location, initial tumor volume (log_2 transformed) and age at inclusion were statistically significant predictors for growth, and were thus included in our prediction model (table 4.0.2). The hazard ratio of age was constant over time. This was however not true for carotid versus vagal body tumors. Therefore, tumor location was included in our prediction model as a stratification factor. Also, volume was nonproportional, but only for values between 0.03 cm^3 and 1.58 cm^3 (boundary to first internal knot), the associated parameter estimate was interpreted as an average effect [21].

Table 4.0.2: Multivariate Cox proportional hazards analysis predicting growth

	Hazard ratio (95% CI)	**p-value**
Age at inclusion [1]*	0.81 (0.69-0.95)	p = 0.01
Volume log_2 transformed *	0.86 (0.79-0.93)	p < 0.001
Location (ref = CBT) [2]*	0.63 (0.44-0.89)	p = 0.01
p.Asp92Tyr vs other SDHD variants (ref = other)	1.17 (0.72-1.91)	p = 0.53
Screening vs clinically detected (ref = screening detected)	1.34 (0.86-2.08)	p = 0.19
Sex (ref = male)	0.97 (0.65-1.46)	p = 0.88

[1] Hazard ratio for a 10-year increase in age
[2] Vagal body versus carotid body paragangliomas
* Included in our prediction model for growth

Prediction of growth

The predicted probability of growth decreased with increasing age and volume, increased over time and was higher for carotid body tumors compared with vagal body tumors (figure 4.0.3). For instance, if growth was predicted for a patient of 60 years with a carotid body tumor of 15 cm^3, the predicted probability of growth (volume increase to at least 16.5 cm^3) was 32% after 1 year of follow-up, 49% after 2 years, and increased to 60% after 5 years. In comparison, for a patient of 20 years with a carotid body tumor of 5 cm^3, the predicted probability of growth (volume increase to at least 5.5 cm^3) was 59%, 78% and 88%, respectively (appendix 4.0.6, an interactive version of the model is available at https://hnpgl.shinyapps.io/growth/).

Model performance

Median predicted probabilities were 35% (range 15 - 97%) for nongrowing tumors and 51% (range 17 - 92%) for growing tumors after the first year of follow-up, corresponding to an area under the curve (AUC) of 0.71. After 3 years of follow-up the median predicted probabilities were 72% (range: 41 - 100%) and 60% (range: 42 - 92%) for growing and nongrowing tumors, respectively (AUC: 0.64, figure 4.0.4a-b).

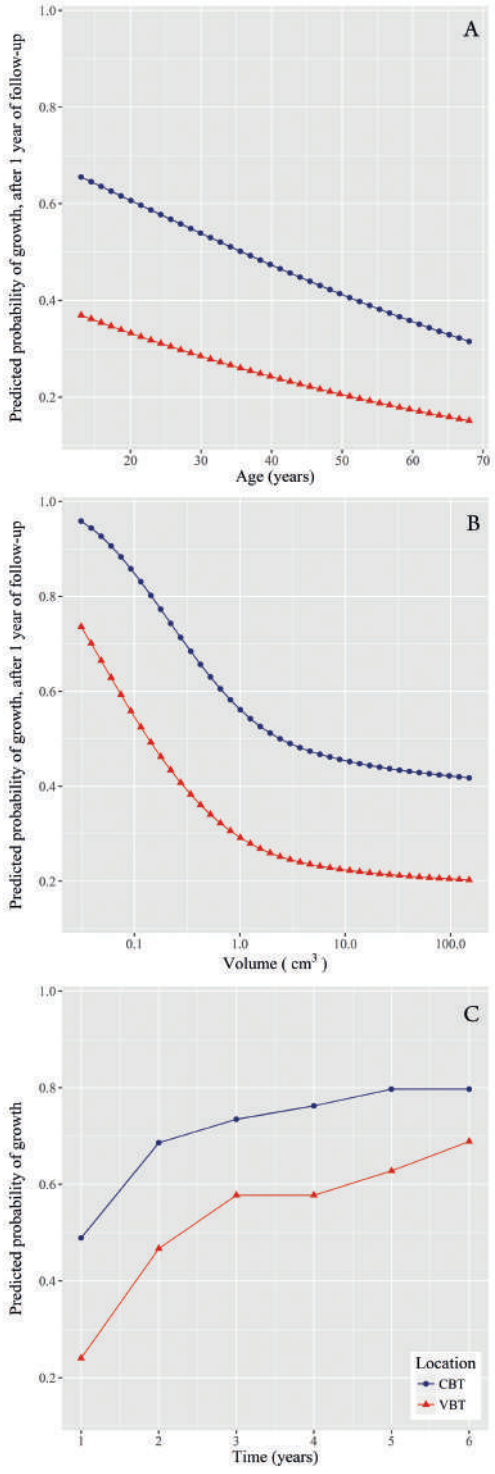

Figure 4.0.3: With increasing age and volume, the predicted probability of growth decreases. Figure 3a displays the relation between age (x-axis) and the predicted probability of growth after 1 year of follow-up (y-axis). The effect is illustrated for the median volume of carotid and vagal body paragangliomas (3.0 cm^3 and 3.8 cm^3). The relation between volume (x-axis) and predicted probability (y-axis) is illustrated in figure 3b, and displayed for a median age of 37 and 40 years for carotid and vagal body tumors, respectively. As shown in figure 3c, the predicted probability of growth increases over time (displayed for median values of age and volume).

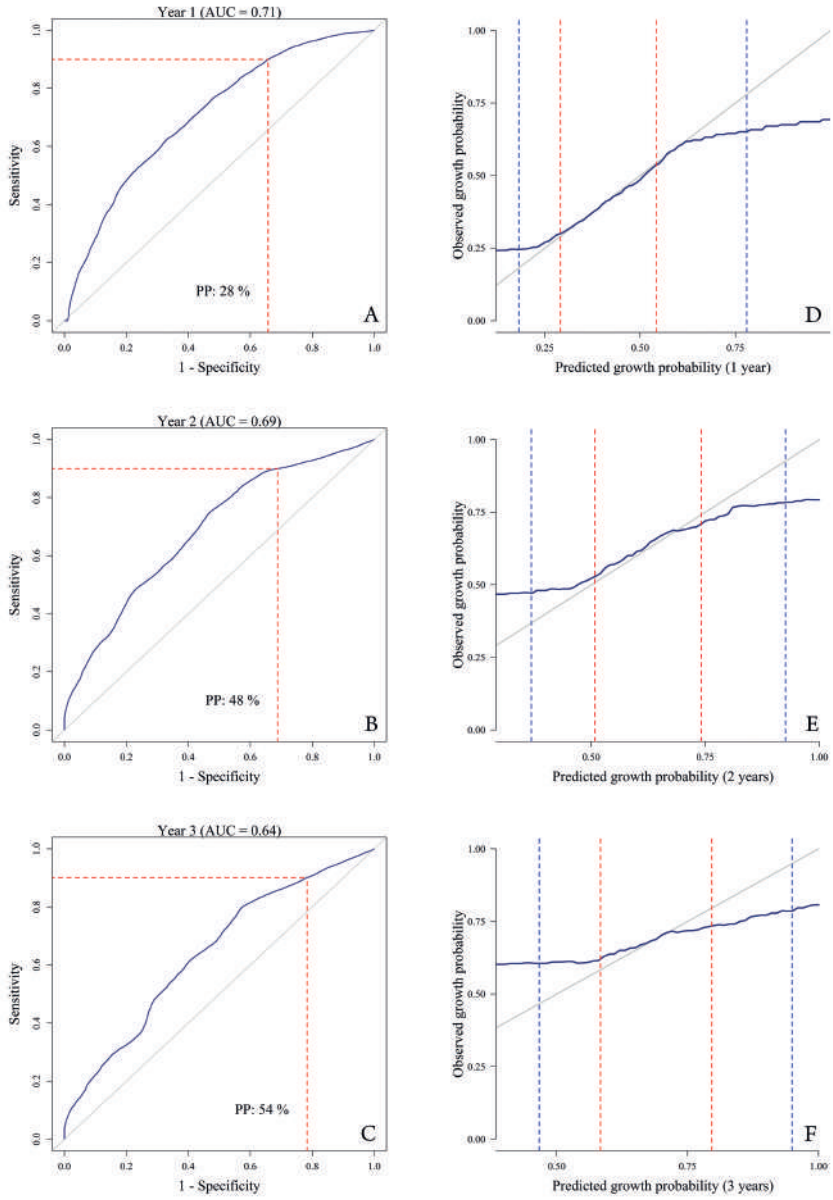

Figure 4.0.4: Time-dependent (after 1, 2, and 3 years of follow-up) ROC curves (figure 4 a-c) with the red lines indicating the 1- specificity and the predicted probability (PP) associated with a sensitivity of 90%. Figure 4 d-f: the corresponding calibration plots with the interquartile range (red lines) and 5th and 95th percentiles (blue dotted lines).

The observed and predicted growth probabilities were approximately equal for the interquartile range, the first 2 years of follow-up but diminished after that (figure 4.0.4 d-f).

Cut-offs for the predicted probability of growth

The consequences of using different cut-off values to make an MRI scan after 1 year of follow-up, with respect to scan reduction as well as number and characteristics of detected and missed growth are shown in table 4.0.3. A similar table with cut-offs for predicted probability after 2 years is provided in the appendix (table 4.0.5). If instead of screening all cases after 1 year, a scan would only be made if the predicted probability is equal to or higher than 34% (corresponding with a sensitivity of 80%), the number of scans would be reduced by 36%. By subsequently using 40% as cut-off value to make an MRI after 2 years (figure 4.0.5), the detection of growth would be delayed with 1 year in 19 cases (17%) and with 2 years in only one case (0.9%). Fast progression, defined as growth of more than 50% per year, was observed in a total of 19 cases and would be detected with 1-year delay in 3 (16%) cases (table 4.0.3 and appendix, table 4.0.6).

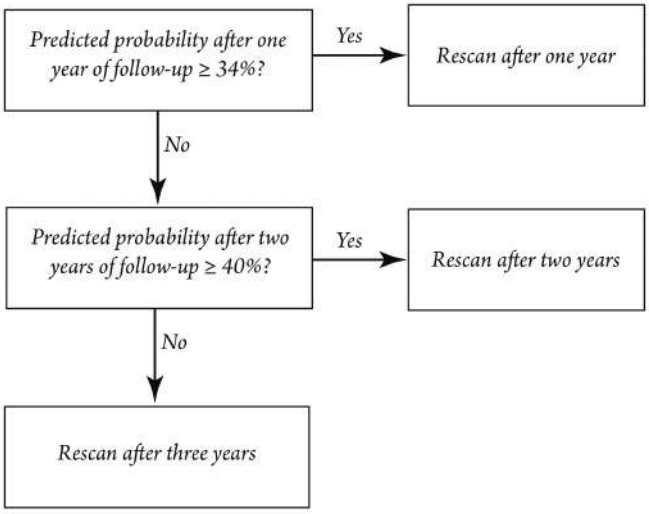

Figure 4.0.5: Screening strategy

Table 4.0.3: Number of detected and missed growth for several cut-offs of predicted probability

Cut-off value PP[1]	Sensitivity	No. of scans	Scan reduction (%)[2]	Detected growth	Missed growth (%)[3]	Detected fast progression [4]	Missed fast progression (%) [4,5]
18	99	171	8 (4)	76	1 (1)	19	0 (0)
24	95	150	29 (16)	73	4 (5)	17	2 (11)
28	90	138	41 (23)	70	7 (9)	16	3 (16)
32	85	125	54 (30)	65	12 (16)	16	3 (16)
34	80	115	64 (36)	62	15 (19)	16	3 (16)
37	75	106	73 (41)	59	18 (23)	15	4 (21)
40	70	93	86 (48)	53	24 (31)	15	4 (21)
42	65	86	93 (52)	51	26 (34)	14	5 (26)
46	60	75	104 (58)	47	30 (39)	13	6 (32)

[1] Cut-off values for predicted probability
[2] After 1 year 179 (97%) cases were still under follow-up
[3] % of total growth
[4] Fast progression is defined as progression > 50% /year
[5] % of total fast progression

Discussion

This study is the first to use multivariate Cox proportional hazards regression to examine the growth of head and neck paragangliomas, and thus factoring in varying follow-up time. We used tumor and measurement specific cut-off values for growth, resulting in a more robust estimation of tumor progression. A perhaps even more significant advantage of the model mentioned earlier is the possibility to study predictors. We found a statistically significant effect of volume, age, and tumor location on the probability of growth and created a prediction model for growth with fairly good discrimination and capability to correctly estimate the likelihood of growth.

With long follow-up growth is observed in most carotid and vagal body tumors, with the estimated fraction of growing tumors ranging from 42% after 1 year of follow-up to 85% after 11 years. However, with a median growth rate of 10.4% and 12.0% per year for carotid and vagal body tumors, respectively, progression is slow, especially in comparison with malignant tumors. In untreated glioblastoma, for instance, a median growth rate of 1.4% per day was observed [22]. Furthermore, cranial nerve impairment was reported in only one case, underlining the indolent natural course and safety of a "wait and scan" strategy. Carotid body tumors are measured more consistently compared with vagal body tumors, resulting in a smaller cut-off value for growth [14]. Consequently, the growth of carotid body tumors was observed earlier during follow-up, despite the higher growth rate of vagal body tumors.

Two earlier studies have addressed the growth of carotid and vagal body tumors; both also concluded that rapid progression is rare [6, 7]. Langerman and colleagues reported tumor growth in only 17 of 47 (38%) paragangliomas, during a mean follow-up time of 5 years. This relatively small percentage, compared with our results, may be partially explained by the comparatively high mean age of 56 (range: 17-86) years. Furthermore, it should be noted that three dimensions were available in only a limited number of cases and it was not clear how they differentiated between progressive and stable tumors. The current results are in agreement with our prior study, with the variation primarily the result of a different definition of growth (20% versus 10% and 25%). Also, the accuracy of measurements has increased as result of improved imaging techniques and digital available images (in our previous study all measurements were performed on hard copies).

Jugulotympanic tumors were not included in our present study. However, the growth of these tumors (Fish C1 to D1) was investigated by Carlson and colleagues [8]. They reported growth, defined as a volume increase of more than 20%, in 42% of tumors during a median follow-up time of 4.8 years. The relatively high median age of 70 years, may again partially explain the lower proportion of growing tumors. Also, the fact that the petrous bone largely surrounds these tumors may have influenced growth rate as well.

The decreasing probability of growth with both increasing volume and patients age, strongly indicate that paragangliomas exhibit a decelerating growth pattern. Both Gompertz and logistic models have been used to successfully model growth of tumors, predominantly in vitro [23]. Tumor doubling time was first introduced by Collins and colleagues to quantify growth rate and is based on exponential growth [24]. Although this model presumably describes early tumor growth, we anticipate that in the long run, a decelerating growth pattern is more accurate. The calculated median tumor doubling, of 5.9 and 4.7 years for carotid and vagal body tumors, is therefore likely to be an underestimation of true doubling time [23].

Currently, MR imaging of the head and neck is, at our institution, generally performed at intervals of 1 to 2 years. Our prediction model enables a more individualized approach. In addition to the predictive value of volume, age, and tumor location, these predictors largely determine treatment possibilities and outcome, as well as, the decision to switch from watchful waiting to active treatment if tumor growth is observed. Surgery for small carotid body tumors is relatively safe. However, the risk of cranial nerve impairment increases with tumor size and is particularly high (12.5% - 78.6%) if the tumor surrounds the carotid vessels. Other complications include permanent stroke and hemorrhage, and are more likely to occur if vascular repair is required [25, 26]. Therefore, surgery should be considered if growth is observed in a carotid body tumor, which may still be treated with low risk for complications. In comparison, surgery for vagal body tumors almost inevitably results in functional loss of the vagus nerve. Therefore, surgery is only advisable if tumor progression already resulted in lower cranial nerve impairment, if excessive catecholamine secretion is accompanied by symptoms or in the case of malignant disease (i.e., the presence of nodal or distant metastasis). Radiation therapy may also be used to gain local control. However, the risk of late complications, for instance, radiation-induced malignancy and carotid stenosis, should be weighed against the natural course [26,

27]. Considering the implications of tumor progression and the likelihood of changing to active treatment if growth is observed, our prediction model can be used to individualize screening intervals and thereby reduce the number of "unnecessary" scans.

It should be noted that although bootstrap cross-validation was used to prevent overfitting, the model is not (yet) externally validated. Also, the results presented here may not be applicable to sporadic cases. Even though a statistically significant difference between growth of hereditary and sporadic cases has previously not been observed, a comparatively lower growth rate is, considering sporadic HNPGL are on average diagnosed approximately 15 years later compared with hereditary cases, plausible [6, 8, 28]. Furthermore, the retrospective nature of this study, as well as the multifocality associated with mutations in the SDHD gene, preclude definitive conclusions regarding clinical progression.

Conclusion

This study, confirms the indolent growth of carotid and vagal body paragangliomas. We also established the predictive value of tumor location, volume, and patients' age. With increasing age and volume the probability of growth decreases, indicating a decelerating growth pattern. The use of these predictors in a model for growth facilitates a more individualized approach to "watchful waiting".

References

1. B. E. Baysal, R. E. Ferrell, J. E. Willett-Brozick, et al. "Mutations in SDHD, a mitochondrial complex II gene, in hereditary paraganglioma." In: *Science* 287.5454 (2000), pp. 848–851.
2. H. P. H. Neumann, Z. Erlic, C. C. Boedeker, et al. "Clinical predictors for germline mutations in Head and neck paraganglioma patients: cost reduction strategy in Genetic diagnostic process as fail-out". In: *Cancer Res.* 69.8 (2009), pp. 3650–3656.
3. R. F. Badenhop, J. C. Jansen, P. A. Fagan, et al. "The prevalence of SDHB, SDHC, and SDHD mutations in patients with head and neck paraganglioma and association of mutations with clinical features." In: *J. Med. Genet.* 41.7 (2004), e99.
4. D. E. Benn, B. G. Robinson, and R. J. Clifton-Bligh. "15 Years of paraganglioma: Clinical manifestations of paraganglioma syndromes types 1-5." In: *Endocr. Relat. Cancer* 22.4 (2015), T91–103.
5. L. T. van Hulsteijn, O. M. Dekkers, F. J. Hes, J. W. A. Smit, and E. P. M. Corssmit. "Risk of malignant paraganglioma in SDHB-mutation and SDHD-mutation carriers: a systematic review and meta-analysis". In: *J. Med. Genet.* (2012), pp. 768–776.
6. J. C. Jansen, R. van den Berg, A. Kuiper, A. G. van der Mey, A. H. Zwinderman, and C. J. Cornelisse. "Estimation of growth rate in patients with head and neck paragangliomas influences the treatment proposal." In: *Cancer* 88.12 (2000), pp. 2811–2816.
7. A. Langerman, S. M. Athavale, S. V. Rangarajan, R. J. Sinard, and J. L. Netterville. "Natural History of Cervical Paragangliomas: Outcomes of Observation of 43 Patients". In: *Arch. Otolaryngol. - Head Neck Surg.* 138.4 (2012), pp. 341–345.
8. M. L. Carlson, A. D. Sweeney, G. B. Wanna, J. L. Netterville, and D. S. Haynes. "Natural History of Glomus Jugulare: A Review of 16 Tumors Managed with Primary Observation". In: *Otolaryngol. – Head Neck Surg.* 152.1 (2014), pp. 98–105.
9. S. C. Prasad, H. A. Mimoune, F. D'Orazio, et al. "The role of wait-and-scan and the efficacy of radiotherapy in the treatment of temporal bone paragangliomas." In: *Otol. Neurotol.* 35.5 (2014), pp. 922–31.
10. J. C. Sniezek, J. L. Netterville, and A. N. Sabri. "Vagal paragangliomas". In: *Otolaryngol. Clin. North Am.* 34.5 (2001), pp. 925–939.
11. M. G. Moore, J. L. Netterville, W. M. Mendenhall, B. Isaacson, and B. Nussenbaum. "Head and Neck Paragangliomas: An Update on Evaluation and Management." In: *Otolaryngol. – Head Neck Surg.* 154.4 (2016), pp. 597–605.
12. P. Gilbo, C. G. Morris, R. J. Amdur, et al. "Radiotherapy for benign head and neck paragangliomas: A 45-year experience". In: *Cancer* 120.23 (2014), pp. 3738–3743.
13. B. L. Heesterman, J. P. Bayley, C. M. Tops, et al. "High prevalence of occult paragangliomas in asymptomatic carriers of SDHD and SDHB gene mutations." In: *Eur. J. Hum. Genet.* 21.4 (2013), pp. 469–70.
14. B. L. Heesterman, B. M. Verbist, A. G. L. van der Mey, et al. "Measurement of head and neck paragangliomas: is volumetric analysis worth the effort? A method comparison study." In: *Clin. Otolaryngol.* 41.5 (2016), pp. 571–8.

15. R. van den Berg. "Imaging and management of head and neck paragangliomas". In: *Eur. Radiol.* 15.7 (2005), pp. 1310–1318.
16. R. C. Team. *R: A Language and Environment for Statistical Computing*. Vienna, Austria, 2016.
17. T. M. Therneau. *A Package for Survival Analysis in S*. 2015.
18. J. T.-Y. Wang, A. Y.-Y. Wang, S. Cheng, L. Gomes, and M. Da Cruz. "Growth Rate Analysis of an Untreated Glomus Vagale on MRI". In: *Case Rep. Otolaryngol.* 2016 (2016), pp. 1–6.
19. U. B. Mogensen, H. Ishwaran, and T. A. Gerds. "Evaluating Random Forests for Survival Analysis using Prediction Error Curves." In: *J. Stat. Softw.* 50.11 (2012), pp. 1–23.
20. P. J. Heagerty and P. Saha-Chaudhuri. *survivalROC: Time-dependent ROC curve estimation from censored survival data*. 2013.
21. P. D. Allison. "Survival Analysis". In: *Rev. Guid. to Quant. Methods Soc. Sci.* Routledge, 2010, pp. 413–424.
22. A. L. Stensjøen, O. Solheim, K. A. Kvistad, A. K. Håberg, Ø. Salvesen, and E. M. Berntsen. "Growth dynamics of untreated glioblastomas in vivo". In: *Neuro. Oncol.* 17.10 (2015), pp. 1402–1411.
23. A. Talkington and R. Durrett. "Estimating Tumor Growth Rates In Vivo." In: *Bull. Math. Biol.* 77.10 (2015), pp. 1934–54.
24. V. P. Collins, R. K. Loeffler, and H. Tivey. "Observations on growth rates of human tumors." In: *Am. J. Roentgenol. Radium Ther. Nucl. Med.* 76.5 (1956), pp. 988–1000.
25. K. E. van der Bogt, M.-P. F. M. Vrancken Peeters, J. M. van Baalen, and J. F. Hamming. "Resection of carotid body tumors: results of an evolving surgical technique." In: *Ann. Surg.* 247.5 (2008), pp. 877–884.
26. C. Suárez, J. P. Rodrigo, W. M. Mendenhall, et al. "Carotid body paragangliomas: a systematic study on management with surgery and radiotherapy." In: *Eur. Arch. Otorhinolaryngol.* 271.1 (2014), pp. 23–34.
27. C. Suárez, J. P. Rodrigo, C. C. Bödeker, et al. "Jugular and vagal paragangliomas: Systematic study of management with surgery and radiotherapy." In: *Head Neck* 35.8 (2013), pp. 1195–204.
28. N. Burnichon, V. Rohmer, L. Amar, et al. "The succinate dehydrogenase genetic testing in a large prospective series of patients with paragangliomas." In: *J. Clin. Endocrinol. Metab.* 94.8 (2009), pp. 2817–2827.

Appendix

Table 4.0.4: Generalized estimation equation predicting the development of additional signs

	Odds ratio (95% CI)	p-value
Volume increase [1]	1.21 (0.98; 1.49)	p = 0.07
Initial volume [2]	1.23 (1.01; 1.50)	p = 0.04
Location (ref = CBT)	0.93 (0.49; 1.76)	p = 0.82

[1] Volume increase was categorized into 8 groups based on quantiles
[2] Initial volume (cm^3) was log2 transformed

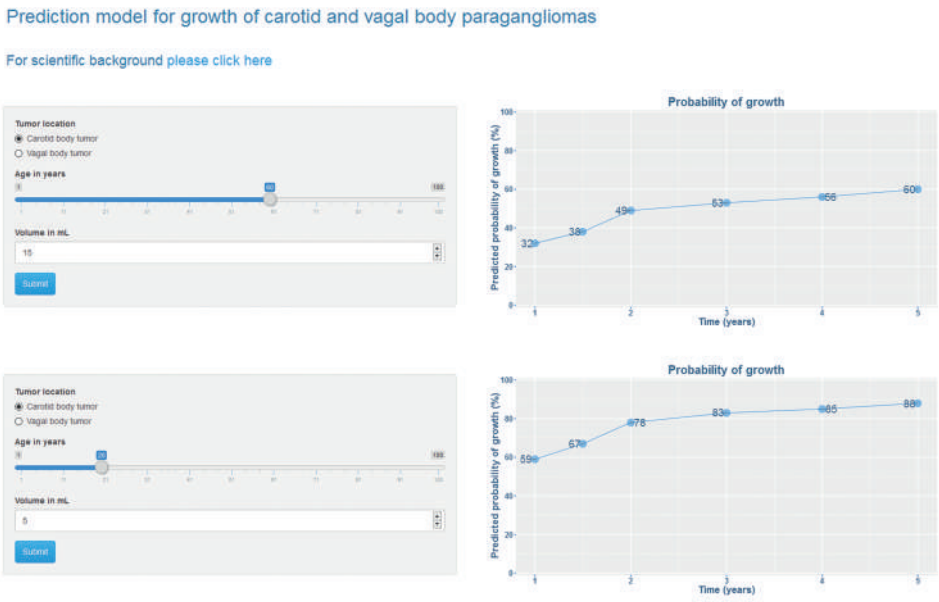

Figure 4.0.6: Prediction of growth for two fictitious patients, interactive version of model is available at https://hnpgl.shinyapps.io/growth/

Table 4.0.5: Number of detected and missed growth for several cut-offs of predicted probability, after 2 years of follow-up (assuming that no scans are made after 1 year of follow-up)

Cut-off value PP[1]	Sensitivity	No. of scans	Scan reduction (%)[2]	Detected growth	Missed growth (%)[3]	Detected fast progression [4]	Missed fast progression (%) [4,5]
33	99	165	2 (1)	109	1 (1)	19	0 (0)
40	95	154	13 (8)	104	6 (5)	19	0 (0)
48	90	140	27 (16)	100	10 (9)	17	2 (11)
51	85	125	42 (25)	93	17 (15)	17	2 (11)
53	80	116	51 (31)	88	22 (20)	16	3 (16)
55	75	108	59 (35)	83	27 (25)	16	3 (16)
57	70	100	67 (40)	78	32 (29)	16	3 (16)
59	65	91	76 (46)	71	39 (35)	16	3 (16)
61	60	87	80 (48)	69	41 (37)	16	3 (16)

[1] Cut-off values for predicted probability
[2] After 2 years 167 (91%) cases were still under follow-up
[3] % of total growth
[4] Fast progression is defined as progression > 50% /year
[5] % of total fast progression

Table 4.0.6: Number of detected and missed growth for several cut-offs of predicted probability after 2 years of follow-up, for cases that would not have been scanned after 1 year based on the screening strategy illustrated in figure 4.0.5. If subsequently 40% would be used as cut-off value to make an MRI after 2 years (screening algorithm illustrated in figure 4.0.5), growth would be missed in 6 additional cases. However, only in 1 out of these 6 cases growth could already have been detected after 1 year of follow-up. Therefore, the detection of growth would be delayed with 1 year in 19 cases (17%) and with 2 years in 1 case (0.9%). Furthermore, growth not yet detectable after 1 year of follow-up would be observed in 9 cases.

Cut-off value PP[1]	Sensitivity	No. of scans	Scan reduction (%)[2]	Detected growth (one year delay)	Missed growth (two years delay)	Detected fast progression [3]	Missed fast progression (%) [3,4]
33	99	58	2 (3)	28 (15)	1 (0)	3	0 (0)
40	95	47	13 (22)	23 (14)	6 (1)	3	0 (0)
48	90	33	27 (45)	19 (11)	10 (4)	1	2 (67)
51	85	18	42 (70)	12 (7)	17 (8)	1	2 (67)
53	80	13	47 (78)	8 (5)	21 (10)	0	3 (100)

[1] Cut-off values for predicted probability
[2] 93% of the cases with a predicted probability of less then 34% at year 1 were still under follow-up after 2 years. In the remaining 4 cases growth was not detected during follow-up
[3] Fast progression is defined as progression > 50% /year
[4] % of total fast progression

Berdine L Heesterman, John-Melle Bokhorst, Lisa M H de Pont, Berit M Verbist, Jean-Pierre Bayley, Andel G L van der Mey, Eleonora P M Corssmit, Frederik J Hes, Peter Paul G van Benthem and Jeroen C Jansen

Journal of Neurological Surgery Part B: Skull Base, 2018

5

Mathematical models for tumor growth and the reduction of overtreatment

Abstract

Background: To improve our understanding of the natural course of head and neck paragangliomas and ultimately differentiate between cases that benefit from early treatment and those that are best left untreated, we studied the growth dynamics of 47 carotid and 30 vagal body paragangliomas managed with primary observation.

Methods: Using digitally available MR Images, tumor volume was estimated at three time points. Subsequently, nonlinear least squares regression was used to fit seven mathematical models to the observed growth data. Goodness of fit was assessed with the coefficient of determination (R^2) and root mean squared error (RMSE). The models were compared with Kruskal-Wallis one-way analysis of variance and subsequent post-hoc tests. In addition, the credibility of predictions (age at onset of neoplastic growth and estimated volume at age 90) were evaluated.

Results: Equations generating sigmoidal-shaped growth curves (Gompertz, logistic, Spratt and Bertalanffy) provided a good fit (median R^2 of 0.996 - 1.00) and better described the observed data compared with the linear, exponential, and Mendelsohn equations ($p < 0.001$). Although there was no statistically significant difference between the sigmoidal-shaped growth curves regarding the goodness of fit, a realistic age at onset and estimated volume at age 90 were most often predicted by the Bertalanffy model.

Conclusions: Growth of head and neck paragangliomas is best described by decelerating tumor growth laws, with a preference for the Bertalanffy model. To the best of our knowledge, this is the first time that this often-neglected model has been successfully fitted to clinically obtained growth data.

Introduction

Head and neck paragangliomas (HNPGLs) are generally benign tumors that arise from nonchromaffin paraganglion cells associated with the autonomic nervous system. They are most commonly located at the bifurcation of the carotid artery, but also occur at the nodose and jugular ganglion of the vagus nerve, and within the temporal bone, where they arise at the adventitia of the jugular bulb and along Arnold's and Jacobson's nerve. Head and neck paragangliomas at other locations, including the thyroid gland and larynx, are extremely rare [1–3].

Paragangliomas are associated with germline mutations in numerous genes, but mutations in SDHD are currently the most common cause of hereditary paragangliomas [4, 5]. An increasing number of paragangliomas are detected following surveillance in subjects with a genetic predisposition [6]. These "screening detected" paragangliomas are usually small and asymptomatic. However, as tumors become larger, symptoms related to compression and destruction of adjacent structures, including lower cranial nerve paralysis, may occur.

The risk of postoperative cranial nerve dysfunction and other serious complications, including stroke and aspiration/pneumonia, is relatively low following surgery for small carotid body tumors (8.3-26.7%) but increases to around 80% when the internal and external carotid arteries are completely encased by tumor tissue [7]. With this in mind, one could argue that all small carotid body tumors should be surgically resected. However, although tumor progression is, with long follow-up, observed in most HNPGL, progression is generally slow and tumors may remain asymptomatic throughout life [8–10]. Thus, even though surgery for small carotid body tumors is reasonably safe, it remains uncertain whether the benefits outweigh the potential harm caused by treatment. Ideally, we would be able to differentiate between tumors that will never cause symptoms, and those that can best be treated while still small.

A better understanding of the natural course of tumors is vital to determine optimal screening intervals, model treatment response, and prevent overtreatment. Unsurprisingly, tumor growth laws have been of interest for over a century, and a variety of mathematical models have been proposed. As most tumors are treated shortly after diagnosis, tumor growth is primarily studied using mouse models or in vitro experiments [11–13].

We studied growth of HNPGLs using sequential MR imaging obtained during routine patient care. We previously observed a decreasing growth probability with increasing age and tumor volume, consistent with a decelerating growth pattern [9]. We, therefore, propose that a sigmoidal-shaped growth curve will best describe the growth of HNPGLs.

Methods

Subjects

SDHD mutation carriers were identified as previously described [9]. MRI scans were digitally available from 2002 onwards and sufficient follow-up was required to study growth patterns. To avoid selection of an atypically favorable subset of untreated tumors (i.e., tumors that were left untreated while already under surveillance), only patients diagnosed with HNPGL between January 2002 and 2009 were eligible for inclusion. For reasons earlier described, only carotid and vagal body paragangliomas were included [9]. In addition, a minimum of three consecutive MRI scans, before any intervention, was deemed a prerequisite for inclusion. In accordance with the Dutch law, approval of the institutional ethics committee was not obtained because all data were collected in the course of routine patient care.

Volume estimation

Three perpendicular dimensions were measured using a linear digital caliper tool, at three different time points. Tumor volume was subsequently calculated, assuming an ellipsoid shape (5.1). Measurements were performed by two observers (BLH and LMHP) and executed as described in our earlier work on growth of HNPGL [9, 14].

$$Volume(V) = \frac{4}{3}\pi(\frac{1}{2}A * \frac{1}{2}B * \frac{1}{2}C) \tag{5.1}$$

Mathematical models

Seven mathematical models of tumor growth were investigated (figure 5.0.1 on page 96).

Linear model

The simplest model to describe the increase in tumor volume (V) over time (t) is linear growth, with a constant growth rate (r) independent of tumor size.

$$V(t) = V_0 + rt \tag{5.2}$$

Exponential model

If all tumor cells are proliferating at a constant rate, tumor volume increases exponentially. Relative growth rate and thus tumor doubling time (T_d) remain constant over time [11, 12, 15].

$$V(t) = V_0 e^{rt} \tag{5.3}$$

$$T_d = \frac{ln2}{r} \tag{5.4}$$

Mendelsohn model

Although tumor doubling is probably constant during early tumor growth, T_d eventually increases. An adjustment to exponential growth was therefore proposed by Mendelsohn in 1963. If $a = \frac{2}{3}$, growth is proportional to the surface area of the tumor, consistent with linear growth of tumor diameter [11, 12].

$$V(t) = (V_0^{1-a} + (1-a)rt)^{\frac{1}{1-a}} \tag{5.5}$$

Gompertz model

Perhaps the best-known tumor growth model, the Gompertz model was introduced in 1825 as a tool to determine the value of life insurance, and was first used by Anna Laird for the explanation of tumor growth [11, 16]. The inflection point of this sigmoid-shaped model occurs once 37% of the maximum tumor volume (V_∞) has been reached. Thereafter, the growth rate decreases exponentially.

$$V(t) = V_0 e^{ln(V_\infty/V_0)(1-e^{-rt})} \tag{5.6}$$

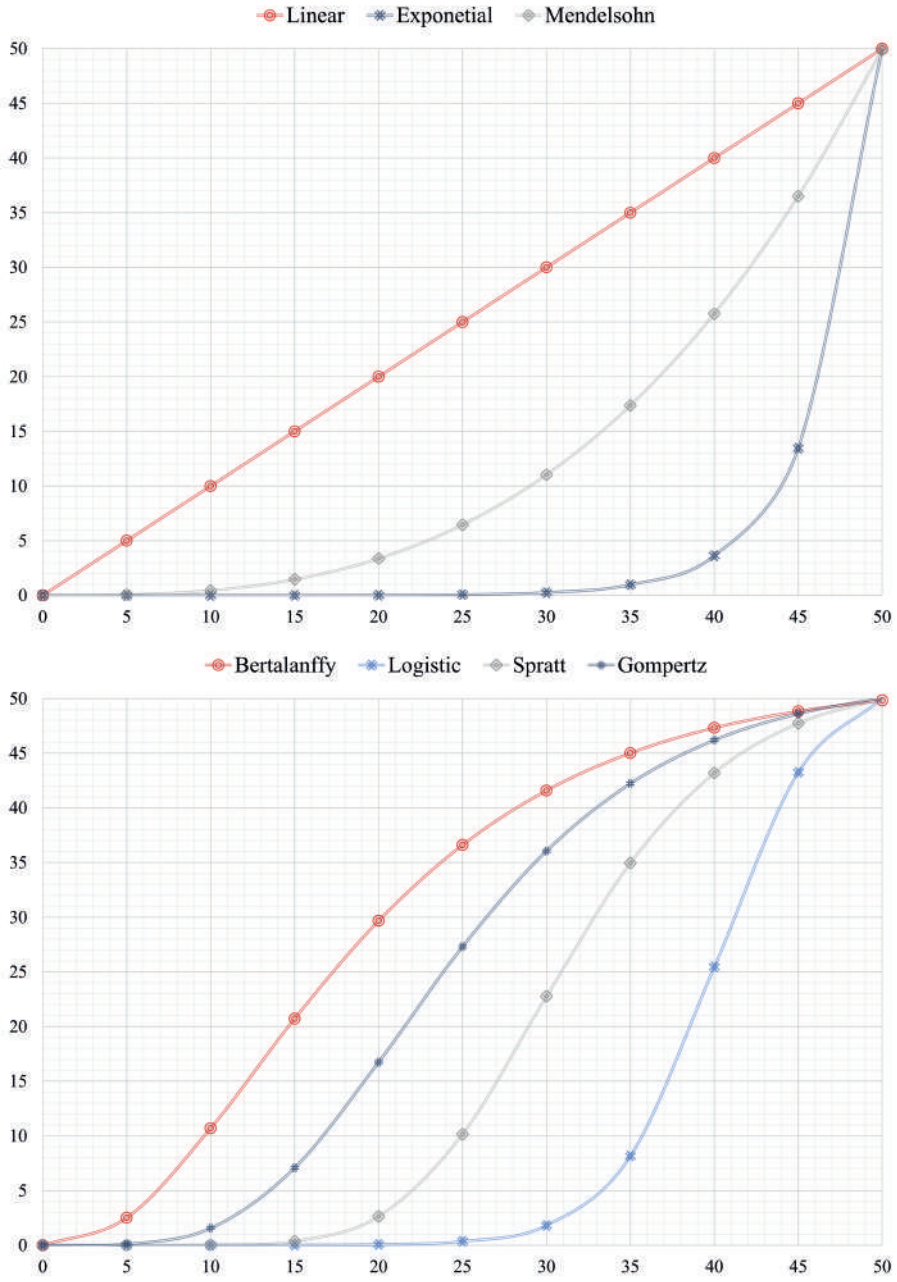

Figure 5.0.1: The investigated models could be subdivided in equations generating a sigmoidal-shaped growth curve (bottom panel) and those predicting ever-expanding tumor volume (upper panel).

Logistic model

The second model originating in the 19th century is the Logistic model, also sigmoidal in shape and first used to describe population dynamics. After 50% of the final size has been reached, growth rate decreases linearly with tumor size [11].

$$V(t) = V_\infty[1 + ((V_\infty/V_0) - 1)e^{-rt}]^{-1} \tag{5.7}$$

Spratt model

Spratt et al. found that a generalized logistic model with $\beta = \frac{1}{4}$ best described the growth of human breast cancer [17].

$$V(t) = V_\infty[1 + ((V_\infty/V_0)^{\frac{1}{4}} - 1)e^{-\frac{1}{4}rt}]^{-4} \tag{5.8}$$

Bertalanffy model

The final model we considered is the Bertalanffy model. This model is based on the assumption that growth results from a balance between cell proliferation and cell death. Proliferation occurs in proportion to the surface area ($\gamma = \frac{2}{3}$) and loss of tumor mass due to cell death is proportional to tumor volume (with constant β) [11, 13, 18]. Areas of necrosis are usually observed when head and neck paragangliomas become larger [19].

$$V(t) = (\frac{\alpha}{\beta} + (V_0^{1-\gamma} - \frac{\alpha}{\beta})e^{-\beta(1-\gamma)t})^{\frac{1}{1-\gamma}} \tag{5.9}$$

Statistics

The mathematical models were fitted using nonlinear least squares regression, with a convergence tolerance for parameters of 10^{-6}. Subsequently, the predicted age at onset of neoplastic growth and tumor volume at age 90 were calculated. Considering that the largest HNPGL we have encountered thus far had an estimated volume of 820 cm^3 (patients age $\approx$ 60 years), a volume of 1000 cm^3 was regarded as the maximum realistic predicted volume at age 90. Goodness of fit statistics, including the coefficient of determination (R^2) and root mean squared error (RMSE) were used to compare the

different models. Kruskal-Wallis one-way analysis of variance, followed by post-hoc tests, was performed to determine statistical significance. Continuous data are, if normally distributed, expressed as mean ± SD, otherwise the median and interquartile range (IQR) are provided. A p-value < 0.05 was considered statistically significant.

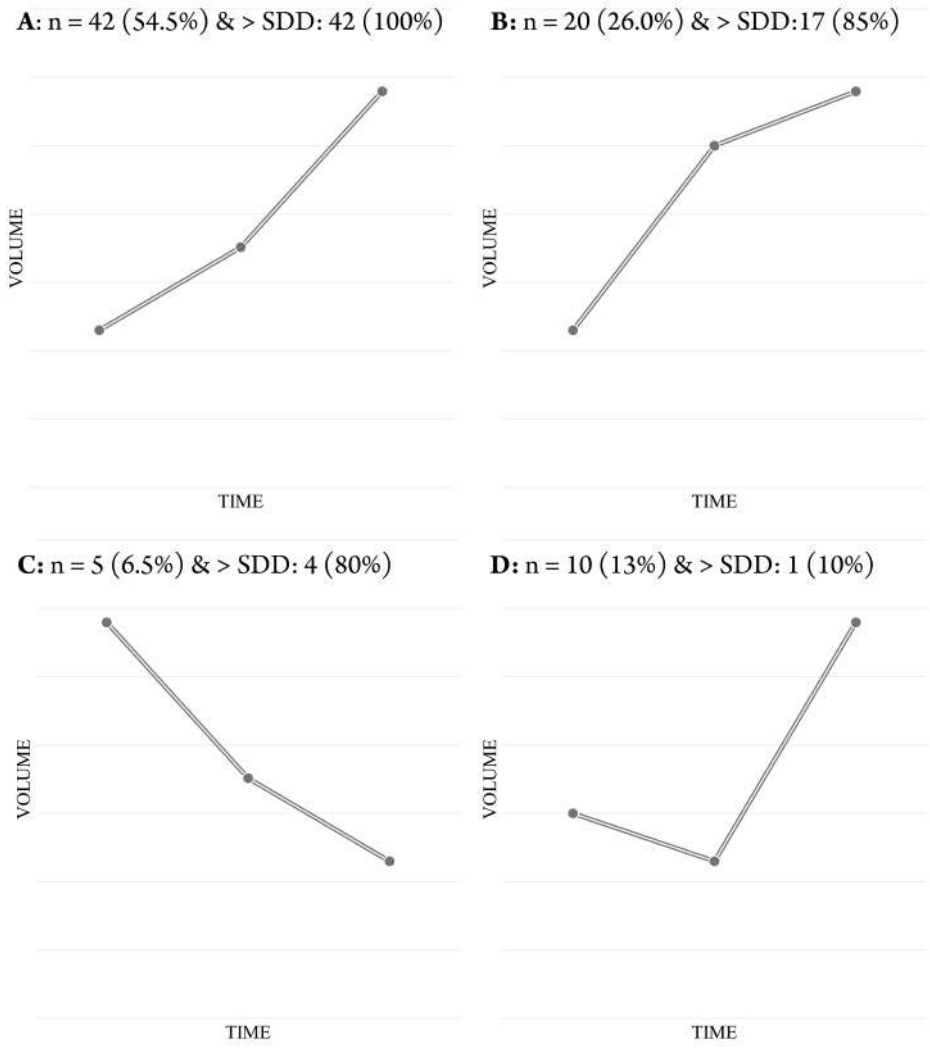

Figure 5.0.2: The observed growth patterns, accelerating (a) and decelerating (b) growth, gradual regression (c) and alternated progression and regression (d). The frequency and how often progression or regression exceeded the smallest detectable difference (SDD) are provided for each pattern.

Results

Subjects

Sequential MR imaging was obtained for 47 (61%) carotid body and 30 (39%) vagal body paragangliomas, managed with primary observation. These 77 HNPGL were diagnosed in 44 patients, with a mean age at baseline of 42 $\pm$ 12 years. Twenty-seven (61%) subjects were male and 91% carried the c.274G>T, p.Asp92Tyr Dutch founder mutation, while the remaining patients carried other known germline mutations in SDHD. Median tumor volume was 4.6 cm^3 at baseline and increased to 8.0 cm^3 during a mean observation period of 6.9 $\pm$ 2.0 years (range: 3.0-11.8). The cases presented here were also included in our previous work on growth of HNPGL [9].

Observed growth patterns

Four growth patterns could be distinguished (figure 5.0.2). Gradual increase in tumor volume was observed in 62 cases (80.5%), and could be further subdivided in accelerating (figure5.0.2a) and decelerating (figure5.0.2b) growth. Spontaneous regression was observed in five cases (6.5%). In the remaining cases (13%) growth was characterized by alternating progression and regression (figure5.0.2d). In 83%, progression or regression exceeded the previously determined smallest detectable difference (SDD) of 10% and 25% for carotid and vagal body tumors, respectively. Particularly when a gradual increase or decrease of tumor volume was observed, growth or regression exceeded the SDD.

Mathematical models & goodness of fit

The median R^2, interquartile range and outliers are shown in figure 5.0.3 on the next page. A box and whisker diagram is also provided for the root mean squared error (figure 5.0.3). There was a statistically significant difference between the different mathematical models, with test statistic $H(6) = 80.23$ and $p < 0.001$. Focused comparisons of the mean ranks revealed that the sigmoidal-shaped growth curves (logistic, Spratt, Gompertz and Bertalanffy equation) better described the observed data compared with the linear, exponential, and Mendelsohn equations. Within the two groups (sigmoidal and nonsigmoidal-shaped growth curves) there was no statistically significant difference. An example of all models fitted to patient data is presented in figure 5.0.4 on page 103.

A realistic predicted age at onset (i.e., after conception) can, by the very nature of the proposed models, not be expected if the estimated volume is smaller at the end compared with the start of follow-up. Therefore, these cases (n = 9) were not included in further analysis. Dependent on the mathematical model fitted, the predicted age at onset was regarded as realistic in 28%-87% of cases, with the median age ranging from 13-34 years (table 5.0.1 on the next page). In the remaining cases, the estimated volume at birth was generally small (median: 0.32-1.46), although outliers were observed. Volume at age 90 years was predicted to be less than 1000 cm^3, in 41-96% of cases, with the median predicted volume ranging from 23.7-74.9 cm^3. A realistic predicted age at onset and volume at age 90 were most often observed for the linear model, followed by the Bertalanffy model.

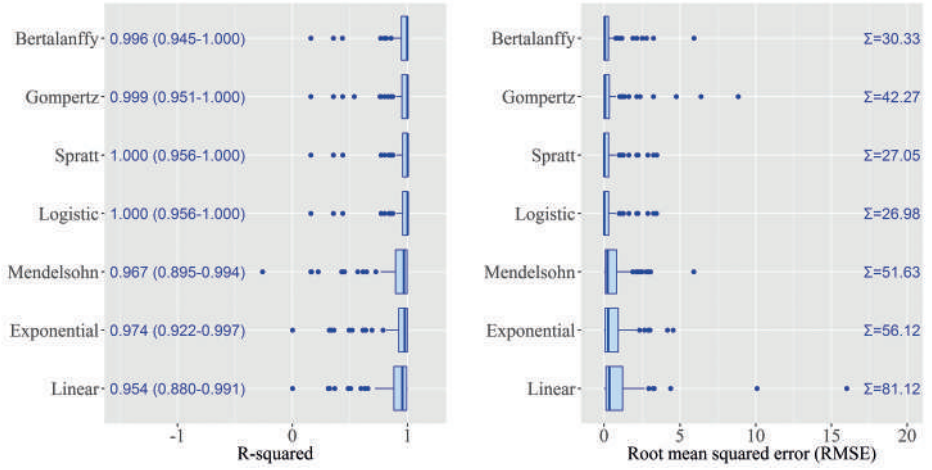

Figure 5.0.3: Box and whisker diagram for the R^2 (left panel) and root mean squared error (right panel). The median R^2 (IQR) is provided for all mathematical models, a value of R^2= 1 indicates a perfect fit. For each model, the root mean squared error (RMSE) was summed for all patients, with the lowest value indicating the best fit. The lower whiskers (left panel) represent the smallest observed $R^2 \geq$ first quartile (Q_1) - 1.5* IQR and the upper whiskers (right panel) represent the largest observed RMSE $\leq$ third quartile (Q_3) + 1.5 * IQR. The blue dots represent the outliers.

Table 5.0.1: The number and proportion of cases with a realistic age at onset[1] and predicted volume at age 90[2] detailed for each model. Median age at onset and volume at age 90 are given for cases with realistic values. The 68 cases in which the tumor volume at the end of follow-up exceeded the initial volume were included in this table

	Number (%) or Median (IQR)						
	Linear	**Exponential**	**Mendelsohn**	**Logistic**	**Spratt**	**Gompertz**	**Bertalanffy**
Realistic[1] age at onset	59 (87%)	19 (28%)	47 (69%)	44 (65%)	44 (65%)	50 (74%)	57 (84%)
Median age (years) at onset (if realistic[1])	34 (23-43)	13 (3-18)	21 (13-31)	13 (7-23)	20 (12-30)	23 (14-32)	28 (21-36)
Volume (cm^3) at birth (if onset < conception)	1.46 (0.70-6.01)	0.33 (0.02-2.01)	0.81 (0.30-5.69)	0.37 (0.02-1.90)	0.32 (0.02-1.89)	0.82 (0.04-2.58)	0.76 (0.46-6.38)
Realistic[2] volume at age 90	68 (100%)	41 (60%)	60 (88%)	57 (84%)	55 (81%)	60 (88%)	65 (96%)
Median volume (cm^3) at age 90 (if realistic[2])	32.5 (11.9-83.3)	74.9 (21.5-350.1)	63.7 (27.6-143.3)	23.7 (8.0-58.5)	25.0 (8.1-61.6)	31.1 (10.7-78.2)	35.7 (12.9-81.5)

Note 1: i.e., after conception (defined as 9 months before birth)

Note 2: i.e., if $\leq$ 1000 cm^3

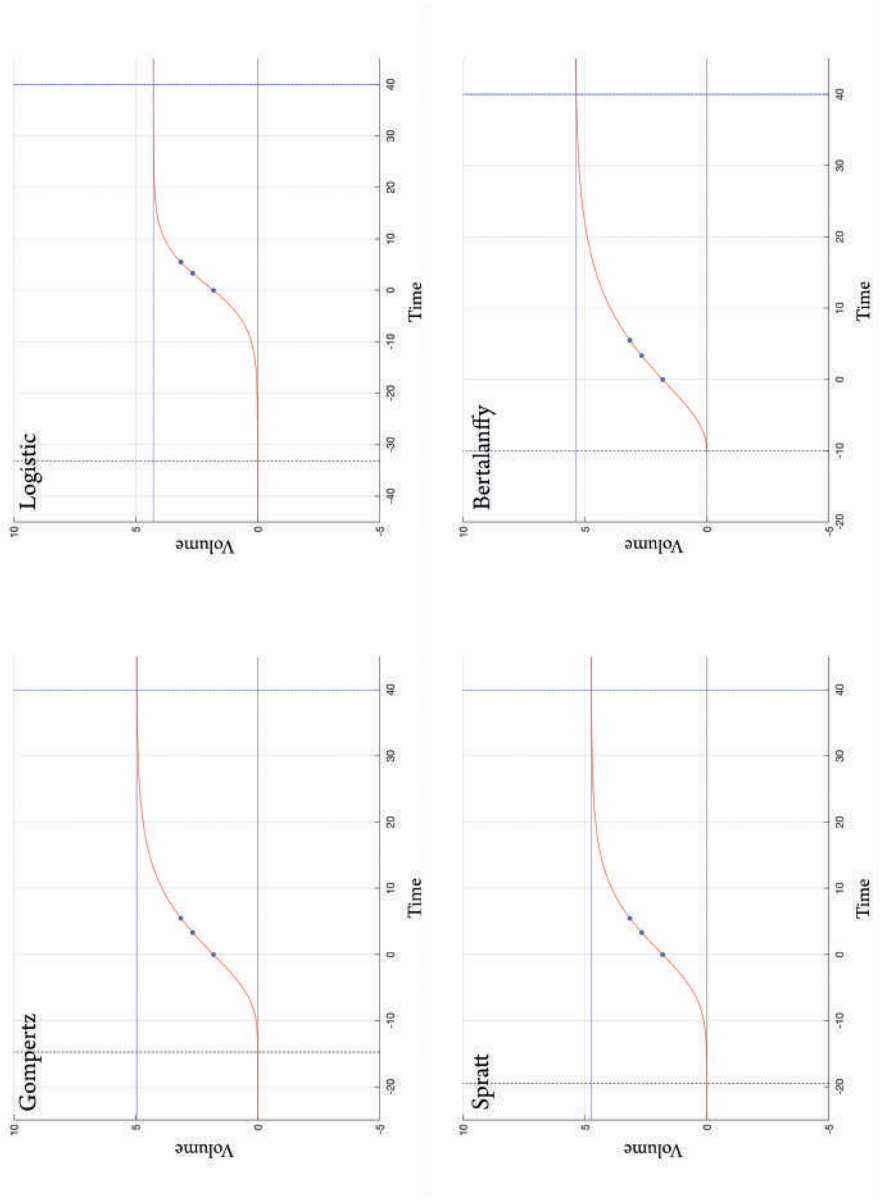
Logistic
Bertalanffy
Gompertz
Spratt
Volume
Time

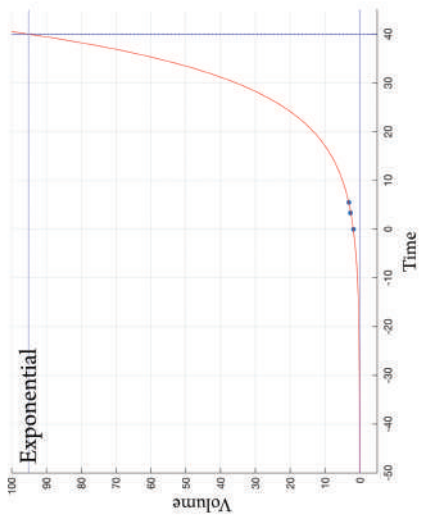

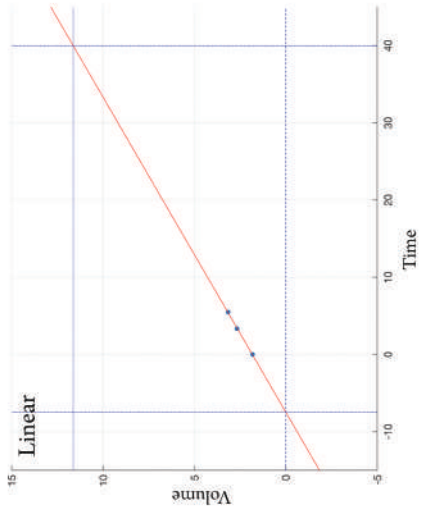

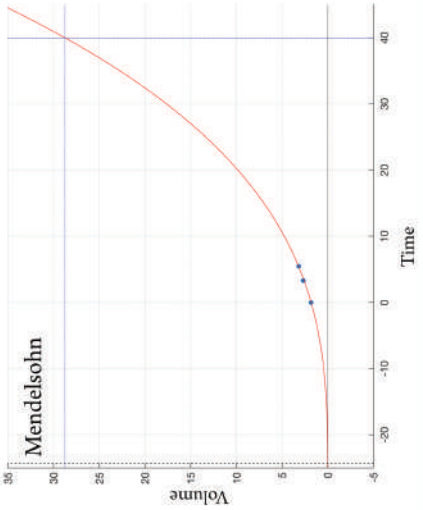

Figure 5.0.4: An example of the seven investigated mathematical models fitted to observed data points. Although all equations describe the observed data points relatively well, the RMSE of the linear, exponential, and Mendelsohn model range from 0.03-0.11, while the RMSE of the sigmoid-shaped curves was substantially smaller (all < 0.00001). The four sigmoid curves yielded a similar estimated volume at age 90 (as apparent from the results in table 5.0.1, this is not true in all cases), while the calculated age at onset was more variable.

Discussion

Decelerating tumor growth laws, i.e., the Gompertz, logistic, Spratt, and Bertalanffy equations, were better suited to model growth of head and neck paragangliomas compared with the linear, exponential, or Mendelsohn models. This finding is in line with a previous observation of decreasing growth rates with increasing volume and age [9]. By definition, none of the investigated models could provide a perfect fit to alternating progression and regression as depicted in figure5.0.2 d. However, as the smallest detectable difference was only exceeded in one of these cases, we propose growth, or rather the lack of it, was consistent with the plateau phase reached by all sigmoidal-shaped growth curves.

As stated by Vaidya et al, in addition to providing a good fit, a mathematical model should have a physiological basis [18]. Retardation of cell cycle speed was suggested as the mechanism behind the Gompertzian model [16]. However, this was contradicted by a more recently observed constant mitotic rate in renal cell carcinomas [11, 20]. Likewise, a solid physiological basis is lacking for the logistic, and Spratt models. Considering that the Bertalanffy equation is a derived from basic cellular principles, we suggest this as an advantage over the other models, a proposal further reinforced by the observation that a realistic age at onset and volume at age 90 were generally predicted by the Bertalanffy model, while this was less clear in the Gompertz, logistic and Spratt models.

As most tumors are treated promptly following diagnosis, studies that use clinical images to model tumor growth are scarce. To the best of our knowledge, this is the first time that the Bertalanffy equation has been successfully fitted to clinically obtained growth data. In agreement with the current analysis, sigmoidal-shaped growth curves have been found to best describe growth of meningiomas and breast carcinomas [17, 21]. Evidence in favor of decelerating tumor growth is further provided by the observation of growth retardation with increasing age and volume, not only in paragangliomas but also in other benign and malignant tumors [22–25]. In fact, sigmoid curves were first used to model tumor growth, in view of the ever diminishing growth rate with increasing volume observed in animal models [11, 16]. Considering that the Gompertz, logistic, Spratt, and Bertalanffy models all fit our data almost equally well, we propose that the Bertalanffy model will also provide a good fit to growth data of tumors other than paragangliomas.

A minimum of three data points is required to model sigmoid-shaped growth curves. Therefore, tumors were only included if three consecutive MRI scans, before any intervention, were available. This may have resulted in a cohort with more favorable tumors, i.e., tumors that were left untreated after the second MRI. However, as the equations used are not restricted by growth rate, it is unlikely that the results are influenced by this potential bias.

Although we have not yet evaluated the accuracy of predictions, we believe we have made steps toward unraveling the natural course of head and neck paragangliomas. Neoplastic growth was estimated to commence in the third or fourth decade of life in most cases. However, dependent on the mathematical model used, neoplastic growth actually appeared to start prior to conception in a non-negligible number of cases. While this clearly indicates an imperfect fit, it probably indicates that neoplastic growth started very early in life in at least a few of these cases.

Following validation, mathematical models can, once three measurements are available, be used to differentiate between tumors that will probably cause serious symptoms and those that will likely remain asymptomatic. Subsequently, one can decide to switch to active treatment or continue conservative management.

Overdiagnosis, i.e., detection of occult disease that would have remained unnoticed throughout life, and subsequent overtreatment are not only associated with early detection of hereditary head and neck paragangliomas, but are intrinsic to cancer screening [26]. Although it is more or less possible to estimate the incidence of overdiagnosis at a population level, it is not as straightforward when it concerns individual patients [27, 28]. The benefits of screening, such as reduction of disease-specific morbidity and mortality, would be compromised if attempts were made to reduce overdiagnosis. However, by introducing conservative management strategies such as "watchful waiting", harmful side effects of unnecessary treatment can be reduced. Perhaps the most well-known example is active surveillance for men with low-risk prostate cancer [29]. More recently, active surveillance was also introduced for clinical T1a renal lesions and low-risk ductal carcinoma in situ (DCIS) [30, 31]. We recognize that knowledge of tumor growth dynamics alone may not be sufficient to differentiate between aggressive and nonaggressive tumors, and additional criteria, including pathologic tumor features (e.g., Gleason upgrading in prostate cancer) or radiologic characteristics (e.g., increased density around calcifica-

tions of DCIS), will be required. However, we are now convinced that mathematical modeling of tumor growth is a useful determinant, as it provides not only the opportunity to estimate future tumor growth and thereby reduce overtreatment, but may also be used to estimate the age at onset and improve screening strategies.

Conclusion

Decelerating tumor growth laws best describe growth of carotid and vagal body paragangliomas. In addition, we have provided evidence that the often-neglected Bertalanffy equation can be used to model clinically obtained growth data and, in light of the generally realistic predicted age at onset of neoplastic growth and predicted volume at age 90, may even be the most appropriate mathematical model in this context. A better understanding of tumor growth dynamics will provide possibilities to optimize surveillance and reduce overtreatment.

References

1. L. T. van Hulsteijn, B. Heesterman, J. C. Jansen, et al. "No evidence for increased mortality in SDHD variant carriers compared with the general population." In: *Eur. J. Hum. Genet.* 23.12 (2015), pp. 1713–6.
2. C. C. Boedeker. "Paragangliomas and paraganglioma syndromes." In: *GMS Curr. Top. Otorhinolaryngol. Head Neck Surg.* 10 (2011), Doc03.
3. J. L. Weissman and B. E. Hirsch. "Beyond the promontory: The multifocal origin of glomus tympanicum tumors". In: *Am. J. Neuroradiol.* 19.1 (1998), pp. 119–122.
4. C. C. Boedeker, E. F. Hensen, H. P. H. Neumann, et al. "Genetics of hereditary head and neck paragangliomas." In: *Head Neck* 36.6 (2014), pp. 907–16.
5. D. Taïeb, A. Kaliski, C. C. Boedeker, et al. "Current approaches and recent developments in the management of head and neck paragangliomas." In: *Endocr. Rev.* 35.5 (2014), pp. 795–819.
6. B. L. Heesterman, J. P. Bayley, C. M. Tops, et al. "High prevalence of occult paragangliomas in asymptomatic carriers of SDHD and SDHB gene mutations." In: *Eur. J. Hum. Genet.* 21.4 (2013), pp. 469–70.
7. C. Suárez, J. P. Rodrigo, W. M. Mendenhall, et al. "Carotid body paragangliomas: a systematic study on management with surgery and radiotherapy." In: *Eur. Arch. Otorhinolaryngol.* 271.1 (2014), pp. 23–34.
8. E. F. Hensen, J. C. Jansen, M. D. Siemers, et al. "The Dutch founder mutation SDHD.D92Y shows a reduced penetrance for the development of paragangliomas in a large multigenerational family." In: *Eur. J. Hum. Genet.* 18.1 (2010), pp. 62–66.
9. B. L. Heesterman, L. M. H. de Pont, B. M. Verbist, et al. "Age and tumor volume predict growth of carotid and vagal body paragangliomas". In: *J Neurol Surg B Skull Base* 78.6 (2017), pp. 497–505.
10. M. L. Carlson, A. D. Sweeney, G. B. Wanna, J. L. Netterville, and D. S. Haynes. "Natural History of Glomus Jugulare: A Review of 16 Tumors Managed with Primary Observation". In: *Otolaryngol. – Head Neck Surg.* 152.1 (2014), pp. 98–105.
11. P. Gerlee. "The model muddle: In search of tumor growth laws". In: *Cancer Res.* 73.8 (2013), pp. 2407–2411.
12. A. Talkington and R. Durrett. "Estimating Tumor Growth Rates In Vivo." In: *Bull. Math. Biol.* 77.10 (2015), pp. 1934–54.
13. S. Benzekry, C. Lamont, A. Beheshti, et al. "Classical mathematical models for description and prediction of experimental tumor growth." In: *PLoS Comput. Biol.* 10.8 (2014), e1003800.
14. B. L. Heesterman, B. M. Verbist, A. G. L. van der Mey, et al. "Measurement of head and neck paragangliomas: is volumetric analysis worth the effort? A method comparison study." In: *Clin. Otolaryngol.* 41.5 (2016), pp. 571–8.
15. V. P. Collins, R. K. Loeffler, and H. Tivey. "Observations on growth rates of human tumors." In: *Am. J. Roentgenol. Radium Ther. Nucl. Med.* 76.5 (1956), pp. 988–1000.
16. a. K. Laird. "Dynamics of Tumor Growth." In: *Br. J. Cancer* 13.1953 (1964), pp. 490–502.

17. J. A. Spratt, D. von Fournier, J. S. Spratt, and E. E. Weber. "Decelerating growth and human breast cancer." In: *Cancer* 71.6 (1993), pp. 2013–2019.
18. V. G. Vaidya and F. J. Alexandro. "Evaluation of some mathematical models for tumor growth." In: *Int J Biomed Comput* 13.1 (1982), pp. 19–36.
19. P. Som and H. Curtin. "Chapter 38 parapharyngeal and masticator space lesions". In: *Head neck imaging*. Ed. by P. Som and H. Curtin. 4th. Mosby, St. Louis, 2003, pp. 1954–2003.
20. W. T. Knöfel, U. Otto, H. Baisch, and G. Klöppel. "Stability of human renal cell carcinomas during long term serial transplantation into nude mice: histopathology, nuclear grade, mitotic rate, and DNA content in thirty tumors." In: *Cancer Res.* 47.1 (1987), pp. 221–4.
21. S. Nakasu, Y. Nakasu, T. Fukami, J. Jito, and K. Nozaki. "Growth curve analysis of asymptomatic and symptomatic meningiomas". In: *J. Neurooncol.* 102.2 (2011), pp. 303–310.
22. C. An, Y. A. Choi, D. Choi, et al. "Growth rate of early-stage hepatocellular carcinoma in patients with chronic liver disease." In: *Clin. Mol. Hepatol.* 21.3 (2015), pp. 279–286.
23. Y. Park, D. Choi, H. K. Lim, et al. "Growth rate of new hepatocellular carcinoma after percutaneous radiofrequency ablation: Evaluation with multiphase CT". In: *Am. J. Roentgenol.* 191.1 (2008), pp. 215–220.
24. P. L. Crispen, A. Soljic, G. Stewart, A. Kutikov, D. Davenport, and R. G. Uzzo. "Enhancing renal tumors in patients with prior normal abdominal imaging: Further insight into the natural history of renal cell carcinoma". In: *J. Urol.* 188.4 (2012), pp. 1089–1093.
25. J. Honegger, S. Zimmermann, T. Psaras, et al. "Growth modelling of non-functioning pituitary adenomas in patients referred for surgery". In: *Eur. J. Endocrinol.* 158.3 (2008), pp. 287–294.
26. M. Jung. "Breast, prostate, and thyroid cancer screening tests and overdiagnosis." In: *Curr. Probl. Cancer* 41.1 (2016), pp. 71–79.
27. G. Draisma, R. Etzioni, A. Tsodikov, et al. "Lead time and overdiagnosis in prostate-specific antigen screening: Importance of methods and context". In: *J. Natl. Cancer Inst.* 101.6 (2009), pp. 374–383.
28. J. R. Benson, I. Jatoi, and M. Toi. "Treatment of low-risk ductal carcinoma in situ: is nothing better than something?" In: *Lancet. Oncol.* 17.10 (2016), e442–e451.
29. L. P. Bokhorst, R. Valdagni, A. Rannikko, et al. "A Decade of Active Surveillance in the PRIAS Study: An Update and Evaluation of the Criteria Used to Recommend a Switch to Active Treatment". In: *Eur. Urol.* 70.6 (2016), pp. 954–960.
30. L. E. Elshof, K. Tryfonidis, L. Slaets, et al. "Feasibility of a prospective, randomised, open-label, international multicentre, phase III, non-inferiority trial to assess the safety of active surveillance for low risk ductal carcinoma in situ - The LORD study". In: *Eur. J. Cancer* 51.12 (2015), pp. 1497–1510.
31. M. Nayyar, P. Cheng, B. Desai, et al. "Active Surveillance of Small Renal Masses: A Review on the Role of Imaging With a Focus on Growth Rate." In: *J. Comput. Assist. Tomogr.* 40.4 (2016), pp. 517–23.

Berdine L Heesterman, Lisa M H de Pont, Andel G L van der Mey, Jean-Pierre Bayley, Eleonora P M Corssmit, Frederik J Hes, Berit M Verbist, Peter Paul G van Benthem and Jeroen C Jansen

European Journal of Human Genetics, 2018

6

Clinical progression and metachronous paragangliomas in a large cohort of SDHD germline variant carriers

Abstract

Background: Although it is well established that paternally transmitted germline variants in SDHD are associated with multifocal paragangliomas and lifelong follow-up is generally advised, the risk of metachronous lesions is presently unknown. In a large Dutch cohort of SDHD variant carriers, we studied the development of new paragangliomas, and the evolution of symptoms and cranial nerve impairment.

Methods: Recurrent event analysis and the Kaplan-Meier product limit estimator were used to study the risk of new lesions. The relation between several predictors and development of new symptoms was assessed using logistic regression.

Results: Of the 222 SDHD variant carriers included, 65% presented with symptoms and 11% with cranial nerve dysfunction. Over a median period of 8 years, 42% reported new symptoms, and new cranial nerve impairment was observed in 11% of subjects. The estimated fraction of subjects that developed new HNPGL increased to 73% (95% CI: 52-85%) after 22 years of follow-up. Males were more likely to develop new HNPGL compared to females (HR: 1.63, 95% CI: 1.10-2.40), as were subjects that presented with symptoms, compared to subjects that were asymptomatic at baseline (HR: 1.61, 95% CI: 1.01-2.55). In addition, the risk of new lesions decreased with number of HNPGL present at first diagnosis (HR: 0.68 and 95% CI: 0.56-0.82).

Conclusions: Carriers of a paternally inherited SDHD variant face a considerable risk for new HNPGL. In addition, nearly 50% of subjects reported new symptoms. However, new cranial nerve deficits were observed in only 11%, which is less than reported in surgical series. These risks should be taken into account when considering treatment strategies and counseling.

Introduction

Hereditary head and neck paragangliomas (HNPGL) are primarily associated with germline variants in the genes encoding subunits of succinate dehydrogenase (SDHA, SDHB, SDHC, and SDHD) or its assembly factor (SDHAF2). SDHD variants are the leading cause of hereditary head and neck paragangliomas in the Netherlands, and a high prevalence of two founder variants, c.274G>T, p.(Asp92Tyr) and c.416T>C, p.(Leu139Pro), is observed in the Dutch population [1–3]. A remarkable parent-of-origin effect characterizes inheritance of SDHD-related paragangliomas (PGL). Carriers of a germline variant in this gene develop a phenotype almost exclusively upon paternal transmission. Although still unproven, the hypothesis that a second paternally imprinted gene, presumably located on 11p15, is involved in tumorigenesis seems the most plausible explanation to date. A requirement for complex mitotic recombination of the maternal 11q and paternal 11p region, followed by loss of the paternal 11q and maternal 11p region, explains the rare occurrence of maternally transmitted disease [4–7].

Numerous authors have studied genotype-phenotype correlations, and SDHD variants are typically associated with head and neck paragangliomas, multifocal disease, and a low malignancy rate. Germline variants in SDHD also predispose carriers to develop pheochromocytomas (PCC) and extra-adrenal sympathetic paragangliomas (sPGL) [8–12]. Patients may present with symptoms related to mass effect or occasionally with symptoms caused by excessive catecholamine secretion. In addition, HNPGLs are increasingly detected following screening by genetic testing and imaging in the context of hereditary disease [13].

Although a few authors have reported metachronous lesions in individual patients, the risk of developing new head and neck paragangliomas during follow-up has not been previously studied [14–18]. In addition, there are no large studies describing clinical progression in patients with untreated HNPGL.

With the aim to further optimize surveillance and counseling of both patients and their family members, we studied symptoms and cranial nerve dysfunction at initial presentation, clinical progression, and the development of new paragangliomas in a large Dutch cohort of SDHD variant carriers.

Methods

Subjects

The database of the Laboratory for Diagnostic Genome Analysis (LDGA) of the Leiden University Medical Center, a tertiary referral center for patients with PGL in the Netherlands, was used to identify SDHD variant carriers. Molecular genetic testing was performed as previously described (reference sequence: NT_033899.7 NM_003002.2) [19]. In addition, family members known at the Leiden University Medical Center with an obligate carrier status, which requires at least one diagnosed paraganglioma and a family member with a germline SDHD variant, were eligible for inclusion. Subjects diagnosed with PGL between January 1990 and October 2015 were included if, following first diagnosis, they underwent imaging in our institution at least once and visited the departments of Otorhinolaryngology, Endocrinology, or Surgery. Carriers of a paternally inherited SDHD variant, with no evidence of disease at initial surveillance, were included if at least one additional MRI or CT scan was available.

In accordance with the Dutch law, approval of the institutional ethics committee was not required because all data used were collected for routine patient care.

Surveillance

Magnetic resonance imaging (MRI) is generally used in our institution for the detection and follow-up of HNPGL (contrast-enhanced 3D Time of Flight MR Angiography sequence has been used since the late 1990s). If there are contraindications for magnetic resonance imaging (e.g., implanted cardioverter-defibrillator or claustrophobia), computed tomography (CT) is used. Measurement of urinary catecholamines and their *O*-methylated metabolites, to detect hormonally active paragangliomas, was performed as described by Havekes et al. and was followed by MRI or CT scans of the thorax, abdomen, and pelvis in case of excessive catecholamine secretion [18, 20]. If a sPGL or PCC was suspected, ^{123}I metaiodobenzylguanidine (MIBG) scintigraphy was performed. Since 2002, biochemical screening has been performed at 2-year intervals and MR imaging at intervals of 1 to 2 years (every 5 years if no evidence of disease is found).

Occasionally, carotid body tumors were detected by head and neck ultrasonography and jugulotympanic tumors by CT imaging of the temporal bone. In light of the risk of multifocal disease associated with SDHD variants, cross-sectional imaging of the head and neck region should be added to discover additional PGLs. With this in mind, the development of a new primary paraganglioma was defined as the detection of a tumor at least one year after initial diagnosis. Accordingly, tumors detected within the first year of follow-up were classified as present at baseline.

The starting point for follow-up was the first MRI or CT scan of the head and neck region of SDHD variant carriers without evidence of disease at initial surveillance. For the remaining subjects, the starting point was equivalent to the date of diagnosis of the first PGL. The time of most recent imaging of the head and neck region was considered the end of follow-up, as it was the most recent point at which new HNPGL could be detected. Relevant clinical data were retrieved from medical records, and comprised the period to the last PGL-related visit to the LUMC. Common PGL-related signs and symptoms (e.g., neck swelling, hearing loss, tinnitus, dysphonia, palpitations, hypertension, and cranial nerve dysfunction) were routinely assessed.

Statistics

For statistical analysis, IBM SPSS Statistics version 23 (IBM Corp.: Armonk, NY, USA) and R version 3.2.5 were used. To assess the risk of developing new (metachronous) HNPGL, recurrent event analysis was used (more specifically a Prentice, Williams and Peterson Total Time model, an extension of Cox proportional hazards regression) [21, 22]. The proportional hazards assumption was checked using scaled Schoenfeld residuals. Age at the start of follow-up, gender, whether a patient was symptomatic or asymptomatic at baseline, and the number of head and neck paragangliomas present at the start of follow-up were considered possible predictors. As imaging techniques have improved over time, we also included the year follow-up started as predictor. Although we intended to include several SDHD variants in our analysis, the high prevalence of the c.274G >T, p.(Asp92Tyr) variant and the much lower number of subjects and observed events for other variants precluded reliable comparison. Only seven patients developed more than three new primary head and neck paragangliomas, therefore a dataset limited to a maximum of three events was used for recurrent event analysis [21]. The estimated

fraction of subjects developing at least one new HNPGL and the median time to this first event was provided by the Kaplan-Meier product limit estimator. To illustrate the effect of binary predictors, Cox proportional hazards regression was used.

The relation between aforementioned predictors, as well as the number of new HNPGL, the development of new symptoms (attributable to paragangliomas located in the head and neck region), and cranial nerve paresis or paralysis was assessed with logistic regression. To correct for varying follow-up times, the duration of follow-up was included in the analysis. To compare the age at onset, defined as the age a patient retrospectively first experienced symptoms, of males versus females, an independent sample t-test was performed. If continuous data followed a Gaussian distribution, the mean and standard deviation are provided, if not, the median and interquartile range (IQR) are given unless stated otherwise. A p-value of less than 0.05 was considered statistically significant.

Results

Patients

A total of 222 Dutch SDHD variant carriers were included, 121 (55%) of whom were male. One subject had developed HNPGL upon maternal transmission, whereas in the remaining 221 subjects the SDHD variant was transmitted via the paternal line. Figure 6.0.1 depicts the number of patients under follow-up from 1990-2016. The SDHD c.274G>T, p.(Asp92Tyr) variant was present in 80%, and the SDHD c.416T>C, p.(Leu139Pro) variant in 12% of subjects. The LOVD database (www.lovd.nl/sdhd) identification numbers and SDHD variants present in the remaining subjects are listed in the appendix (table 6.0.5). In fourteen subjects there was no evidence of disease at the start of follow-up (i.e., the first CT or MRI scan of the head and neck region), five developed one or multiple paragangliomas (five HNPGL and one sPGL) and nine remained unaffected during a median follow-up time of 5.24 years (IQR: 3.26-6.54). In all other cases follow-up started at diagnosis of the first PGL. Almost two-thirds of subjects (n=145; 65%) presented with symptoms, and the median age at baseline was 39 years (range: 13-73; table 6.0.1). All but one subject visited the department of otorhinolaryngology, and biochemical screening was performed in 94%.

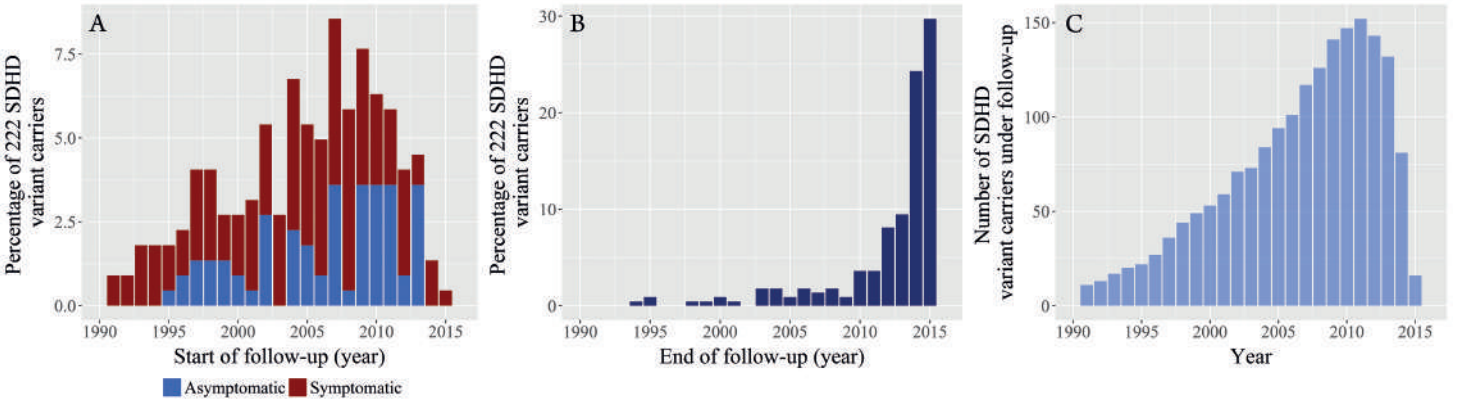

Figure 6.0.1 : The year subjects were included is depicted in figure 6.0.1a. In addition, the proportion of subjects that presented with symptoms versus the proportion of subjects that were asymptomatic at the start of follow-up is specified. The end of follow-up (year of most recent imaging) is depicted in figure 6.0.1b and the total number of SDHD variant carriers under follow-up each year is provided in figure 6.0.1c.

Table 6.0.1: Baseline characteristics

	Median/N	IQR/%
Gender		
Male	121	55%
Female	101	45%
Mutation [1]		
c.274G>T p.(Asp92Tyr)	177	80%
c.416T>C p.(Leu139Pro)	27	12%
Other	18	8%
Age		
Age at the start follow-up (n= 222)[2]	39	29 - 49
Age at diagnosis (n= 213)[2]	39	29 - 49
Symptomatic at baseline	145	65%
Asymptomatic at baseline	77	33%
Median no. of head and neck paragangliomas	2	1 - 3

[1] SDHD germline variants were detected/confirmed by molecular genetic testing (reference sequence: NT_033899.7 NM_003002.2) in 179 cases (81%); the remaining subjects were obligate carriers. The other SDHD variants detected in the study population are listed in the appendix.
[2] The date of diagnosis was equal to the start of follow-up for 208 patients. Five subjects developed the first paraganglioma during follow-up (age at diagnosis > age at the start of follow-up) and nine SDHD variant carriers remained disease free. For 27 patients only the year of diagnosis was known, month and day were set to January first.

Development of new paragangliomas

During a median follow-up time of 7 years (IQR: 4-12), 75 SDHD variant carriers (34%) developed new head and neck paragangliomas and the number of subjects diagnosed with multiple HNPGL increased from 137 (62%) to 171 (77%). In addition, PCC or sPGL were detected in 21 subjects. Overall, 40% of all SDHD variant carriers developed new paragangliomas during follow-up. Carotid body tumors were encountered most frequently, followed by vagal body and jugulotympanic tumors (the distribution was approximately equal between males and females). In addition, HNPGL at other locations (e.g., proximal to the thyroid gland) were detected in five patients (table 6.0.2).

The estimated fraction of SDHD variant carriers that developed at least one new head and neck paraganglioma ranged from 7% (95% CI: 3-10%) after 2 years of follow-up to

73% (95% CI: 52-85%) after 22 years, with a median time of 14.6 years (95% CI: 11.5-16.1; figure 6.0.2a). Males were more likely to develop new HNPGL compared to females (hazard ratio: 1.63, p = 0.01), as were subjects that presented with symptoms compared to subjects that were asymptomatic at baseline (hazard ratio: 1.61, p = 0.04). The chance of developing new tumors decreased if more head and neck paragangliomas were already present (hazard ratio: 0.68, $p < 0.001$; figure 6.0.2c-d and appendix table 6.0.6). There was no statistically significant effect of age.

Table 6.0.2: Number of subjects affected with paragangliomas and detected tumors at the start and end of follow-up (median follow-up time: 7 years).

	Start of follow-up	**End of follow-up**
Subjects	n = 222	n = 222
No evidence of disease	14 (6%)	9 (4%)
Affected with paragangliomas	208 (94%)	213 (96%)
Head and neck paragangliomas	207 (93%)	211 (95%)
Single head and neck paraganglioma	70 (32%)	40 (18%)
Multiple head and neck paragangliomas	137 (62%)	171 (77%)
Pheochromocytoma and/or extra-adrenal sympathetic paraganglioma [1]	10 (5%)	31 (15%)
Tumors	n = 437	n = 570
Head and neck paragangliomas	424 (97%)	531 (93%)
Carotid body tumors	271 (62%)	315 (55%)
Vagal body tumors	100 (23%)	147 (26%)
Jugulotympanic tumors	51 (12%)	64 (11%) [2]
Head and neck paragangliomas at other locations	2 (0.5%)	5 (1%)
Pheochromocytomas	4 (1%)	16 (3%)
Extra-adrenal sympathetic paragangliomas	9 (2%)	23 (4%)

[1] 208 patients underwent biochemical screening. At the end of follow-up 8 patients were diagnosed with multiple pheochromocytomas/ extra-adrenal sympathetic paragangliomas
[2] 23 Jugular paragangliomas and 12 tympanic paragangliomas. In the remaining 29 cases, no distinction could be made (i.e., jugulotympanic paragangliomas)

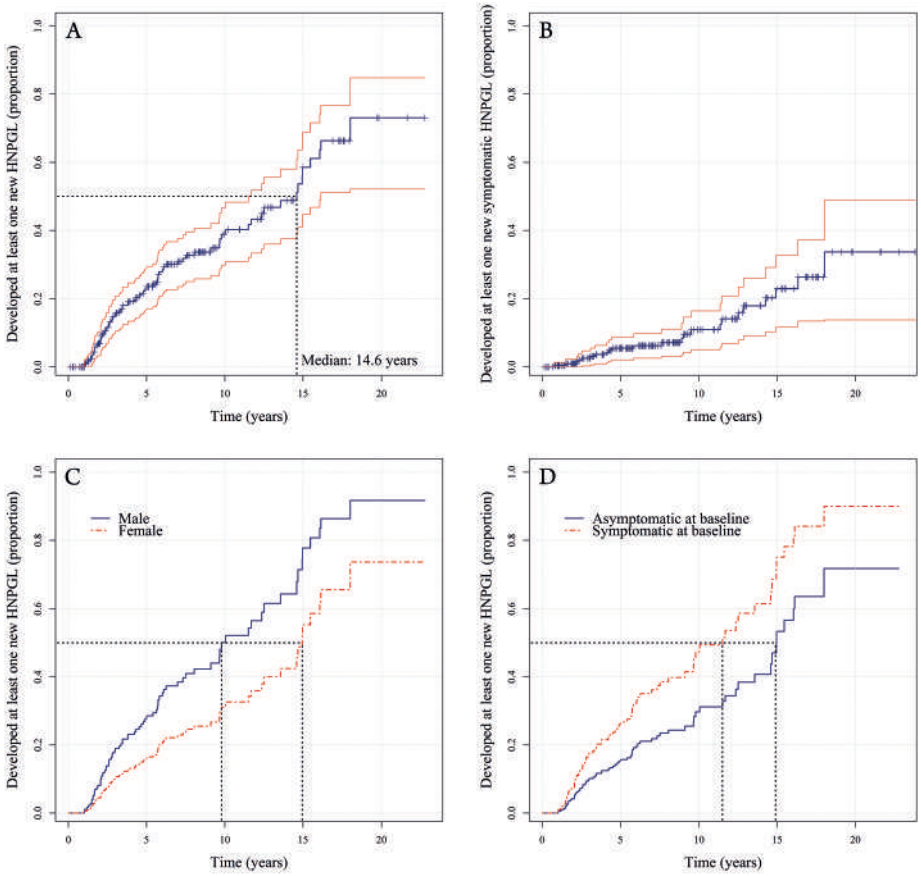

Figure 6.0.2: The cumulative proportion of subjects that developed at least one new (symptomatic or asymptomatic) head and neck paraganglioma over time (a) and the cumulative proportion of subjects that developed at least one new symptomatic head and neck paraganglioma (b), with 95% confidence interval. (c) The risk of males versus females and (d) symptomatic versus asymptomatic patients, represented both for median or mean values of other predictors. The black dotted lines illustrate the estimated median time to the detection of a new tumor.

Clinical progression

At the start of follow-up, 65% of SDHD variant carriers were symptomatic. In addition, 24 (31%) of previously asymptomatic subjects developed symptoms during follow-up, and 70 (48%) already symptomatic patients reported new symptoms. In seven cases, the evolution of symptoms was unknown. In total, 94 (42%) subjects reported new symptoms, including symptoms in 23 cases (24%) attributable to tumors that devel-

oped during follow-up (the cumulative risk of developing a new symptomatic tumor is depicted in figure 6.0.2b). Furthermore, 70 (48%) patients experienced progression of preexisting symptoms, of whom 37 also reported new symptoms. Both the exact date of diagnosis and the duration of symptoms were known for 79% of symptomatic patients. The mean age at onset was 36 (± 13; range 9 - 72) years, and there was no statistically significant difference between males and females (p= 0.73). In the remaining patients, symptoms had often been present for years, suggesting that the actual age at onset was lower. Jugulotympanic tumors were most often symptomatic, with hearing loss and tinnitus being the most commonly reported symptoms. Carotid and vagal body tumors most often caused a neck swelling, and to a lesser extent, pain, sensitivity, or a pressure sensation (table 6.0.3).

In total, 211 SDHD variant carriers were diagnosed with head and neck paragangliomas. Twenty-three (11%) subjects presented with cranial nerve dysfunction, of whom three developed additional cranial nerve palsies during follow-up. In total, 24 (11%) patients developed new cranial nerve paresis or paralysis during follow-up, 21% of which was attributable to new head and neck paragangliomas (table 6.0.4).

Females more often reported new symptoms compared to males (odds ratio: 1.92, p= 0.03), as did younger compared to older subjects (odds ratio per 10 years age increase: 0.76, p= 0.02; appendix table 6.0.7). Both the number of HNPGL present at baseline and the number of new tumors were statistically significant predictors for the development of new symptoms (odds ratio of 1.53 and 1.90, with p-values of 0.01 and 0.003). The former was the only significant predictor for the development of new cranial nerve paresis or paralysis (odds ratio of 1.69, p = 0.03). Urinary catecholamine and/or *O*-methylated metabolites levels were elevated in 79 (40%) patients at some point during follow-up, and one or multiple pheochromocytoma or extra-adrenal sympathetic paragangliomas were detected in 30 patients. In the remaining cases, increased urinary excretion rates of catecholamines and/or *O*-methylated metabolites were attributable to head and neck paragangliomas. In addition, in nine cases catecholamine excess persisted or recurred after treatment for a PCC or sPGL, and could be attributed to the presence of HNPGL. In four other cases both HNPGL and sPGL were biochemically active. A biochemically silent extra-adrenal sympathetic paraganglioma was detected in one patient.

Eight (4%) patients were diagnosed with metastatic paragangliomas. In four cases this involved metastatic spread to locoregional lymph nodes, while in the remaining cases distant metastasis (pulmonary, skeletal, and/or hepatic metastasis) were present. Two patients died of metastatic disease, in a third case the cause of death was unknown and five patients are still in follow-up (mean follow-up time: 7.7 years). In four cases the primary tumor was located in the head and neck region and in two cases the primary tumor was a sPGL. The remaining two patients were diagnosed with both HNPGL and sPGL and the location of the primary tumor was uncertain.

Treatment

A total of 108 patients were treated for 163 head and neck paragangliomas (112 carotid body, 18 vagal body, 13 jugulotympanic, 11 tympanic, 6 jugular paragangliomas, and 3 HNPGL at other locations). The majority of tumors were treated surgically (83%), but radiation therapy (15%), embolization (5%), and octreotide (4%) and lutetium (2%) therapy were also used (as primary or adjuvant therapy). Treatment caused permanent cranial nerve injury in 24 patients (22%), all but two cases of which were attributable to surgical treatment. The vagus nerve was most often affected, followed by the hypoglossal nerve (appendix table 6.0.8). In addition, serious complications, including respiratory insufficiency and stroke, were reported in seven cases.

A total of 27 patients were treated for 16 PCC and 18 sPGL. Serious complications (such as pneumonia, radiation myelopathy and terminal kidney insufficiency) occurred in five cases.

Discussion

Lifelong follow-up is generally recommended in cases of hereditary paragangliomas. However, the risk of developing metachronous lesions has never been studied, nor are there any sizable studies reporting the evolution of symptoms or cranial nerve damage. In this study, we focused on SDHD variant carriers. SDHD variants are predominantly associated with head and neck paragangliomas, with an estimated penetrance at age 70 ranging from approximately 85-100%. Pheochromocytomas and extra-adrenal sympathetic paragangliomas are observed less frequently [8, 11, 20, 23–26]. This distinction

Table 6.0.3: Symptoms present at diagnosis for both patients (211 SDHD variant carriers who were diagnosed with at least one head and neck paraganglioma and 2 with only an extra-adrenal sympathetic paraganglioma) and tumor locations separately. Occasionally, symptoms were attributable to a conglomerate of multiple tumors, or it could not be determined which tumor caused symptom(s).

	Patients (%)	**Carotid body tumors (%)**	**Vagal body tumors (%)**	**Jugulotympanic tumors (%)**
	n = 213	n = 315	n = 147	n = 64
Asymptomatic at diagnosis[1]	67 (31%)	191 (61%)	103 (70%)	13 (20%)
Symptomatic at diagnosis[1]	146 (69%)	112 (36%)	43 (29%)	48 (75%)
	n = 140 [1]	n = 112	n = 43	n = 48
Neck swelling[2]	94 (67%)	103 (92%)	23 (53%)	0 (0%)
Pain/sensitivity/pressure	24 (17%)	15 (13%)	5 (12%)	7 (15%)
Dysphagia	13 (9%)	7 (6%)	10 (23%)	5 (10%)
Tinnitus (pulsatile)	35 (25%)	2 (2%)	3 (7%)	33 (69%)
Tinnitus (non-pulsatile)	4 (3%)	0 (0%)	0 (0%)	4 (8%)
Hearing loss	30 (21%)	0 (0%)	0 (0%)	33[3] (69%)
Dizziness	6 (4%)	4 (4%)	2 (5%)	4 (8%)
Obstructive sleep apnea syndrome	2 (1%)	4 (4%)	0 (0%)	0 (0%)
Dysphonia	15 (11%)	5 (4%)	13 (30%)	8 (17%)
Other[4]	19 (14%)	9 (8%)	5 (12%)	12 (25%)
Symptomatic catecholamine excess[5]	8 (6%)	6 (5%)	3 (7%)	4 (8%)

[1]Discrepancies due to incomplete data; [2]Bilateral in 17 subjects (12%); [3]Objectified in 85%; [4]e.g., symptoms related to cranial nerve impairment (NVII, NIX and NXII), syncope, coughing, dyspnea, globus sensation, (bloody) otorrhea, recurrent otitis, and fatigue; [5]Attributable to catecholamine secreting head and neck paragangliomas in three subjects, and to pheochromocytomas or extra-adrenal sympathetic paragangliomas in five subjects.

Table 6.0.4: Cranial nerve paresis or paralysis for both patients (211 SDHD variant carriers diagnosed with head and neck paragangliomas, and 44 patients who presented with or developed cranial nerve dysfunction) and individual tumors. This table displays paresis or paralysis attributable to tumor progression, cranial nerve damage related to treatment is listed in the appendix (table 6.0.8).

	Patients (% of 211)	**Carotid body tumors (% of 315)**		**Vagal body tumors (% 147)**		**Jugulotympanic tumors (% of 64)**	
		Present at diagnosis	*Developed during follow-up*	*Present at diagnosis*	*Developed during follow-up*	*Present at diagnosis*	*Developed during follow-up*
Facial nerve	9 (4%)	0 (0%)	0 (0%)	0 (0%)	0 (0%)	4 (6%)	5 (8%)
Glossopharyngeal nerve	5 (2%)	1 (0.3%)	0 (0%)	0 (0%)	1 (1%)	2 (3%)	1 (2%)
Vagus nerve	30 (14%)	3 (1%)	5 (2%)	15 (10%)	6 (4%)	9 (14%)	4 (6%)
Accessory nerve	6 (3%)	1 (0.3%)	0 (0%)	1 (1%)	0 (0%)	2 (3%)	3 (5%)
Hypoglossal nerve	18 (9%)	4 (1%)	0 (0%)	5 (3%)	6 (4%)	8 (13%)	2 (3%)
Other	3 (1%)	0 (0%)	0 (0%)	0 (0%)	0 (0%)	1 (2%)	2 (3%)
Cranial nerve dysfunction	44 (21%)	5 (2%)	5 (2%)	19 (13%)	10 (7%)	15 (23%)	11 (17%)

Note 1: There were no patients with bilateral vocal cord paralysis.
Note 2: In two patients, a deficit of the vagus nerve and in an additional patient a deficit of the hypoglossal nerve, could have been caused by treatment.
Note 3: In one patient, it was unknown if deficits of cranial nerves NIX, NX and NXII (attributable to a conglomerate of a vagal and jugulotympanic tumor) developed during follow-up.
Note 4: In 16 cases, it was not certain which tumor caused cranial nerve dysfunction, and in 8 cases cranial nerve dysfunction was attributable to a conglomerate of multiple tumors.

was also apparent from our results, with 95% of subjects diagnosed with HNPGL, compared to 15% with a PCC and/or sPGL.

On average, SDHD variant carriers face an approximately 75% (95% CI: 52-85%) risk for a new HNPGL over a follow-up period of 22 years. This risk is dependent on the number of tumors already present at first presentation. A surprising finding was that men were more prone to develop new head and neck paragangliomas compared to women. We previously found no statistically significant relation between sex and growth of HNPGL [27]. An increased growth rate of central nervous system hemangioblastomas, as well as an increased tumor burden, has been reported in male compared to female patients with von Hippel-Lindau disease (VHL). The authors suggested that this might be due to male hormonal influences [28]. Considering that PGLs are also a manifestation of VHL disease, that both VHL and SDHD tumors exhibit stabilization of HIF-1α, and that testosterone has been found to induce HIF-1α function in rats, we postulate that male hormones may affect the development of paragangliomas [28–31]. However, further research will be required to establish whether testosterone is involved in tumorigenesis of SDHD-related paragangliomas and to confirm sex-related differences in SDHD-related disease.

Patients symptomatic at the start of follow-up were more likely to develop new HNPGL, indicating that asymptomatic SDHD variant carriers, i.e., screening-detected patients, may have a more favorable natural course. Furthermore, it should be noted that although recurrent event analysis revealed no significant relation between age and the development of new tumors, the hazard ratio depicts a risk ratio per time unit. Thus, subjects with a higher life expectancy do have a higher cumulative risk of developing new paragangliomas.

The relatively high percentage of SDHD variant carriers diagnosed with HNPGLs in this cohort, in comparison to previous reports, is attributable to our surveillance regimen and inclusion criteria [11, 13, 20, 26]. In agreement with previous studies, carotid body tumors were most common, followed by vagal and jugulotympanic tumors. Due to their anatomic location, jugulotympanic tumors most frequently presented with symptoms [32, 33].

At the start of follow-up 65% of subjects were symptomatic. During a median follow-up time of 8 years, 42%, including previously asymptomatic SDHD variant carriers, reported new symptoms, 24% of which were attributable to new tumors. Not surprisingly, both the number of tumors present at the start of follow-up, as well as the number of new tumors were statistically significant predictors for the development of new symptoms. In line with an earlier observation of decreasing growth rates of carotid and vagal body paragangliomas with increasing age, there was a negative correlation between age and the development of new symptoms [27]. In addition, females reported new symptoms more often, independent of number of PGL and age. It is well established that there are gender-related differences in reporting physical symptoms [34, 35]. Whether the underlying cause is primarily related to biological differences, bodily vigilance, recall bias, or social standards is unclear, but in population samples and in samples of medical patients women report symptoms more frequently [34, 35].

Twenty-three subjects (11%) presented with cranial nerve dysfunction and 24 subjects (11%) developed new cranial nerve deficits during follow-up. In most cases, dysfunction, primarily involving the vagus and hypoglossal nerve, was attributable to jugulotympanic and/or vagal body paragangliomas. It is noticeable that 21% of cranial nerve dysfunction was attributable to newly developed tumors. Treatment (mainly surgery) resulted in permanent cranial nerve dysfunction in 22% of treated patients. In particular, carotid and vagal body PGL treatment more often resulted in cranial nerve deficits compared to a "wait and scan" strategy. It should be noted that evaluation of treatment was not the main objective of this study and we have not reported results for different treatment modalities separately. However, we know from previous research that the risk of postoperative cranial nerve impairment is high, and almost inevitable if vagal body tumors are resected [36, 37]. The risk of cranial nerve damage following radiotherapy is considerably lower (0-7.4%), although acute and late side effects should be taken into account and weighed against the generally favorable natural course of these tumors [36, 37].

It is generally thought that head and neck paragangliomas seldom release catecholamines. However, if biochemical screening includes the measurement of urinary 3-methoxytyramine, catecholamine excess is observed in approximately 30% of patients with exclusively HNPGL [38]. Finally, the observed malignancy rate was comparable to the rate reported in literature [11, 39].

As imaging of the thorax and abdomen was only performed if there was evidence for increased catecholamine secretion or in case of suspect signs or symptoms, biochemically silent pheochromocytomas and extra-adrenal sympathetic paragangliomas may have gone undetected. In addition, the sensitivity and specificity of newer functional imaging techniques such as ^{18}F-fluordopa and ^{68}Ga-DOTATATE PET/CT have proven superior compared to ^{123}I MIBG scintigraphy [40, 41]. An increased risk of pheochromocytoma has been associated with certain SDHD variants [11]. Although there is only limited evidence for other genotype-phenotype correlations, the results presented here may not be applicable to carriers of all SDHD variants [12]. Lastly, due to the retrospective nature of this study, symptoms may have been underreported.

Conclusion

As SDHD variants are associated with multifocal disease, lifelong follow-up is generally advised. In addition to confirming the high prevalence of multifocal disease, importantly we also showed that SDHD variant carriers face a substantial risk for new head and neck paragangliomas during follow-up (approximately 75% after 22 years). In addition, we detailed the clinical characteristics of 222 SDHD variant carriers, presenting the evolution of symptoms and cranial nerve dysfunction. While up to 50% of SDHD variant carriers reported new symptoms during a median of 8 years, new cranial nerve dysfunction was observed in only 11%, less than in previous surgical series. The risks reported here should be taken into account when considering treatment strategies and counseling.

References

1. E. F. Hensen, N. van Duinen, J. C. Jansen, et al. "High prevalence of founder mutations of the succinate dehydrogenase genes in the Netherlands". In: *Clin. Genet.* 81.3 (2012), pp. 284–288.
2. P. E. M. Taschner, J. C. Jansen, B. E. Baysal, et al. "Nearly all hereditary paragangliomas in the Netherlands are caused by two founder mutations in the SDHD gene". In: *Genes Chromosom. Cancer* 31.3 (2001), pp. 274–281.
3. D. Taïeb, A. Kaliski, C. C. Boedeker, et al. "Current approaches and recent developments in the management of head and neck paragangliomas." In: *Endocr. Rev.* 35.5 (2014), pp. 795–819.
4. E. F. Hensen, E. S. Jordanova, I. J. H. M. van Minderhout, et al. "Somatic loss of maternal chromosome 11 causes parent-of-origin-dependent inheritance in SDHD-linked paraganglioma and phaeochromocytoma families." In: *Oncogene* 23.23 (2004), pp. 4076–4083.
5. J.-P. Bayley, R. a. Oldenburg, J. Nuk, et al. "Paraganglioma and pheochromocytoma upon maternal transmission of SDHD mutations." In: *BMC Med. Genet.* 15.1 (2014), p. 111.
6. A. S. Hoekstra, P. Devilee, and J.-P. Bayley. "Models of parent-of-origin tumorigenesis in hereditary paraganglioma". In: *Semin. Cell Dev. Biol.* (2015), pp. 1–8.
7. A. S. Hoekstra, R. D. Addie, C. Ras, et al. "Parent-of-origin tumorigenesis is mediated by an essential imprinted modifier in SDHD -linked paragangliomas: SLC22A18 and CDKN1C are candidate tumor modifiers". In: *Hum. Mol. Genet.* 25.17 (2016), ddw218.
8. H. P. H. Neumann, C. Pawlu, M. Peczkowska, et al. "Distinct clinical features of paraganglioma syndromes associated with SDHB and SDHD gene mutations." In: *JAMA* 292.8 (2004), pp. 943–51.
9. H. J. L. M. Timmers, A. P. Gimenez-Roqueplo, M. Mannelli, and K. Pacak. "Clinical aspects of SDHx-related pheochromocytoma and paraganglioma". In: *Endocr. Relat. Cancer* 16.2 (2009), pp. 391–400.
10. V. Piccini, E. Rapizzi, A. Bacca, et al. "Head and neck paragangliomas: Genetic spectrum and clinical variability in 79 consecutive patients". In: *Endocr. Relat. Cancer* 19.2 (2012), pp. 149–155.
11. C. J. Ricketts, J. R. Forman, E. Rattenberry, et al. "Tumor risks and genotype-phenotype-proteotype analysis in 358 patients with germline mutations in SDHB and SDHD". In: *Hum. Mutat.* 31.1 (2010), pp. 41–51.
12. L. Evenepoel, T. G. Papathomas, N. Krol, et al. "Toward an improved definition of the genetic and tumor spectrum associated with SDH germ-line mutations". In: *Genet. Med.* 17.8 (2015), pp. 610–620.
13. B. L. Heesterman, J. P. Bayley, C. M. Tops, et al. "High prevalence of occult paragangliomas in asymptomatic carriers of SDHD and SDHB gene mutations." In: *Eur. J. Hum. Genet.* 21.4 (2013), pp. 469–70.
14. C. Lepoutre-Lussey, C. Caramella, F. Bidault, et al. "Screening in asymptomatic SDHx mutation carriers: added value of (18)F-FDG PET/CT at initial diagnosis and 1-year follow-up." In: *Eur. J. Nucl. Med. Mol. Imaging* 42.6 (2015), pp. 868–76.

15. A. Mediouni, S. Ammari, M. Wassef, et al. "Malignant head/neck paragangliomas. Comparative Study". In: *Eur. Ann. Otorhinolaryngol. Head Neck Dis.* 131.3 (2014), pp. 159–166.
16. J. Fruhmann, J. B. Geigl, P. Konstantiniuk, and T. U. Cohnert. "Paraganglioma of the carotid body: Treatment strategy and SDH-gene mutations". In: *Eur. J. Vasc. Endovasc. Surg.* 45.5 (2013), pp. 431–436.
17. H. P. Neumann, B. Bausch, S. R. McWhinney, et al. "Germ-Line Mutations in Nonsyndromic Pheochromocytoma". In: *N. Engl. J. Med.* 346.19 (2002), pp. 1459–1466.
18. B. Havekes, A. A. van Der Klaauw, M. M. Weiss, et al. "Pheochromocytomas and extra-adrenal paragangliomas detected by screening in patients with SDHD-associated head-and-neck paragangliomas". In: *Endocr. Relat. Cancer* 16.2 (2009), pp. 527–536.
19. L. T. van Hulsteijn, B. Heesterman, J. C. Jansen, et al. "No evidence for increased mortality in SDHD variant carriers compared with the general population." In: *Eur. J. Hum. Genet.* 23.12 (2015), pp. 1713–6.
20. L. T. van Hulsteijn, A. C. den Dulk, F. J. Hes, J. P. Bayley, J. C. Jansen, and E. P. M. Corssmit. "No difference in phenotype of the main Dutch SDHD founder mutations". In: *Clin. Endocrinol. (Oxf).* 79.6 (2013), pp. 824–831.
21. L. D. A. F. Amorim and J. Cai. "Modelling recurrent events: A tutorial for analysis in epidemiology". In: *Int. J. Epidemiol.* 44.1 (2015), pp. 324–333.
22. T. M. Therneau. *A Package for Survival Analysis in S*. 2015.
23. E. F. Hensen, J. C. Jansen, M. D. Siemers, et al. "The Dutch founder mutation SDHD.D92Y shows a reduced penetrance for the development of paragangliomas in a large multigenerational family." In: *Eur. J. Hum. Genet.* 18.1 (2010), pp. 62–66.
24. D. E. Benn, A. P. Gimenez-Roqueplo, J. R. Reilly, et al. "Clinical presentation and penetrance of pheochromocytoma/paraganglioma syndromes". In: *J. Clin. Endocrinol. Metab.* 91.3 (2006), pp. 827–836.
25. D. E. Benn, B. G. Robinson, and R. J. Clifton-Bligh. "15 Years of paraganglioma: Clinical manifestations of paraganglioma syndromes types 1-5." In: *Endocr. Relat. Cancer* 22.4 (2015), T91–103.
26. F. Schiavi, S. Demattè, M. E. Cecchini, et al. "The endemic paraganglioma syndrome type 1: Origin, spread, and clinical expression". In: *J. Clin. Endocrinol. Metab.* 97.4 (2012), pp. 637–641.
27. B. L. Heesterman, L. M. H. de Pont, B. M. Verbist, et al. "Age and tumor volume predict growth of carotid and vagal body paragangliomas". In: *J Neurol Surg B Skull Base* 78.6 (2017), pp. 497–505.
28. R. R. Lonser, J. a. Butman, K. Huntoon, et al. "Prospective natural history study of central nervous system hemangioblastomas in von Hippel-Lindau disease." In: *J. Neurosurg.* 120.5 (2014), pp. 1055–62.
29. M. A. Selak, S. M. Armour, E. D. MacKenzie, et al. "Succinate links TCA cycle dysfunction to oncogenesis by inhibiting HIF-*a* prolyl hydroxylase". In: *Cancer Cell* 7.1 (2005), pp. 77–85.
30. I. Hussain, Q. Husain, S. Baredes, J. A. Eloy, R. W. Jyung, and J. K. Liu. "Molecular genetics of paragangliomas of the skull base and head and neck region: implications for medical and surgical management." In: *J. Neurosurg.* 120.2 (2014), pp. 321–30.

31. Y. Chen, L. Fu, Y. Han, et al. "Testosterone replacement therapy promotes angiogenesis after acute myocardial infarction by enhancing expression of cytokines HIF-1a, SDF-1a and VEGF". In: *Eur. J. Pharmacol.* 684.1-3 (2012), pp. 116–124.
32. A. P. Gimenez-Roqueplo, A. Caumont-Prim, C. Houzard, et al. "Imaging work-up for screening of paraganglioma and pheochromocytoma in SDHx mutation carriers: A multicenter prospective study from the PGL.EVA investigators". In: *J. Clin. Endocrinol. Metab.* 98.1 (2013), pp. 4578–4587.
33. S. Woolen and J. J. Gemmete. "Paragangliomas of the Head and Neck." In: *Neuroimaging Clin. N. Am.* 26.2 (2016), pp. 259–78.
34. A. J. Barsky, H. M. Peekna, and J. F. Borus. "Somatic symptom reporting in women and men". In: *J. Gen. Intern. Med.* 16.4 (2001), pp. 266–275.
35. C. M. T. Gijsbers Van Wijk and A. M. Kolk. "Sex differences in physical symptoms: The contribution of symptom perception theory". In: *Soc. Sci. Med.* 45.2 (1997), pp. 231–246.
36. C. Suárez, J. P. Rodrigo, C. C. Bödeker, et al. "Jugular and vagal paragangliomas: Systematic study of management with surgery and radiotherapy." In: *Head Neck* 35.8 (2013), pp. 1195–204.
37. C. Suárez, J. P. Rodrigo, W. M. Mendenhall, et al. "Carotid body paragangliomas: a systematic study on management with surgery and radiotherapy." In: *Eur. Arch. Otorhinolaryngol.* 271.1 (2014), pp. 23–34.
38. N. van Duinen, D. Steenvoorden, I. P. Kema, et al. "Increased urinary excretion of 3-methoxytyramine in patients with head and neck paragangliomas". In: *J. Clin. Endocrinol. Metab.* 95.1 (2010), pp. 209–214.
39. N. Burnichon, V. Rohmer, L. Amar, et al. "The succinate dehydrogenase genetic testing in a large prospective series of patients with paragangliomas." In: *J. Clin. Endocrinol. Metab.* 94.8 (2009), pp. 2817–2827.
40. V. L. Martucci and K. Pacak. "Pheochromocytoma and paraganglioma: Diagnosis, genetics, management, and treatment". In: *Curr. Probl. Cancer* 38.1 (2014).
41. A. Archier, A. Varoquaux, P. Garrigue, et al. "Prospective comparison of 68Ga-DOTATATE and 18F-FDOPA PET/CT in patients with various pheochromocytomas and paragangliomas with emphasis on sporadic cases". In: *Eur. J. Nucl. Med. Mol. Imaging* 43.7 (2016), pp. 1248–1257.

Appendix

Table 6.0.5: SDHD variants as observed in the study population. All variants are considered pathogenic or likely pathogenic, except the last one (c.299C>T) which has not been described previously and classified as variant of unknown significance (VUS).

SDHD variant	Number (%)	LOVD_ID[2]
c.274G>T p.(Asp92Tyr)	177 (80%)	SDHD_000004
c.416T>C p.(Leu139Pro)	27 (12%)	SDHD_000016
c.284T>C p.(Leu95Pro)	6 (3%)	SDHD_000039
c.-8828_169+442 del	4 (2%)	SDHD_000121
c.169_169+9 del TGTATGTTCT	2 (1%)	SDHD_000074
c.337_340 del GACT p.(Asp113Metfs*21)	2 (1%)	SDHD_000022
c.242C>T p.(Pro81Leu)	1 (0.5%)	SDHD_000003
c.3G>C p.(Met1Ile)	1 (0.5%)	SDHD_000015
c.284T>G p.(Leu95Arg)	1 (0.5%)	SDHD_000172
c.299C>T p.(Thr100Ile)	1 (0.5%)	SDHD_000171

Note 1: reference sequence: NT_033899.7 NM_003002.2
Note 2: www.lovd.nl/sdhd

Table 6.0.6: Multivariate recurrent event analysis predicting development of new head and neck paragangliomas.

	Hazard ratio (95% CI)	**p-value**
Gender (ref = Female)	1.63 (1.10-2.40)	p = 0.01
Symptomatic versus asymptomatic at baseline (ref = asymptomatic)	1.61 (1.01-2.55)	p = 0.04
No. of head and neck paragangliomas present at baseline	0.68 (0.56-0.82)	p < 0.001
Year follow-up started (1990-2015)	1.04 (1.00-1.08)	p = 0.06

Table 6.0.7: Logistic regression predicting the development of new symptoms at any point between the start of follow-up and the last PGL-related visit. For 215 SDHD variant carriers it was known if they developed new symptoms during a median time of 8 years (IQR: 5 - 13), these patients were included in the analysis.

	Odds ratio (95% CI)	**p-value**
Gender (ref = Male)	1.92 (1.06-3.53)	p = 0.03
Symptomatic versus asymptomatic at baseline (ref = asymptomatic)	1.55 (0.82-2.98)	p = 0.18
Age at the start of follow-up of follow-up[1]	0.76 (0.60-0.95)	p = 0.02
No. of HNPGLs at start of follow-up	1.53 (1.13-2.10)	p = 0.01
No. of HNPGLs developed during follow-up	1.90 (1.26-2.99)	p = 0.003
Follow-up time	1.03 (0.98-1.09)	p = 0.25

Note 1: Odds ratio for a 10-year increase in age.

Table 6.0.8: Treatment-related cranial nerve paralysis/ paresis. In total, treatment for 22 (20%) carotid body tumors, 5 (28%) vagal body tumors, 7 (23%) jugulotympanic paragangliomas caused cranial nerve injury. Five vagal body tumors were treated surgically, in all cases there was postoperative vocal cord paralysis.

Nerve	**Patients**	**Carotid body tumors**	**Vagal body tumors**	**Jugulotympanic tumors**[1]
	Total (Recovered)	Total (Recovered)	Total (Recovered)	Total (Recovered)
Trigeminal nerve	1 (0)	1 (0)	0 (0)	0 (0)
Facial nerve	10 (7)	5 (5)	0 (0)	5 (2)
Vestibulocochlear nerve	1 (0)	0 (0)	0 (0)	1 (0)
Glossopharyngeal nerve	4 (2)	1 (0)	1 (0)	2 (2)
Vagus nerve	24 (4)	15 (3)	5[2] (0)	4 (1)
Accessory nerve	5 (4)	4 (4)	1 (0)	0 (0)
Hypoglossal nerve	15 (7)	8 (6)	5[2] (0)	2 (1)
Cranial nerve dysfunction	33 (9)	22 (7)	5 (0)	7 (1)

Note 1: Five Jugular paragangliomas, one tympanic and one jugulotympanic paraganglioma
Note 2: Combined surgery for a carotid and vagal body tumor in four cases.

Leonie T van Hulsteijn, Berdine L Heesterman*, Jeroen C Jansen, Jean-Pierre Bayley, Frederik J Hes, Eleonora P M Corssmit and Olaf M Dekkers *These authors contributed equally to this work*

European Journal of Human Genetics, 2015

7

No evidence for increased mortality in SDHD variant carriers compared with the general population

Abstract

Background: Germline variants in subunit-D of the succinate dehydrogenase gene (SDHD variants) are associated with an increased risk of developing paragangliomas. The aim of this study was to compare mortality rates and survival in a Dutch cohort of SDHD variant carriers with those in the general population. The study was conducted at the Leiden University Medical Center, a tertiary referral center for patients with paragangliomas.

Methods: Included subjects all tested positive for SDHD variants before 1 July 2012 and visited the departments of Otorhinolaryngology or Endocrinology at least once or had a diagnosed paraganglioma and a SDHD variant-positive family history. Clinical data were retrieved from medical records, information on mortality was obtained from the Municipal Personal Records Database, and mortality rates for the Dutch population were obtained from the Dutch Central Bureau of Statistics, stratified by sex, age and date. SDHD variant carriers were followed from the date of first SDHD variant-related contact until death, emigration or 12 December 2012 and the standardized mortality ratio (SMR) was calculated.

Results: Two-hundred and seventy-five SDHD variant carriers were included in the study, of which 80% carried the c.274G>T, p.(Asp92Tyr) variant, had a mean duration of follow-up of 7.6 years, yielding 2242 person-years of observation for analysis. There were 18 deaths in the SDHD variant carrier group; two were paraganglioma related. The SMR for the whole cohort was 1.07 (95% confidence interval 0.67–1.73).

Conclusions: Mortality in SDHD variant carriers is not substantially increased. Additional studies are required to confirm these findings.

Introduction

Germline variants in subunit-D of the succinate dehydrogenase (SDH) gene predispose carriers to the development of paragangliomas (PGLs) [1]. SDHD variants are mainly associated with multifocal PGLs in the head and neck region (HNPGLs), although sympathetic PGLs (sPGLs; extra-adrenal PGLs) and adrenal PGLs (i.e., pheochromocytomas, PCC) also occur [2–4]. Although the majority of HNPGLs are benign and indolent tumors [5], their location in close proximity to important neurovascular structures may lead to serious morbidity [6]. Neurovascular complications occur in up to 60% of cases following surgical treatment, for example, cranial nerve injury and lesions to the carotid artery [7, 8]. It is therefore of great importance to carefully consider whether HNPGL should be treated, and a "wait and scan" policy is often the best option [5].

Because of their ability to hypersecrete catecholamines, PCC and sPGLs can give rise to severe cardiovascular complications, such as shock, myocardial infarction, dissecting aortic aneurysms or heart failure due to toxic cardiomyopathy [9–12]. In order to avoid these potentially lethal complications, adrenalectomy is indicated for PCC [13], and with implementation of appropriate preoperative care to modulate the effects of catecholamine release, perioperative mortality is nil [14–16].

The pooled incidence of malignant PGL, defined as the presence of metastases [17–19], in populations comprising both unaffected SDHD variant carriers and SDHD variant carriers with manifest nonmalignant PGL is about 8% [20]. Prognosis in malignant PGL is poor, with reported 5-year survival rates of 20–55% for malignant sPGL and PCC [21, 22] and 60% for malignant HNPGL [23], although a few cases of survival for >20 years after diagnosis have been described [24, 25].

An increasing number of SDHD variant carriers are now being identified through (presymptomatic) testing of family members of SDHD variant carriers with manifest disease, that is, index cases. It is important that these newly identified variant carriers receive reliable prognostic information, including the impact of SDHD variants on mortality and survival. As SDHD variants are associated with a high risk for HNPGLs, and fatal cases of (untreated) PCC have been described, it is important to know whether this translates into increased mortality risk. As this question has not yet been addressed for SDHD variant carriers, the objective of this study was to compare mortality rates

and survival in a Dutch cohort of SDHD variant carriers with that of the general Dutch population.

Subjects and methods

Eligibility criteria

The database of the Laboratory for Diagnostic Genome Analysis of the Leiden University Medical Center (LUMC), a tertiary referral center for patients with PGLs, was used to identify carriers of SDHD variants. Screening for SDH variants was performed in all persons diagnosed with PGL who agreed to genetic testing. Informed consent of both parents was required for individuals aged between 12 and 16 years.

In index patients, all exonic and adjacent intronic regions of the SDH genes were tested for the presence of variants by direct sequencing using the Sanger method on an ABI 377 Genetic Analyzer (Applied Biosystems, Carlsbad, CA, USA) and multiplex ligation-dependent probe amplification (MLPA) was carried out with the P226 MLPA Kit (MRC Holland, Amsterdam, the Netherlands) [3]. Family members of index patients were tested for the family-specific variant. The reference sequence NG_012337.1 covering SDHD transcript NM_003002.2, available from the TCA Cycle Gene Variant Database LOVD database, was used to describe variants. All variants described in this study were previously submitted to the above LOVD database (http://chromium.liacs.nl/lovd_-sdh).

Consecutive SDHD variant carriers who tested positive before 1 July 2012 and who visited the departments of Otorhinolaryngology or Endocrinology at least once were included. In addition, persons with a PGL diagnosis and a SDHD variant-positive family history and known to the outpatient clinics of the departments of Endocrinology and Otorhinolaryngology of the LUMC were also included, as they were considered to be obligate SDHD variant carriers. Only SDHD variant carriers with paternal inheritance were included. Persons for whom no information could be retrieved at the Municipal Personal Records Database (see below) were excluded.

Clinical characteristics

Clinical data were retrieved from medical records. Since 2002, a standard evaluation protocol has been implemented at the departments of Endocrinology and Otorhinolaryngology (figure 7.0.1). In order to detect (hormonally active) PGLs, biochemical screening and head-and-neck magnetic resonance imaging (MRI) were performed at intervals of 2 years (at 3-yearly intervals in unaffected variant carriers). The original diagnostic protocol for patients in the period before 2002 was identical to that from 2002 onwards, with the exception of protocolized follow-up every 2 years.

Biochemical screening included the measurement of (nor)epinephrine, vanillylmandelic acid and dopamine in two 24-h urinary samples. From 2005 onwards, (nor)metanephrine and 3-methoxytyramine were added to these measurements [4]. In cases with excessive catecholamine secretion (i.e., any value above the upper reference limit), radiological assessment by MRI or computed tomographic scans of thorax, abdomen and pelvis was performed to identify potential sources of excessive catecholamine production outside the head and neck region, followed by whole-body ^{123}I-metaiodobenzylguanidine scans if a suspected lesion was found. Patients with PCC or sPGLs operated at the LUMC are generally prepared with adequate preoperative α- and, if necessary, β-adrenergic blockade. In all surgically resected PGLs, diagnosis was confirmed by pathological investigation.

Mortality and survival

For this study, follow-up data on SDHD variant carriers were included from the date of genetic testing. In cases where clinical follow-up was available for the period before SDHD genetic testing, this period was not considered in the mortality analysis, because it would have introduced immortal time bias with an underestimation of mortality rates [26]. Because our aim was to determine the relation between mortality and carriage of a SDHD variant and not between mortality and a diagnosis of PGL, obligate SDHD variant carriers were included from their first PGL-related contact at the LUMC. We also included these patients in the mortality analyses.

Follow-up ended 12 December 2012, or at date of death or, in case of emigration, on the date of emigration. Ten patients are currently being followed-up at another hospital.

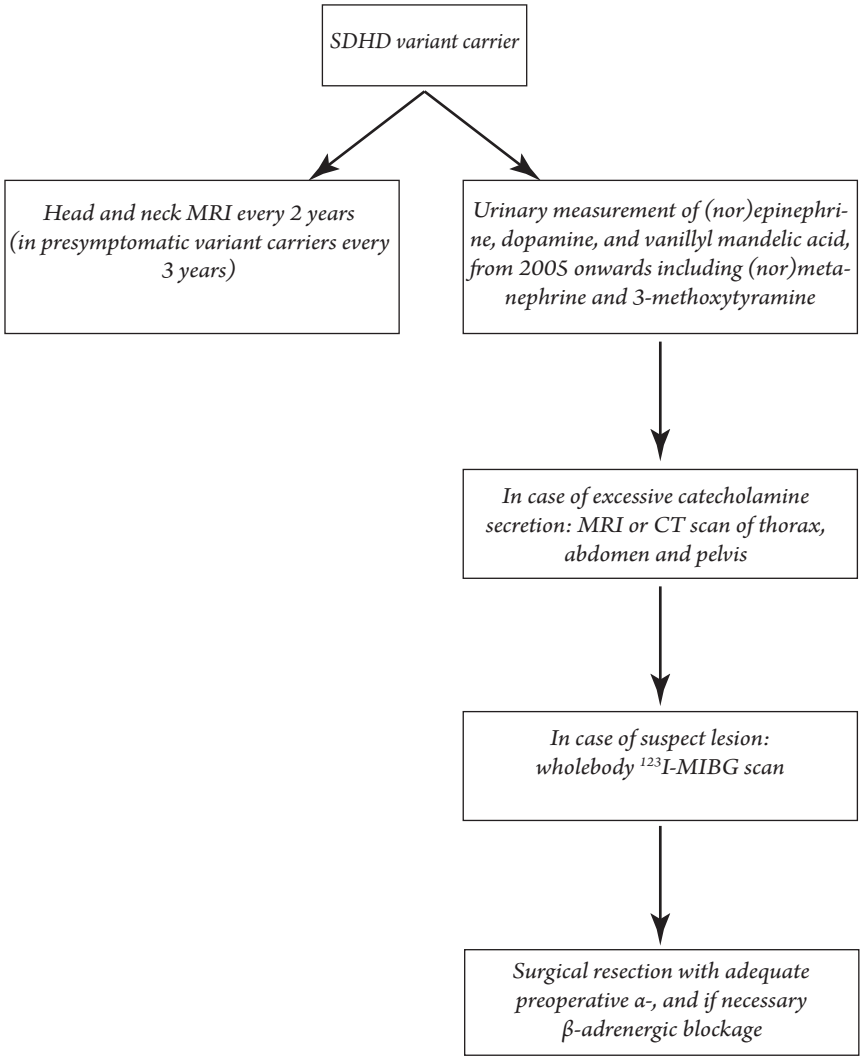

Figure 7.0.1: Screening policy in SDHD variant carriers

For all included (obligate) SDHD variant carriers, an enquiry was sent to the Municipal Personal Records Database (GBA) on 12 December 2012. The GBA registers all deaths

of Dutch inhabitants. To compare mortality between (obligate) SDHD variant carriers and the general population, the standardized mortality ratio (SMR) was estimated. Mortality rates for the Dutch population were obtained from the Dutch Central Bureau of Statistics (The Netherlands), using rates stratified by sex, age (per 1 year) and date (1-year periods). The SMR was calculated by dividing the observed number of deaths in the SDHD cohort, and the expected number of deaths calculated as the sum of the stratified number of expected deaths (stratum specific mortality rates from the general population times follow-up time at risk). Post-hoc power calculations revealed sufficient power ($>$0.8) to detect a difference in mortality of $>$7%.

Survival curves were produced for SDHD variant carriers and the general population, depicting observed and expected survival, respectively. STATA 12.0 (Stata Corp, College Station, TX, USA) was used for statistical analysis.

Results

Clinical characteristics

Of the 275 SDHD variant carriers included, 131 (48%) were female. Clinical characteristics are detailed in table 7.0.1. Molecular genetic testing was used to identify 193 cases (70%), with the remaining 82 individuals characterized as obligate SDHD variant carriers. The SDHD c.274G$>$T, p.(Asp92Tyr) variant (SDHD LOVD ID: SDHD_00004) was present in 80% of the cohort, 11% carried the SDHD c.416T$>$C, p.(Leu139Pro) variant (SDHD LOVD ID: SDHD_00016) and 3% the SDHD c.284T$>$C, p.(Leu95Pro) variant (SDHD LOVD ID: SDHD_00039). Six other SDHD variants were found in the remaining subjects.

Mean age at first identification of a SDHD variant or PGL-related contact at the LUMC was 43.5 $\pm$ 14.4 years. By the end of follow-up, a total of 620 HNPGLs had been found in 246 patients (89%), with 200 patients showing multiple HNPGLs. Treatment was initiated for 143 patients (52%), and a "wait and scan" policy was chosen for the remaining cases. The primary therapy option was surgery, and only seven patients were exclusively treated with radiotherapy or embolization. The disease status of five patients (2%) could not be determined, because these patients declined radiological imaging of the head and neck region owing to an absence of the symptoms.

Table 7.0.1: Clinical characteristics

	Number of patients (%)
Male/female	144 (52%)/131 (48%)
Mean age at first SDHD variant or PGL-related contact	43.5 ± 14.4 years
Mean duration of follow-up	7.6 years (range 0 - 45)
HNPGL	246 (89%)
Percentage of treated tumors	35%
Carotid body PGL	229 (83%)
Percentage of treated tumors	38%
Vagal body PGL	126 (46%)
Percentage of treated tumors	13%
Jugulotympanic PGL	74 (27%)
Percentage of treated tumor	56%
Other HNPGL	5 (2%)
Percentage of treated tumors	40%
sPGL	20 (7%)
Percentage of treated tumors	80%
Pheochromocytoma	18 (7%)
Percentage of treated tumors	94%
Malignant PGL	10 (4%)
Unaffected	20 (7%)

Head and neck paraganglioma (HNPGL), Paraganglioma (PGL), Extra-adrenal sympathetic paraganglioma (sPGL)

In total, 231 (84%) patients underwent biochemical screening at least once at the department of Endocrinology, thereby identifying 20 sPGLs and 18 PCCs. The remaining

44 patients were seen at the department of Otorhinolaryngology. A "watchful waiting" policy was adopted for four sPGL cases: the lesions were surgically difficult to assess, and because of a low risk of malignant transformation and the lack of symptoms related to catecholamine excess, a decision to postpone surgery was preferred. One patient with a non-secretory pheochromocytoma declined surgery. Fifteen patients with sPGL and 17 patients with pheochromocytoma were surgically treated, and the resection of one sPGL is scheduled. A malignant PGL was diagnosed in 10 patients (4%), and the primary tumor was a HNPGL in 7 of these cases. Finally, 20 individuals (7%) showed no signs of manifest disease during follow-up, that is, they were unaffected SDHD variant carriers.

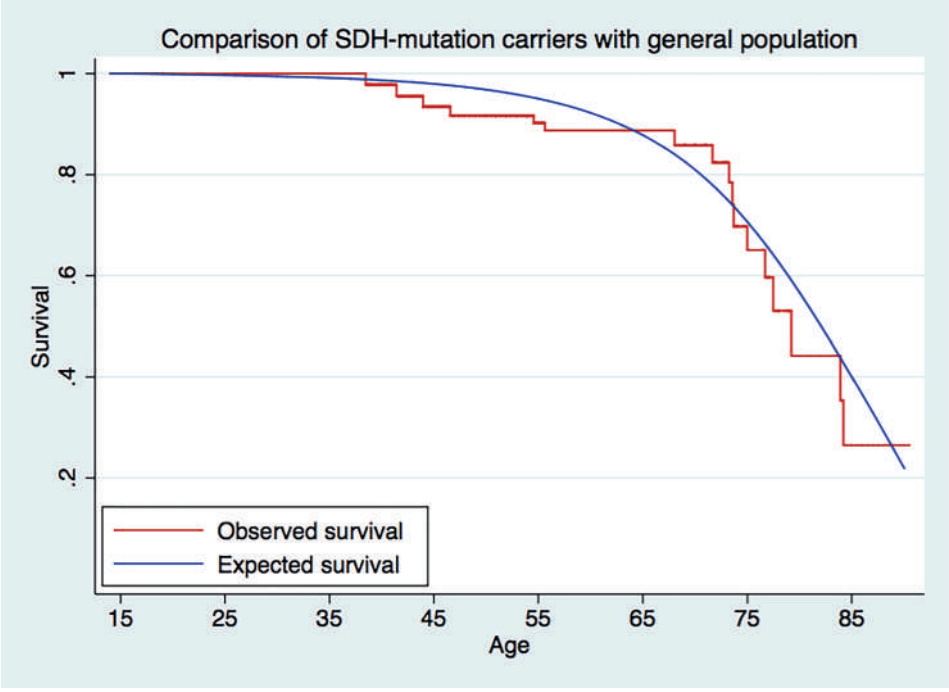

Figure 7.0.2: Survival of SDHD variant carriers (observed survival) and of the general population (expected survival).

Mortality, SMR and survival

Mortality data were available for all 275 cases, with none lost to follow-up. Over a mean follow-up period of 7.6 years (range 0 - 45 years), 18 SDHD variant carriers died at a

mean age of 65 years. Of the 18 deaths in the SDHD variant carrier group, two were PGL-related (i.e., these people died of metastatic disease). Four people died of a cause not related to PGL, and of the 12 people, cause of death was unknown.

A total of 2242 person-years were available for comparison with normative data of the Dutch population. The SMR was 1.07 (95% confidence interval (CI) 0.67 - 1.73) for the whole cohort, indicating no substantial mortality in SDHD variant carriers compared with the general population. The SMR for female SDHD variant carriers was 1.24 (95% CI 0.56 - 2.76) and 1.00 (95% CI 0.55 - 1.81) for male carriers.

Survival curves of the SDHD variant carriers ("observed survival") and of the general population ("expected survival") are depicted in figure 7.0.2.

Discussion

The aim of the present study was to compare mortality rates and survival in SDHD variant carriers with those of the general population. Our results show that mortality in SDHD variant carriers is not substantially increased compared with the general population, despite the presence of HNPGL in a majority of variant carriers. As the prevalence of SDHD-related morbidity is high, these results convey an important message to (newly identified) SDHD variant carriers. However, this study cannot determine whether mortality risk and survival are influenced by the protocolized screening for catecholamine overproduction and subsequent surgical treatment of PCC/sPGL when necessary.

To the best of our knowledge, this is the first investigation of mortality and survival in SDHD variant carriers. The high prevalence of SDHD variants in the Netherlands and the long history of PGL research at the LUMC provided access to a large cohort of SDHD variant carriers with a long duration of follow-up. Although our results provided no evidence for substantially increased mortality in SDHD variant carriers, the upper limit of the confidence interval, at 1.73, indicates that some uncertainty remains. Therefore, additional large cohort studies are needed to confirm and expand these results.

The high prevalence of founder variants in the Netherlands is probably due to the fact that Dutch society was segregated based on socioeconomic and religious differences until the mid-twentieth century, leading to endogamy in isolated populations. This facilitated

the proliferation of many Dutch founder variants [27]. The c.274G>T, p.(Asp92Tyr) and c.416T>C, p.(Leu139Pro) founder variants in SDHD are the most prevalent cause of hereditary PGLs in the Netherlands [3, 4, 28]; however, these specific variants are very rare in other series. Although this, strictly, prohibits simple generalization of our results to other cohorts of SDHD variant carriers, it is worth noting that no convincing genotype-phenotype correlation has ever been described for a specific disease-causing SDH variant.

Our main result - that survival in SDHD carriers is not substantially decreased compared with the general population - may be surprising. Considering the poor prognosis of malignant PGL, an increased mortality in SDHD variant carriers would be expected if malignant PGL was common. However, the low incidence (8%) of malignant PGL in Dutch SDHD variant carriers probably means that it has little influence on overall mortality rates [4]. An expected increase in mortality due to the serious morbidity that may result from (treatment of) HNPGLs and the potentially fatal course of (untreated) PCC [6, 8, 29, 30] was not seen, which could be partly due to the LUMC follow-up policy. First, although 90% of SDHD variant carriers in our cohort developed a HNPGL, only 35% of these patients were treated. This "wait and scan" policy may have resulted in a decreased treatment-related morbidity and possibly mortality. Second, the variant carriers included in our cohort were regularly screened for the presence of PCC. Early detection of PCC by screening results in a much lower prevalence of symptoms, lower catecholamine excess and smaller tumors compared with sporadic PCC detected by signs and symptoms [31]. This may have led to a decrease in both disease- and treatment-related morbidity and, possibly, mortality. It should also be kept in mind that the present study may be underpowered to detect a small increase in mortality risk (i.e., <7%).

Our center previously investigated the survival of Dutch patients diagnosed with a HNPGL between 1945 and 1960. In accordance with the present study, this earlier study was also unable to find a significant difference in survival compared with the general population [32]. Although this earlier study did not assess variant status, as most HNPGL patients in the Netherlands are carriers of SDHD variants [3] the majority of patients included in that study must have been SDHD variant carriers. This previous study reported results from an era before the regular screening of HNPGL patients for the presence of PCC. The prevalence of PCC in Dutch SDHD variant carriers is reported

to be 9% [4], but even at this frequency no effect on mortality due to an absence of screening could be detected. In addition, the subjects included in this study are under regular medical surveillance, which may have resulted in the earlier detection of other clinical conditions and therefore lower than expected deaths compared with the general population.

Seven percent of the study cohort did not display any signs of manifest disease, that is, unaffected variant carriers. The number of unaffected variant carriers in our cohort is probably an underestimation of the actual number, as we were only able to include those under regular follow-up. Unaffected variant carriers are more likely to decline regular follow-up and may therefore remain under the clinical radar. Although this could have resulted in a more "diseased cohort", a bias of this type implies that our findings on mortality are actually more robust.

In conclusion, mortality is not substantially increased in SDHD variant carriers. This knowledge brings a previously missing clarity to the prognostic outlook for (newly identified) variant carriers concerning the effect of SDHD variants on mortality and survival.

References

1. B. E. Baysal, R. E. Ferrell, J. E. Willett-Brozick, et al. "Mutations in SDHD, a mitochondrial complex II gene, in hereditary paraganglioma." In: *Science* 287.5454 (2000), pp. 848–851.
2. D. E. Benn, A. P. Gimenez-Roqueplo, J. R. Reilly, et al. "Clinical presentation and penetrance of pheochromocytoma/paraganglioma syndromes". In: *J. Clin. Endocrinol. Metab.* 91.3 (2006), pp. 827–836.
3. E. F. Hensen, M. D. Siemers, J. C. Jansen, et al. "Mutations in SDHD are the major determinants of the clinical characteristics of Dutch head and neck paraganglioma patients". In: *Clin. Endocrinol. (Oxf).* 75.5 (2011), pp. 650–655.
4. L. T. van Hulsteijn, A. C. den Dulk, F. J. Hes, J. P. Bayley, J. C. Jansen, and E. P. M. Corssmit. "No difference in phenotype of the main Dutch SDHD founder mutations". In: *Clin. Endocrinol. (Oxf).* 79.6 (2013), pp. 824–831.
5. J. C. Jansen, R. van den Berg, A. Kuiper, A. G. van der Mey, A. H. Zwinderman, and C. J. Cornelisse. "Estimation of growth rate in patients with head and neck paragangliomas influences the treatment proposal." In: *Cancer* 88.12 (2000), pp. 2811–2816.
6. K. Papaspyrou, W. J. Mann, and R. G. Amedee. "Management of head and neck paragangliomas: review of 120 patients." In: *Head Neck* 31.3 (2009), pp. 381–7.
7. J. W. Bradshaw and J. C. Jansen. "Management of vagal paraganglioma: Is operative resection really the best option?" In: *Surgery* 137.2 (2005), pp. 225–228.
8. L. Li-shan, L. Chang-wei, G. Heng, Z. Yue-hong, C. Xing-ming, and L. Yong-jun. "Efficacy of surgical therapy for carotid body tumors." In: *Chinese Med. Sci. J.* 26.4 (2011), pp. 241–5.
9. B. E. Bergland. "Pheochromocytoma presenting as shock". In: *Am. J. Emerg. Med.* 7.1 (1989), pp. 44–48.
10. J.-H. Park, K. S. Kim, J.-Y. Sul, et al. "Prevalence and patterns of left ventricular dysfunction in patients with pheochromocytoma." In: *J. Cardiovasc. Ultrasound* 19.2 (2011), pp. 76–82.
11. T. H. Schurmeyer, B. Engeroff, H. Dralle, and A. von zur Muhlen. "Cardiological effects of catecholamine-secreting tumours." In: *Eur. J. Clin. Invest.* 27.3 (1997), pp. 189–195.
12. J. C. Triplett and N. O. Atuk. "Dissecting aortic aneurysm associated with pheochromocytoma." In: *South. Med. J.* 68.6 (1975), pp. 748, 753.
13. K. Pacak, G. Eisenhofer, H. Ahlman, et al. "Pheochromocytoma: recommendations for clinical practice from the First International Symposium. October 2005." In: *Nat. Clin. Pract. Endocrinol. Metab.* 3.2 (2007), pp. 92–102.
14. G. Conzo, M. Musella, F. Corcione, et al. "Laparoscopic adrenalectomy, a safe procedure for pheochromocytoma. A retrospective review of clinical series". In: *Int. J. Surg.* 11.2 (2013), pp. 152–156.
15. M. R. Kazic, V. R. Zivaljevic, Z. B. Milan, and I. R. Paunovic. "Perioperative risk factors, morbidity, and outcome of 145 patients during phaeochromocytoma resection." In: *Acta Chir. Belg.* 111.4 (2011), pp. 223–7.

16. M. A. Kinney, M. E. Warner, J. A. VanHeerden, et al. "Perianesthetic risks and outcomes of pheochromocytoma and paraganglioma resection". In: *Anesth. Analg.* 91.5 (2000), pp. 1118–1123.
17. G. Eisenhofer, S. R. Bornstein, F. M. Brouwers, et al. "Malignant pheochromocytoma: Current status and initiatives for future progress". In: *Endocr. Relat. Cancer* 11.3 (2004), pp. 423–436.
18. R. Ilona Linnoila, H. R. Keiser, S. M. Steinberg, and E. E. Lack. "Histopathology of benign versus malignant sympathoadrenal paragangliomas: Clinicopathologic study of 120 cases including unusual histologic features". In: *Hum. Pathol.* 21.11 (1990), pp. 1168–1180.
19. B. Shapiro, J. C. Sisson, R. Lloyd, M. Nakajo, W. Satterlee, and W. H. Beierwaltes. "Malignant phaeochromocytoma: clinical, biochemical and scintigraphic characterization." In: *Clin. Endocrinol. (Oxf).* 20.2 (1984), pp. 189–203.
20. L. T. van Hulsteijn, O. M. Dekkers, F. J. Hes, J. W. A. Smit, and E. P. M. Corssmit. "Risk of malignant paraganglioma in SDHB-mutation and SDHD-mutation carriers: a systematic review and meta-analysis". In: *J. Med. Genet.* (2012), pp. 768–776.
21. H. John, W. H. Ziegler, D. Hauri, and P. Jaeger. "Pheochromocytomas: Can malignant potential be predicted?" In: *Urology* 53.4 (1999), pp. 679–683.
22. A. Szalat, M. Fraenkel, V. Doviner, A. Salmon, and D. J. Gross. "Malignant pheochromocytoma: Predictive factors of malignancy and clinical course in 16 patients at a single tertiary medical center". In: *Endocrine* 39.2 (2011), pp. 160–166.
23. D. J. Moskovic, J. R. Smolarz, D. Stanley, et al. "Malignant head and neck paragangliomas: Is there an optimal treatment strategy?" In: *Head Neck Oncol.* 2.1 (2010), pp. 0–7.
24. P. J. van den Broek and J. de Graeff. "Prolonged survival in a patient with pulmonary metastases of a malignant pheochromocytoma." In: *Neth. J. Med.* 21.6 (1978), pp. 245–7.
25. S. Yoshida, M. Hatori, T. Noshiro, N. Kimura, and S. Kokubun. "Twenty-six-years' survival with multiple bone metastasis of malignant pheochromocytoma". In: *Arch. Orthop. Trauma Surg.* 121.10 (2001), pp. 598–600.
26. S. Suissa. "Immortal time bias in pharmacoepidemiology". In: *Am. J. Epidemiol.* 167.4 (2008), pp. 492–499.
27. M. P. A. Zeegers, F. van Poppel, R. Vlietinck, L. Spruijt, and H. Ostrer. "Founder mutations among the Dutch." In: *Eur. J. Hum. Genet.* 12.October 2003 (2004), pp. 591–600.
28. P. E. M. Taschner, J. C. Jansen, B. E. Baysal, et al. "Nearly all hereditary paragangliomas in the Netherlands are caused by two founder mutations in the SDHD gene". In: *Genes Chromosom. Cancer* 31.3 (2001), pp. 274–281.
29. J. R. Kizer, L. S. Koniaris, J. D. Edelman, and M. G. St John Sutton. "Pheochromocytoma crisis, cardiomyopathy, and hemodynamic collapse." In: *Chest* 118.4 (2000), pp. 1221–3.
30. K. A. Newell, R. A. Prinz, J. Pickleman, et al. "Pheochromocytoma multisystem crisis. A surgical emergency." In: *Arch. Surg.* 123.8 (1988), pp. 956–9.
31. N. Van Duinen, D. Steenvoorden, B. A. Bonsing, et al. "Pheochromocytomas detected by biochemical screening in predisposed subjects are associated with lower prevalence of clinical

and biochemical manifestations and smaller tumors than pheochromocytomas detected by signs and symptoms". In: *Eur. J. Endocrinol.* 163.1 (2010), pp. 121–127.

32. J. de Flines, J. Jansen, R. Elders, et al. "Normal life expectancy for paraganglioma patients: a 50-year-old cohort revisited." In: *Skull Base* 21.6 (2011), pp. 385–8.

"Medicine is a science of uncertainty and an art of probability."

William Osler

8

General discussion

The natural course of head and neck paragangliomas

The primary aim of this thesis was to gain more insight in the natural course of SDHD-related head and neck paragangliomas and ultimately improve counseling, surveillance, and treatment strategies. The risk of occult and metachronous paragangliomas (*chapter 2 and 6*), tumor growth (*chapter 3, 4 and 5*), clinical progression (*chapter 4 and 6*), and survival of SDHD germline mutation carriers (*chapter 7*) were addressed. In this final chapter the acquired knowledge is further discussed.

Penetrance

The age-related penetrance has been estimated by several authors ($\approx$ 85-100% at age 70) [1–4]. However, due to the inclusion of primarily symptomatic patients, these studies are methodologically flawed. Not surprisingly, the estimated penetrance in a large multigenerational family that harbors the c.274G>T, p.Asp92Tyr missense mutation, was lower compared to the thus far reported numbers. Although, bias due to over-representation of symptomatic patients was reduced in this analysis, the question remains if the results can be extrapolated to other SDHD variants [1].

In this thesis the prevalence of occult paragangliomas in asymptomatic SDHD germline mutation carriers was studied (*chapter 1*). A head and neck paraganglioma was detected in nearly 60% of subjects. If subsequently, the chance that unaffected carriers eventually develop head and neck paragangliomas is considered (*chapter 6*, an adapted version of figure 6.0.2c is printed on the facing page), this number increases to approximately 95% after 20 years of follow-up (median age: 55 years, range 36-90). It should be noted that *chapter 6* was not set out to create a prediction model and the predictive value was not validated. In addition, in families with more affected members or severe disease, asymptomatic family members may be more inclined to pursue genetic testing.

Although the most accurately estimated penetrance will be obtained by including multiple families and applying a maximum likelihood approach [5]. It is, considering the hitherto published data and evidence provided in this thesis, safe to say that carriers of a paternally derived germline mutation in SDHD face a very high risk of developing head and neck paragangliomas. As already evident from previous studies and further reinforced by results reported in this thesis (*chapter 6*), most SDHD germline mutation

carriers will even develop multiple (synchronous or metachronous) head and neck paragangliomas [3, 6].

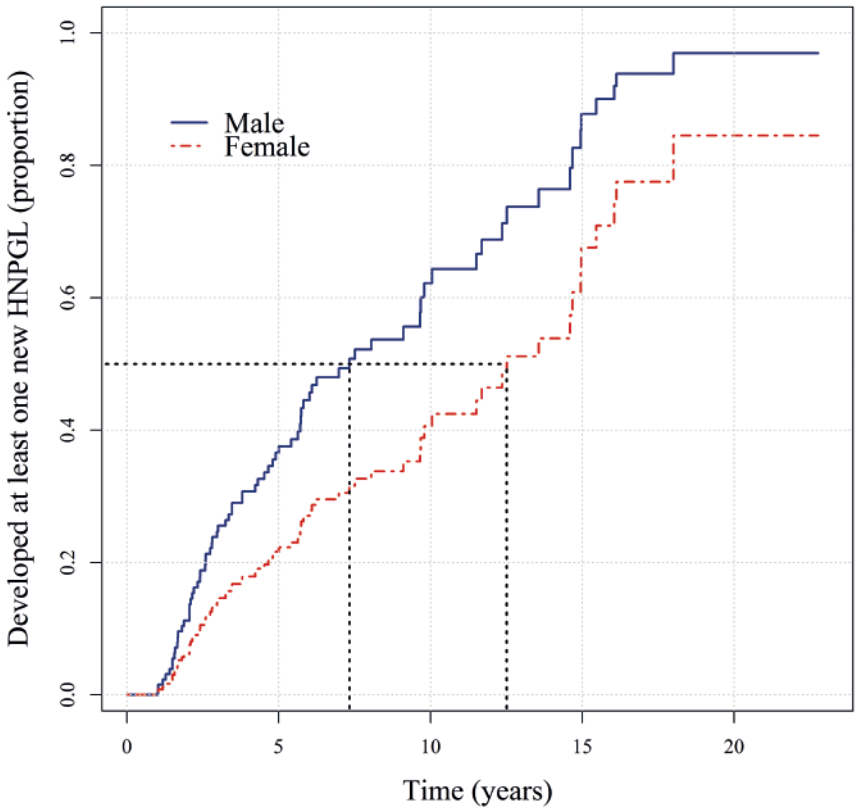

Figure 8.0.1: The cumulative proportion of subjects that developed at least one head and neck paraganglioma. In contrast to figure 6.0.2c, the results are represented for asymptomatic SDHD germline mutation carriers with no evidence of disease at baseline.

Growth of head and neck paragangliomas

Growth of head and neck paragangliomas has been previously addressed in several case series (12-48 paragangliomas), all demonstrating that progression is slow and many tumors (40-65%) remain stable for years [7–10]. Advances in imaging techniques, the use of measurement and tumor specific cut-off values for growth (*chapter 3*), and the inclusion of no less than 118 carotid and 66 vagal body paragangliomas enabled more accurate estimation of tumor growth (*chapter 4*). The use of time to event analysis (Kaplan-

Meier product limit estimator and multivariate Cox proportional hazards regression) provided the opportunity to factor in varying follow-up time and study predictors for tumor growth. Although the generally slow growth rate of head and neck paragangliomas (10.4% and 12.0% annually for carotid and vagal body tumors, respectively) was confirmed, growth will, with long follow-up, be observed in most cases (85% after 11 years). In accordance with a model of retarded growth, age and tumor volume were (independent) negative predictors for growth rate. This observation was further reinforced in *chapter 5*, decelerating tumor growth laws (Gompertz, logistic, Spratt and Bertalanffy equations) described growth of head and neck paragangliomas more accurately compared to a linear, exponential, or Mendelsohn model.

Clinical progression

Even though growth is generally slow and tumors may remain asymptomatic throughout life, the vast majority of SDHD germline mutation carriers will (eventually) develop clinical manifestations (figure 8.0.2). Accordingly, nearly 50% of patients managed with primary observation reported new symptoms during a median follow-up time of 8 years, of whom 26% was previously asymptomatic (*chapter 6*). Moreover, one-fourth was attributable to metachronous tumors. Consistent with decelerating growth, patients reported new symptoms less often with increasing age. Fortunately symptoms were generally mild (figure 8.0.3), and new cranial nerve deficits were reported in only 11% of patients. The relatively high fraction of patients experiencing new symptoms during follow-up, compared to results reported in *chapter 4* (new signs or symptoms were reported in approximately 25% of HNPGL), is readily explained by the fact that most SDHD germline mutation carriers are affected with multiple HNPGL.

Not surprisingly, symptomatic tumors were, with a median volume of 15.2 cm^3 (IQR: 6.4-24.3), considerably larger compared to asymptomatic tumors (median volume: 1.9 cm^3, IQR: 0.7-4.9). Moreover, with increasing volume, new symptoms developed more often.

Malignancy & mortality

The prevalence of malignant disease is low (3%), and even if metastases occur, disease may remain stable for years [11, 12]. In a review including 59 subjects with malignant

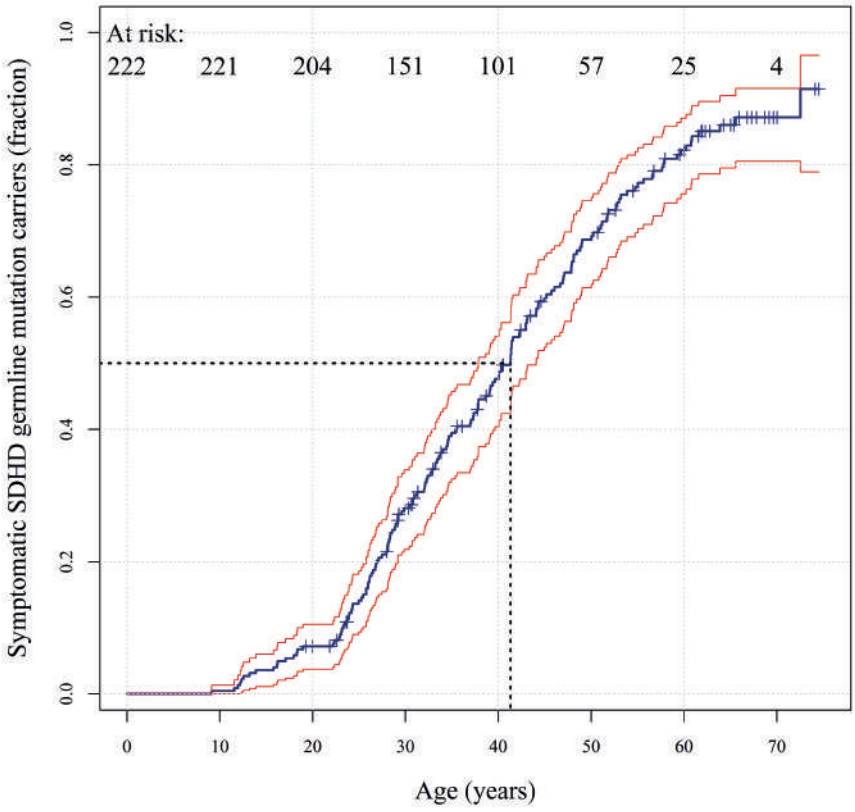

Figure 8.0.2: The fraction of symptomatic SDHD germline mutation carriers was estimated by means of survival analysis (Kaplan-Meier product limit estimator). One hundred forty-five (65%) subjects presented with symptoms, and an additional 24 (11%) subjects became symptomatic during follow-up (*chapter 6*). The age at onset of symptoms was known in 79%. In the remaining cases, symptoms were assumed to be present for 2 years prior to diagnosis (the effect of changing this assumption is limited, data not shown). Asymptomatic SDHD germline mutation carriers were censored at the age of their last PGL-related visit to the LUMC. If the relative under-representation of unaffected carriers is taken into account, by adding fictitious unaffected SDHD-germline mutation carriers (so that the penetrance is ≈90% at age 70), the estimated fraction of symptomatic subjects changes to approximately 80% at age 70.

paraganglioma, the 5 year survival rate was approximately 12% if distant metastases were present and nearly 80% if metastatic spread was restricted to regional lymph nodes. Unfortunately, the genetic status of patients was not reported. However, considering only 2 of the 10 patients diagnosed with malignant disease in our own series died of metastatic disease (*chapter 7*), the prognosis of SDHD-related malignant paragangliomas

is probably more favorable. Moreover, mortality in SDHD germline mutation carriers is not increased compared to the general population (*chapter 7*).

Management of SDHD germline mutation carriers

Seeing that survival of SDHD mutation carriers is not (substantially) reduced and the risk of metastatic transformation low, management of SDHD germline mutation carriers should be focused on the preservation of quality of life, rather than curative treatment. But how do we achieve this?

From previous research we know that the quality of life of SDHD germline mutation carriers is decreased compared to an age adjusted reference population, if patients experience paraganglioma-related symptoms. However, this is not true for SDHD germline mutation carriers without clinical manifestations (i.e., unaffected or asymptomatic) [13]. Should we thus treat all paragangliomas shortly after diagnosis? Not to achieve complete removal, but to prevent clinical progression? Surgery is generally recommended for pheochromocytomas, extra-adrenal sympathetic paragangliomas, and tympanic (Fish type A & B) paragangliomas (*chapter 1*). However, if tumors arise at other locations (or are no longer confined to the tympanomastoid compartment) surgery does not necessarily improve the natural course.

The incidence of postoperative cranial nerve dysfunction and other serious complications have already been discussed in *chapter 1* and are printed alongside results obtained in *chapter 6* on the next page. As already mentioned on multiple occasions throughout this thesis, the risk of iatrogenic damage to cranial nerves is considerable and exceeds the prevalence of cranial nerve dysfunction attributable to tumor progression (*chapter 6*). Due to slow progression and simultaneous compensation, neurological deficits resulting from tumor growth may go unnoticed. In younger patients sufficient compensation usually also occurs following surgery, although the rehabilitation period is prolonged if multiple cranial nerves are affected and interventions such as vocal cord medialization may be required. However, in elderly patients compensation is generally slow and often incomplete [9, 14, 15].

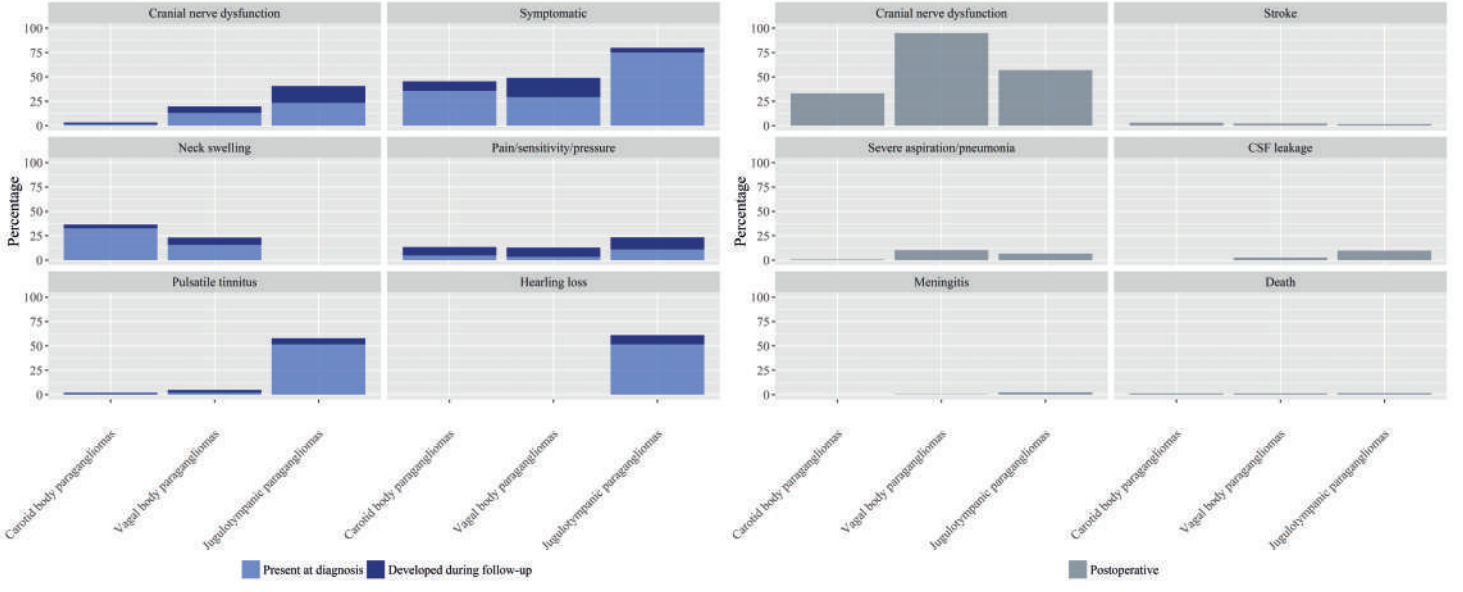

Figure 8.0.3: The reported risk of cranial nerve paralysis and (most common) symptoms attributable to tumor progression are reprinted from *chapter 6* (table 6.0.3 and 6.0.4). The risk of postoperative cranial nerve damage and other serious complications are obtained from literature [16–26].

Should we, considering these risks, refrain from treatment in all cases? And if we do so, is there any added value of (presymptomatic) genetic testing or surveillance? Although one could argue that genetic testing is still useful in terms of exclusion of disease in genuinely healthy subjects, the added value of surveillance is limited if not (in selected cases) followed by intervention. Should surveillance thus be limited to pheochromocytomas and extra-adrenal sympathetic paragangliomas, considering these tumors are generally treated even in the absence of symptoms? Even though growth data can be utilized to improve mathematical modeling (*chapter 5*), ultimately surveillance is only valuable if mathematical modeling is applied to select cases that benefit form early intervention.

In addition to surgery, radiotherapy is increasingly used as primary treatment modality. Although the risk of cranial nerve dysfunction and major complications following irradiation, is significantly less compared to surgery, serious complications may occur in addition to more frequent side effects such as mucositis and fatigue (*chapter 1*) [16, 26, 27]. The efficacy of radiotherapy should be viewed in light of the generally favorable natural course of paragangliomas, unfortunately comparative studies between radiotherapy and primary observation are lacking. However, if the local control rates reported in literature (absence of tumor progression in approximately 80 - 100% during a mean follow-up time of at least 8 years) are compared with the estimated fraction of growing tumors ($\approx$ 80% after 8 years of follow-up, *chapter 4*), it is evident that irradiation effectively induces growth arrest or at least significant growth retardation. Nonetheless, it would be valuable to estimate this effect more accurately by applying radiotherapy after an initial period of primary observation.

Evidence in favor of radiotherapy over surgery is increasing, although surgery may be preferred in case of small carotid body tumors. However, it remains uncertain if the harms of treatment outweigh the advantages. Therefore, a "wait and scan" strategy is often applied, enabling the selection of tumors that will most likely benefit from intervention, while preventing overtreatment. Currently intervals of 1-2 years are maintained, 5 years if there is no evidence of disease. Justification for the latter was provided in *chapter 6*. The median time before the detection of new head and neck paragangliomas was 14.6 years. Even if the negative correlation between number of head and neck paragangliomas present at baseline and risk of developing new tumors is taken into consideration, an

interval of 5 years is sufficient. Particularly, in view of the generally slow growth rate of paragangliomas.

The prediction model created in *chapter 4*, facilitates a more personalized approach to "watchful waiting". By factoring in, age, tumor location, and volume, the likelihood of observing growth beyond the measurement error (*chapter 3*) can be estimated. Hence, the number of unnecessary scans and the chance that growth is overlooked as a result of too small scanning intervals will be reduced.

The proposed model provides the opportunity to predict the occurrence of growth in the near future with fairly good accuracy. Ideally, we would however be able to foresee long-term prospective growth and clinical behavior, and thereby select cases that will benefit from treatment with certainty. In addition, such knowledge would enable further elongation of surveillance intervals. If the evolution of tumor volume over time is accurately described by mathematical models, both the age at onset and long-term tumor growth can be calculated. In *chapter 5* several decelerating tumor growth laws were fitted to observed growth data, yielding excellent results (median R^2 0.996 - 1.00). Although observed growth was captured by the mathematical models almost perfectly, validation of the predictive value is required. Naturally, it is not feasible to verify the accuracy of the calculated age at onset. However, if future growth can be predicted with sufficient precision, estimated age at onset can be utilized to optimize screening. Considering the theoretical justification as well as the generally realistic predicted age at onset and predicted volume at age 90, the Bertalanffy model will probably be best suited to estimate past and predict future growth of head and neck paragangliomas.

In conclusion, important steps toward unraveling the natural course of SDHD-related head and neck paragangliomas and predicting future progression were made. The acquired knowledge, enables direct optimization of counseling and surveillance and may furthermore support the decision to continue a conservative approach or in contrast, opt for intervention.

Future perspectives

As already alluded to in the previous section, the predictive value of mathematical models (especially the Bertalanffy equation) needs to be validated. However, it is not merely

future growth but clinical behavior that will truly support a well-founded treatment decision. It is therefore essential to relate the evolution of clinical manifestations to tumor progression. Considering the estimated volume of symptomatic versus asymptomatic tumors, the transition point will probably be reached if tumors become approximately 5-15 cm^3 in size (*chapter 4*). For further investigation, a prospective study design is best suited, preferably including patients with a single tumor, or at least without multiple ipsilateral tumors as it complicates correct attribution of symptoms. Seeing that SDHD germline mutation carriers are often affected with multiple head and neck paragangliomas, the inclusion of sporadic cases or subjects with a mutation in other susceptibility genes is required. Thereby, a final point of interest is stipulated: can the results reported in this thesis, be generalized to all paraganglioma patients or even beyond the two dutch founder mutations in SDHD? Naturally, the risk of developing paragangliomas and survival are at least specific to germline mutation in SDHD. It is however likely that the observed growth rates and created prediction model are applicable to head and neck paragangliomas beyond the investigated population, although external validation is required.

References

1. E. F. Hensen, J. C. Jansen, M. D. Siemers, et al. "The Dutch founder mutation SDHD.D92Y shows a reduced penetrance for the development of paragangliomas in a large multigenerational family." In: *Eur. J. Hum. Genet.* 18.1 (2010), pp. 62–66.
2. D. E. Benn, A. P. Gimenez-Roqueplo, J. R. Reilly, et al. "Clinical presentation and penetrance of pheochromocytoma/paraganglioma syndromes". In: *J. Clin. Endocrinol. Metab.* 91.3 (2006), pp. 827–836.
3. H. P. H. Neumann, C. Pawlu, M. Peczkowska, et al. "Distinct clinical features of paraganglioma syndromes associated with SDHB and SDHD gene mutations." In: *JAMA* 292.8 (2004), pp. 943–51.
4. C. J. Ricketts, J. R. Forman, E. Rattenberry, et al. "Tumor risks and genotype-phenotype-proteotype analysis in 358 patients with germline mutations in SDHB and SDHD". In: *Hum. Mutat.* 31.1 (2010), pp. 41–51.
5. J. A. Rijken, N. D. Niemeijer, E. P. M. Corssmit, et al. "Low penetrance of paraganglioma and pheochromocytoma in an extended kindred with a germline SDHB exon 3 deletion." In: *Clin. Genet.* 89.1 (2016), pp. 128–32.
6. L. T. van Hulsteijn, A. C. den Dulk, F. J. Hes, J. P. Bayley, J. C. Jansen, and E. P. M. Corssmit. "No difference in phenotype of the main Dutch SDHD founder mutations". In: *Clin. Endocrinol. (Oxf).* 79.6 (2013), pp. 824–831.
7. J. C. Jansen, R. van den Berg, A. Kuiper, A. G. van der Mey, A. H. Zwinderman, and C. J. Cornelisse. "Estimation of growth rate in patients with head and neck paragangliomas influences the treatment proposal." In: *Cancer* 88.12 (2000), pp. 2811–2816.
8. A. Langerman, S. M. Athavale, S. V. Rangarajan, R. J. Sinard, and J. L. Netterville. "Natural History of Cervical Paragangliomas: Outcomes of Observation of 43 Patients". In: *Arch. Otolaryngol. - Head Neck Surg.* 138.4 (2012), pp. 341–345.
9. M. L. Carlson, A. D. Sweeney, G. B. Wanna, J. L. Netterville, and D. S. Haynes. "Natural History of Glomus Jugulare: A Review of 16 Tumors Managed with Primary Observation". In: *Otolaryngol. – Head Neck Surg.* 152.1 (2014), pp. 98–105.
10. S. C. Prasad, H. A. Mimoune, F. D'Orazio, et al. "The role of wait-and-scan and the efficacy of radiotherapy in the treatment of temporal bone paragangliomas." In: *Otol. Neurotol.* 35.5 (2014), pp. 922–31.
11. L. T. van Hulsteijn, O. M. Dekkers, F. J. Hes, J. W. A. Smit, and E. P. M. Corssmit. "Risk of malignant paraganglioma in SDHB-mutation and SDHD-mutation carriers: a systematic review and meta-analysis". In: *J. Med. Genet.* (2012), pp. 768–776.
12. J. W. Bradshaw and J. C. Jansen. "Management of vagal paraganglioma: Is operative resection really the best option?" In: *Surgery* 137.2 (2005), pp. 225–228.
13. L. T. Van Hulsteijn, A. Louisse, B. Havekes, et al. "Quality of life is decreased in patients with paragangliomas". In: *Eur. J. Endocrinol.* 168.5 (2013), pp. 689–697.
14. J. L. Netterville and F. J. Civantos. "Rehabilitation of cranial nerve deficits after neurotologic skull base surgery." In: *Laryngoscope* 103.11 Pt 2 Suppl 60 (1993), pp. 45–54.

15. C. G. Jackson. "Glomus tympanicum and glomus jugulare tumors". In: *Otolaryngol. Clin. North Am.* 34.5 (2001), pp. 941–970.
16. C. Suárez, J. P. Rodrigo, W. M. Mendenhall, et al. "Carotid body paragangliomas: a systematic study on management with surgery and radiotherapy." In: *Eur. Arch. Otorhinolaryngol.* 271.1 (2014), pp. 23–34.
17. K. E. van der Bogt, M.-P. F. M. Vrancken Peeters, J. M. van Baalen, and J. F. Hamming. "Resection of carotid body tumors: results of an evolving surgical technique." In: *Ann. Surg.* 247.5 (2008), pp. 877–884.
18. C. D. Lees, H. L. Levine, E. G. Beven, and H. M. Tucker. "Tumors of the carotid body. Experience with 41 operative cases". In: *Am. J. Surg.* 142.3 (1981), pp. 362–365.
19. D. Kotelis, T. Rizos, P. Geisbüsch, et al. "Late outcome after surgical management of carotid body tumors from a 20-year single-center experience". In: *Langenbeck's Arch. Surg.* 394.2 (2009), pp. 339–344.
20. A. Dardik, D. W. Eisele, G. M. Williams, and B. A. Perler. "A contemporary assessment of carotid body tumor surgery." In: *Vasc. Endovascular Surg.* 36.4 (2002), pp. 277–283.
21. G. Ghilardi, E. M. Bortolani, P. Pizzocari, P. L. Vandone, and M. De Monti. "[Paraganglioma of the neck. Analysis of 32 operated cases]." In: *Minerva Chir.* 46.20 (1991), pp. 1109–17.
22. M. Makeieff, I. Raingeard, P. Alric, A. Bonafe, B. Guerrier, and C. Marty-Ane. "Surgical management of carotid body tumors." In: *Ann. Surg. Oncol.* 15.8 (2008), pp. 2180–6.
23. Z. Wang, Z. Zhang, Q. Huang, J. Yang, and H. Wu. "Surgical management of extensive jugular paragangliomas: 10-year-experience with a large cohort of patients in China". In: *Int. J. Surg.* 11.9 (2013), pp. 853–857.
24. T. K. Nicoli, S. T. Sinkkonen, T. Anttila, A. Mäkitie, and J. Jero. "Jugulotympanic paragangliomas in southern Finland: a 40-year experience suggests individualized surgical management". In: *Eur. Arch. Oto-Rhino-Laryngology* (2016), pp. 1–9.
25. Y. Oestreicher-Kedem, S. Agrawal, R. K. Jackler, and E. J. Damrose. "Surgical rehabilitation of voice and swallowing after jugular foramen surgery." In: *Ann. Otol. Rhinol. Laryngol.* 119.3 (2010), pp. 192–8.
26. C. Suárez, J. P. Rodrigo, C. C. Bödeker, et al. "Jugular and vagal paragangliomas: Systematic study of management with surgery and radiotherapy." In: *Head Neck* 35.8 (2013), pp. 1195–204.
27. C. C. Boedeker. "Paragangliomas and paraganglioma syndromes." In: *GMS Curr. Top. Otorhinolaryngol. Head Neck Surg.* 10 (2011), Doc03.

"Fibro-hemangioom van het slaapbeen en middenoor bij drie zussen"
De titel van de eerste publicatie over paragangliomen geschreven door een Nederlandse auteur.

Goekoop, Deventer 1932

9

Nederlandse samenvatting

Hoofd-hals-paragangliomen (HNPGL) zijn doorgaans benigne tumoren die uitgaan van paraganglion weefsel, dat geassocieerd is met het parasympatische zenuwstelsel. Ze worden het meest frequent gedetecteerd ter plaatse van de carotisbifurcatie, in associatie met de nervus vagus (ter plaatse van het ganglion inferior en minder frequent ter plaatse van het ganglion superior), in de adventitia van de bulbus jugularis en ter plaatste van het promotorium in het middenoor.

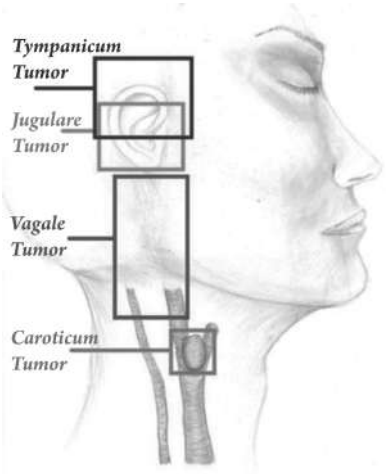

Figure 9.0.1: Locatie van hoofd-hals-paragangliomen

Circa 35-40% van alle HNPGL komt voor in het kader van een erfelijke predispositie. Mutaties in het succinaat-dehydrogenase subunit-D (SDHD) gen komen het meest frequent voor, zeker in Nederland. In het Leids Universitair Medisch Centrum betreft dit circa 90%. Dragers van een SDHD genmutatie hebben een hoog risico op het ontwikkelen van multipele paragangliomen, mits de mutatie via de paternale lijn is doorgegeven. Sinds 2002 is (presymptomatisch) DNA onderzoek mogelijk, dragers van een SDHD gen komen in aanmerking voor frequente screening naar paragangliomen.

Hoewel HNPGL zelden metastaseren, kunnen ze door hun locatie in nabijheid van belangrijke neurovasculaire structuren wel veel morbiditeit veroorzaken. De meest voorkomende symptomen zijn een zwelling in de hals, pijn, pulsatiel oorsuizen en gehoorverlies. Minder frequent leidt tumorprogressie tot uitval van craniale zenuwen. De behandeling van paragangliomen (meestal chirurgische resectie, maar in toenemende mate worden HNPGL primair bestraald) is echter ook niet zonder risico's. Voornamelijk het risico op schade aan craniale zenuwen is, afhankelijk van tumorlocatie en -grootte, aanzienlijk. Daarom wordt frequent een conservatief beleid (surveillance) gehanteerd, waarbij tumorprogressie gemonitord wordt.

Met als voornaamste doel, meer inzicht vergaren in het natuurlijk beloop van SDHD-gerelateerde HNPGL, om uiteindelijk screening, behandeling en counseling van patiënten en hun familieleden te verbeteren, is dit proefschrift tot stand gekomen.

Hoofdstuk 1: Introductie

In dit hoofdstuk komen de geschiedenis, genetica, klinische manifestaties, diagnostiek en behandeling van paragangliomen aan bod. De functie van succinaat-dehydrogenase wordt besproken, alsmede de huidige kennis over de "pathways" betrokken bij het ontstaan van SDHD-gerelateerde paragangliomen. Daarnaast wordt er ingegaan op het zojuist genoemde, opmerkelijke "parent-of-origin" overervingspatroon en wordt er een beknopt overzicht gegeven van de tot dusver bekende genen die betrokken kunnen zijn bij erfelijke paragangliomen. Naast HNPGL, hebben dragers van een SDHD genmutatie een verhoogd risico op het ontwikkelen van paragangliomen in de borst- en buikholte (waaronder het feochromocytoom). Recent zijn ook andere tumoren, o.a. gastro-intestinale stroma tumoren, geassocieerd met SDHD genmutaties. De meest voorkomende symptomen van al deze tumoren worden vermeld. Beeldvorming, classificatie van HNPGL en het toenemende gebruik van functionele beeldvormingstechnieken worden besproken. Evenals het karakteristieke histologische "Zellballen" patroon van type I en II cellen. Tenslotte komen de verschillende behandelopties en potentiele risico's aan de orde.

Hoofdstuk 2: Hoge prevalentie van occulte paragangliomen in asymptomatische dragers van SDHD en SDHB genmutaties

Met als doel de prevalentie van paragangliomen in asymptomatische dragers van een SDHD of SDHB genmutatie te kwantificeren, werden de resultaten van presymptomatisch DNA onderzoek en navolgende screening geanalyseerd. In bijna 60% van de 47 asymptomatische SDHD genmutatie dragers werd een HNPGL gedetecteerd, en in maar liefst 34% werden zelfs meerdere HNPGL gediagnosticeerd. Bij dragers van een SDHB (een ander subunit van succinaat-dehydrogenase) genmutatie, werden significant minder HNPGL gevonden. Abdominale/thoracale paragangliomen werden minder frequent gediagnosticeerd. Concluderend, de prevalentie van HNPGL in dragers van een SDHD genmutatie is hoog, ook in afwezigheid van symptomen.

Hoofdstuk 3: Het meten van hoofd-hals-paragangliomen: is volumetrische analyse de moeite waard?

Om het natuurlijk beloop van HNPGL te kunnen vervolgen is kennis over de reproduceerbaarheid van metingen cruciaal, zonder deze kennis is het immers moeizaam

om tumorprogressie te onderscheiden van meetvariatie. Om die reden werd de intra-observer variabiliteit van drie verschillende meetmethoden vergeleken waarbij ook praktische aspecten (arbeidsintensiteit) in acht werden genomen. Allereerst werd het volume geschat op basis van drie lineaire dimensies, ervan uitgaande dat HNPGLs een ellipsoïde vorm hebben. Daarnaast werden automatische en grotendeels handmatige, volumetrische analyse toegepast. Helaas bleek automatische volumetrische analyse ongeschikt. De reproduceerbaarheid van de andere twee methoden was vergelijkbaar voor caroticum en vagale tumoren, en ook kwam het geschatte volume op basis van lineaire dimensies goed overeen met de meer robuuste volumetrische analyse. Echter, het gebruik van lineaire dimensies was gemiddeld ruim vier keer zo snel. Daarom werd het meten van drie lineaire dimensies als meest geschikte methode beschouwt voor het meten van caroticum en vagale tumoren, met een kleinst meetbaar verschil van respectievelijk 10% en 25%.

Hoofdstuk 4: Leeftijd en tumorvolume zijn voorspellers voor groei van caroticum en vagale tumoren

Met als doel "surveillance" te optimaliseren, werden groei (een volume toename van tenminste het kleinst meetbare verschil) van HNPGL en mogelijk voorspellers voor groei onderzocht. Hoewel het natuurlijk beloop van HNPGL meestal gunstig was (mediane groeisnelheid van circa 10% per jaar) zal, indien HNPGL gedurende een lange periode vervolgd worden, in de meeste gevallen (85%) groei worden waargenomen. De tumorlocatie, tumorvolume en leeftijd van de patiënt bleken statistisch significante voorspellers voor groei en werden geïncludeerd in een predictiemodel dat online beschikbaar is. Met dit model kan, de kans op groei op de korte termijn (circa 2 jaar) redelijk accuraat voorspeld worden. Door de implementatie van dit model kan "surveillance" geïndividualiseerd worden. Met het toenemen van leeftijd en het tumorvolume blijkt de groeisnelheid af te nemen, passend bij decelererende groei.

Hoofdstuk 5: Mathematische modellen voor tumorgroei en de reductie van overbehandeling

Idealiter, zouden we HNPGL die geen (progressie van) symptomen zullen veroorzaken kunnen onderscheiden van HNPGL die juist beter behandeld kunnen worden terwijl ze nog relatief klein zijn. In hoofdstuk 5 werden daarom de eerste stappen gezet om

lange termijn groei te voorspellen. Zeven verschillende wiskundige modellen, variërend van een simpel lineair en exponentieel model tot sigmoïd-vormige modellen, werden aan groeidata gefit. De sigmoïd-vormige modellen verschafte een goede fit (R^2: 0.996-1.00) en beschreven de geobserveerde data beter dan de meer eenvoudige modellen ($p<0.001$), passend bij de bevindingen uit hoofdstuk 4. Van de sigmoïd-vormige modellen, is het Bertalanffy model waarschijnlijk het meeste geschikt om lange termijn groei te voorspellen, mede omdat dit model de beste fysiologische basis heeft.

Hoofdstuk 6: Klinische progressie en metachrone laesies in een groot cohort SDHD variant dragers

Hoewel het welomschreven is dat SDHD genmutaties geassocieerd zijn met multipele HNPGL, was het risico op het ontwikkelen van nieuwe laesies tijdens follow-up tot op heden onbekend. Daarnaast waren er geen grote studies die klinische progressie in patiënten met onbehandelde HNPGL beschreven. Zowel het risico op metachrone laesies en klinische progressie kwamen in dit hoofdstuk aan de orde. Het risico op één of meerdere nieuwe HNPGL nam toe tot 73% na 22 jaar follow-up. Opvallend was het resultaat dat het risico op nieuwe tumoren voor mannen hoger was dan voor vrouwen. Daarnaast bleek het risico op metachrone laesies groter onder patiënten die zich presenteren met symptomen in vergelijking met asymptomatische dragers van een SDHD variant. Gedurende een mediane follow-up tijd van 8 jaar rapporteerde bijna 50% nieuwe symptomen, gelukkig werd in slechts 11% nieuwe dysfunctie van craniale zenuwen geobserveerd. In lijn met de resultaten uit hoofdstuk 4, was leeftijd negatief gecorreleerd met het risico op nieuwe symptomen.

Hoofdstuk 7: Geen bewijs voor verhoogde mortaliteit onder SDHD variant dragers in vergelijking met de algehele bevolking

In dit hoofdstuk werd de overleving in een groot Nederlands cohort SDHD variant dragers vergeleken met de Nederlandse bevolking. Gedurende een gemiddelde follow-up tijd van ruim 7 jaar, overleden 18 van de 275 geïncludeerde SDHD variant dragers. Twee patiënten overleden ten gevolge van gemetastaseerde paragangliomen, in 4 gevallen was de doodsoorzaak niet aan paragangliomen gerelateerd en in de overige gevallen was de doodsoorzaak onbekend. De sterftecijfers werden vergeleken met de sterftecijfers in de Nederlandse populatie (gestratificeerd voor leeftijd, geslacht en datum), hierbij werd

gebruik gemaakt van de standard mortality ratio (SMR). De SMR is het aantal geobserveerde, gedeeld door het aantal verwachte sterfgevallen. Met een SMR van 1.07 bleek dat de sterfte onder SDHD variant dragers niet substantieel verhoogd is ten opzichte van de Nederlandse populatie.

Hoofdstuk 8: Discussie

In dit laatste hoofdstuk werden de bevindingen uit de hoofdstukken 2-7 aan elkaar gerelateerd. Waarbij de belangrijkste conclusies/bevindingen als volgt kunnen worden samengevat. Allereerst is de kans dat een SDHD variant drager één of meerdere paragangliomen ontwikkeld aanzienlijk, ook in afwezigheid van symptomen. Hoewel de groeisnelheid van hoofd-hals paragangliomen doorgaans langzaam is, zullen de meeste SDHD variant dragers uiteindelijk (progressie van) symptomen ervaren. Dysfunctie van craniale zenuwen wordt gelukkig minder vaak geobserveerd. Daarnaast is de levensverwachting van SDHD variant dragers niet substantieel verminderd ten opzichte van de Nederlands populatie. Ten aanzien van de optimalisatie van screening en behandeling van HNPGL werden belangrijke stappen gemaakt. Op de korte termijn kan tumorgroei nu redelijk adequaat voorspeld worden, wat meer geïndividualiseerde screening faciliteert. Ook bleek de groeisnelheid van HNPGL negatief gecorreleerd met leeftijd en volume passend bij decelerende groei. Vermoedelijk is het Bertalanffy model het meest geschikte model om lange termijn groei te voorspellen. De predictieve waarde van dit model moet echter nog wel gevalideerd worden. Aangezien behandelkeuzes idealiter gebaseerd worden op klinische manifestaties en niet op groei alleen, verdient het de aanbeveling om de evolutie van klinische manifestaties en groei aan elkaar te relateren. Prospectief onderzoek is hiervoor het meest geschikt.

Abbreviations
List of contributing authors
List of publications
About the author

A

Appendix

Abbreviations

α-KG	α-ketoglutarate
A	Adenine
Arg	Arginine
Asp	Aspartic acid
AUC	Area under the curve
bp	Base pair
C	Cytosine
c.	Coding DNA reference sequence
CA	California
CBT	Carotid body tumor
CDKN1C	Cyclin-dependent kinase inhibitor 1c
CI	Confidence interval
cm	Centimeter
CNS	Central nervous system
CSF	Cerebrospinal fluid
CT	Computed tomography
DCIS	Ductal carcinoma in situ
del	Deletion
df	Degrees of freedom
DNA	Deoxyribonucleic acid
DSA	Digital substraction angiography
3D TOF MRA	3D Time of Flight MR Angriography
ECA	External carotid artery
EGLN	Elegans homolog
ENT	Ear nose and throat
EPAS1	Endothelial PAS domain protein 1
EPO	Erytropoetin
ERK	Extracellular signal-regulated kinases
FAD	Flavin adenine dinucleotide
^{18}FDOPA	^{18}F-fluordopa
Fe	Iron

FH	Fumurate hydratase
G	Guanine
^{68}Ga	^{68}Gallium
GIST	Gastrointestinal stromal tumor
GN	Ganglioneuroma
GPR91	G-protein-coupled receptor 91
HIF	Hypoxia-inducible factor
HNPGL	Head and neck paraganglioma
HR	Hazard ratio
HRE	HIF-responsive elements
IBM	International Business Machines
ICA	Internal carotid artery
Ile	Isoleucine
^{123}I-MIBG	^{123}I-metaiodobenzylguanidine
IQR	Interquartile range
KIF1Bβ	Kinesin family member1Bβ
LC	Lung carcinoma
LDGA	Laboratory for Diagnostic Genome Analysis
Leu	Leucine
LOVD	Leiden Open (source) Variation Database
LUMC	Leiden University Medical Center
MAX	Myc associated factor X
5mC	5-methylcytosine
MDH2	Malate dehydrogenase 2
MERTK	C-MER proto-oncogene tyrosine kinase
Met	Methionine
MIBG	Metaiodobenzylguanidine
MLPA	Multiplex ligation-dependent probe amplification
mm	Millimeter
MRA	Magnetic resonance angiography
MRI	Magnetic resonance imaging
ms	Millisecond
3MT	3-methoxytyramine

MTC	Medullary thyroid carcinoma
mTOR	Mammalian target of rapamycin
n	Number
NVII	Facial nerve
NIX	Glossopharyngeal nerve
NX	Vagus nerve
NXII	Hypoglossal nerve
NB	Neuroblastoma
NF1	Neurofibromatosis type 1
NGF	Nerve growth factor
NGS	Next generation sequencing
NG_	Genomic sequence
NM_	mRNA reference sequence
NT_	DNA reference sequence
NY	New York
OR	Odds ratio
p.	Protein sequence
PA	Pituitary adenoma
PCC	Pheochromocytoma
PET	Positron emission tomography
PGL	Paraganglioma
PHDs	Prolyl hydroxylase domain proteins
PNMT	Phenylethanolamine N-methyltransferase
PP	Predicted probability
Pro	Proline
PTC	Papillary thyroid carcinoma
Q	Quartile
r	Growth rate
R^2	Coefficient of determination
RCC	Renal cell carcinoma
RET	Rearranged during transfection proto-oncogene
RMSE	Root mean squared error
ROC	Receiver operating characteristic

ROS	Reactive oxygen species
S	Sulfur
SD	Standard deviation
SDD	Smallest detectable difference
SDH	Succinate dehydrogenase
SDHA	Succinate dehydrogenase subunit-A (flavoprotein-subunit)
SDHAF1	Succinate dehydrogenase, assembly factor 1
SDHAF2	Succinate dehydrogenase, assembly factor 2
SDHB	Succinate dehydrogenase subunit-B (iron-sulfur subunit)
SDHC	Succinate dehydrogenase subunit-C (anchoring subunit)
SDHD	Succinate dehydrogenase subunit-D (anchoring subunit)
SLC22A18	poly-specific organic cation transporter
SMR	Standardized mortality ratio
sPGL	Extra-adrenal sympathetic paraganglioma
SPSS	Statistical Package for the Social Sciences
T	Thymine
T	Tesla
t	Time
TCA	Tricarboxylic acid
T_d	Tumor doubling time
Thr	Threonine
TMEM127	Transmembrane protein 127
TX	Texas
Tyr	Tyrosine
USA	United States of America
VEGF	Vascular endothelial growth factor
VHL	Von Hippel-Lindau
V	Volume
WHO	World health organization

List of contributing authors

J.P. Bayley, PhD
Department of Human Genetics, Leiden University Medical Center

Prof. P.P.G. van Benthem, MD, PhD
Department of Otorhinolaryngology, Leiden University Medical Center

B.T.J. van Brussel
Department of Clinical Genetics, Leiden University Medical Center

J.M. Bokhorst, BSc
Eindhoven University of Technology

E.P.M. Corssmit, MD, PhD
Department of Endocrinology, Leiden University Medical Center

Prof. O.M. Dekkers, MD, PhD
Department of Endocrinology & Department of Epidemiology,
Leiden University Medical Center

Prof. J.F. Hamming, MD, PhD
Department of Surgery, Leiden University Medical Center

L.T. van Hulsteijn, MD, PhD
Department of Endocrinology, Leiden University Medical Center

F.J. Hes, MD, PhD
Department of Clinical Genetics, Leiden University Medical Center

J.C. Jansen, MD, PhD
Department of Otorhinolaryngology, Leiden University Medical Center

A.G.L. van der Mey, MD, PhD
Department of Otorhinolaryngology, Leiden University Medical Center

L.H.M. de Pont, BSc
Department of Otorhinolaryngology, Leiden University Medical Center

C.M.J. Tops, PhD
Department of Clinical Genetics, Leiden University Medical Center

B.M. Verbist, MD, PhD
Department of Radiology, Leiden University Medical Center

List of publications

B. L. Heesterman, J. P. Bayley, C. M. Tops, et al. "High prevalence of occult paragangliomas in asymptomatic carriers of SDHD and SDHB gene mutations." In: Eur. J. Hum. Genet. 21.4 (Apr. 2013), pp. 469–70.

L. T. van Hulsteijn, **B.L. Heesterman**, J. C. Jansen, et al. "No evidence for increased mortality in SDHD variant carriers compared with the general population." In: Eur. J. Hum. Genet. 23.12 (Dec. 2015), pp. 1713–6.

B. L. Heesterman, B. M. Verbist, A. G. L. van der Mey, et al. "Measurement of head and neck paragangliomas: is volumetric analysis worth the effort? A method comparison study." In: Clin. Otolaryngol. 41.5 (Oct. 2016), pp. 571–8.

B. L. Heesterman and B. F. Hogewind. "Phacoemulsification and Intraoperative Complications in 452 Patients with Diabetic Retinopathy." In: Semin. Ophthalmol. 32.4 (Apr. 2016), pp. 1–2.

B. L. Heesterman, L.M.H. de Pont, B.M. Verbist, et al. "Age and tumor volume predict growth of carotid and vagal body paragangliomas." In: J Neurol Surg B Skull Base. 78.6 (Dec. 2017), pp. 497–505.

B. L. Heesterman, L.M.H. de Pont, A. G. L. van der Mey, et al. "Clinical progression and metachronous paragangliomas in a large cohort of SDHD germline variant carriers." In: Eur. J. Hum. Genet. (2018).

B. L. Heesterman, J. Bokhorst, L.M.H. de Pont, et al. "Mathematical models for tumor growth and the reduction of overtreatment." In: J Neurol Surg B Skull Base. (in press).

About the author

Berdine Louise Heesterman was born on March 3, 1990 in Baarn, the Netherlands. She completed secondary school at "Het Baarnsch Lyceum" in 2008, after which she started studying medicine at the University of Leiden. During her studies she began her research at the department of Otorhinolaryngology with which she continued after obtaining her medical degree in 2015. Currently she is working as a consultant at IG&H, primarily within the healthcare sector.